5-20-2005

The Kinetics of Particulate Substrate Utilization by Bacterial Films

Joshua Boltz
University of New Orleans

THE KINETICS OF PARTICULATE SUBSTRATE UTILIZATION BY BACTERIAL FILMS

A Dissertation

Submitted to the Graduate Faculty of the
University of New Orleans
in partial fulfillment of the
requirements for the degree of

Doctor of Philosophy
in
Engineering and Applied Sciences

by

Joshua P. Boltz

B.S.C.E., University of South Alabama, 2001
M.S. University of New Orleans, 2003

May 2005

ACKNOWLEDGEMENTS

I would like to express sincere gratitude toward Professor Enrique J. La Motta, whose knowledge allowed for the development of this project. Professor La Motta is a teacher, colleague, and friend. I would also like to acknowledge Professors J. Alex McCorquodale, Adam Faschan, Bhaskar Kura, and Zhide Fang for their participation as members of the dissertation committee. The University of New Orleans Schlieder Urban Environmental Systems Center provided financial support of this research project.

Finally, glory to God for my accomplishments. God bless Rebeca, my life partner and beloved wife, who endured every hardship with compassion, respect, patience, and love. God bless David and Deborah, my Mother and Father, who always have, and always will, support, encourage, and provide me with unconditional love. Finally, I would like to offer special thanks to the little ones, because no hour was too early, or late, to be by my side. Thank you from the bottom of my heart because without you I would not be here. Work hard and never give up!

TABLE OF CONTENTS

LIST OF FIGURES

LIST OF TABLES

ABSTRACT

There is a need to develop a mathematical expression capable of describing the removal of particulate chemical oxygen demand (PCOD) from wastewaters in biological film systems. In this context, organic particles that are maintained in suspension (i.e., not removed during normal settling) are the focus of experimentation, modeling, and discussion. The goal of this research project is to study the kinetics of PCOD removal from wastewaters by bacterial films, or biofilms. To achieve this objective, a bench-scale rotating disc biofilm reactor (RDBR) was operated using methanol (dissolved substrate), Min-U-Sil 10 (inorganic particulates), and Maizena corn starch (organic particulates) dissolved/suspended in the influent stream. The effect of the ratio of biofilm area to volumetric flow rate passing through the RDBR on the concentration of substrate remaining in the final effluent was determined, and the kinetic relationship was established for both dissolved substrate and particle removal. Exocellular polymeric substances (EPS) were extracted and quantified in order to explain the role of biological flocculation, or bioflocculation, in particulate removal.

In the literature, Fick's first law and zero-order kinetics have described the diffusion and biochemical reaction of soluble substrate within the bacterial film matrix (when completely penetrated), respectively. The present study confirms this kinetic behavior for various influent methanol concentrations. On the other hand, the removal of particulates, organic and inorganic, adheres to first-order reaction kinetics. These findings, coupled with the identification of EPS, attribute bioflocculation as the primary removal mechanism of particulates.

A mass balance on the biofilm reactor allowed for the development of a comprehensive rate expression for substrate consumption by biofilms when both dissolved and particulate substrates are available. Total chemical oxygen demand (TCOD) is comprised of dissolved chemical oxygen demand (DCOD) and PCOD, each of which can be readily determined through laboratory analysis. An equation was developed that accurately describes the disappearance of TCOD by the bioflocculation of PCOD and consumption of DCOD in the bench scale RDBR.

1. INTRODUCTION

Several mechanistic models have been developed to describe the kinetics of dissolved substrate utilization by bacterial films, or biofilms. There are two "schools of thought" regarding the kinetics of dissolved substrate utilization by biofilms. Researchers such as Williamson and McCarty (1976a, 1976b) and Rittmann and McCarty (1978, 1980a, 1980b, 1981, 2001) have applied Monod type kinetics to describe biochemical reaction of soluble substrate by biofilms. Another group, including La Motta (1976a), Harremoës (1978) and Trulear and Characklis (1982), have observed that zero-order kinetics accurately describes the intrinsic rate of dissolved substrate utilization by thin (completely penetrated) biofilms. These models, however, have limited application when the primary constituent of chemical oxygen demand (COD) in domestic wastewaters is organic particulates.

Recent research has demonstrated that frequently a small fraction of the total COD (TCOD) in raw sewage and primary effluents is dissolved. Metcalf and Eddy (2003) state that only 20-50% of the TCOD in municipal sewage is dissolved and Levine, et al., (1985, 1991) have pointed out that a major fraction of the organic matter in municipal wastewater is in particulate form. The University of New Orleans (UNO) Urban Waste Management and Research Center (UWMRC) demonstrated that municipal wastewaters in Jefferson Parish, LA, on the west bank of the Mississippi River, contain approximately 15% of dissolved COD (DCOD) and 85% of particulate COD (PCOD) (La Motta, et al., 2003). In this context, DCOD is defined as the COD remaining after the chemical flocculation laboratory method described herein, and PCOD is the difference between TCOD and DCOD. Figure 1 illustrates data

compiled by several researchers within the UWMRC, and indicates that, in fact, a major fraction of COD in wastewater samples taken from the UNO UWMRC pilot-plant located at the Marrero Wastewater Treatment Plant, Marrero, Louisiana, is in particulate form.

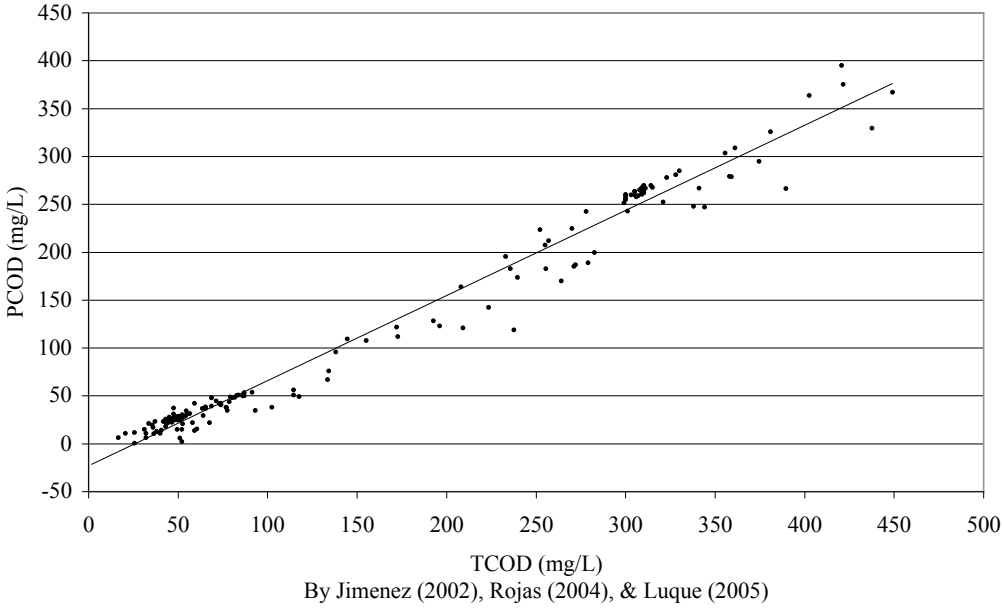

Figure 1. PCOD and TCOD Correlation Observed at the UNO UWMRC Pilot-Plant

A linear regression analysis provided a best-fit equation of PCOD = 0.889.TCOD – 22.85. The coefficient of determination, R^2, is 0.979.

Boltz (2003) demonstrated that the removal of organic and inorganic particulate matter in a pilot-scale trickling filter (TF), located at the aforementioned UWMRC pilot-plant, adheres to first-order reaction kinetics regardless of the amount of DCOD available in the influent stream. This consumption in the pilot-scale TF is well described by a dispersion model, whose solution is similar to the one presented by Wehner and Wilhelm (1956). Additionally, the pilot-scale TF is

more efficient at removing PCOD than DCOD. There is a significant paucity of experimental data pertaining to the kinetics of particulate removal by aerobic fixed-film wastewater treatment processes or the flocculation of particles by the said films. Therefore, there is a need to develop a mathematical expression capable of describing the removal of PCOD from wastewaters by aerobic, biological films.

The primary goal of this research project is to study the kinetics of PCOD removal from wastewaters by biofilms. In this context, organic particles that are maintained in suspension (i.e., not removed during normal settling) are the focus of experimentation, modeling, and discussion. To achieve this objective, a bench-scale rotating disc biofilm reactor (RDBR) is operated using methanol (dissolved substrate), Min-U-Sil 10 (inorganic particulates), and Maizena corn starch (organic particulates) dissolved/suspended in the influent stream. The transport of dissolved substrate from the bulk of the liquid to the wastewater/biofilm interface has been well documented. The literature has used Fick's first law and zero-order kinetics to describe diffusion and biochemical reaction of soluble substrate within the biofilm matrix, respectively. Since particulate, organic and inorganic, removal in the aforementioned pilot-scale TF adheres to first-order reaction kinetics, and La Motta, et al., (2003) have described bioflocculation in the activated sludge system as a first-order process, then the removal of dissolved and particulate substrates by biofilms can, theoretically, be differentiated by their removal kinetics. Consequently, the rate of removal of each substrate can be measured when the system is fed dissolved and particulate substrates simultaneously.

This research project was designed to implement a mass balance approach, utilizing the RDBR, to develop a comprehensive expression capable of describing overall substrate consumption by biological films when both dissolved and particulate substrates are available. Assuming that TCOD is comprised of DCOD and PCOD, each of which can be readily determined through laboratory analysis, an equation will be developed that accurately describes the disappearance of TCOD by the bioflocculation of PCOD and consumption of DCOD. This research also identifies the role extracellular polymeric substances (EPS) play in the removal of particles by biofilms.

2. LITERATURE REVIEW

2.1. PHYSICAL AND BIOLOGICAL PROPERTIES OF BIOFILMS

A biofilm is a complex community containing bacterial cultures. Algae, fungi, protozoan, and metazoan, such as worms, insect larvae, and snails, may also be present in the ecosystem. The composition of biofilms is generally dictated by the conditions under which they are grown. The physical properties of biofilms are directly related to those of their primary constituents, namely microbial cells and EPS. Macroscopic properties generally dictate the rate and extent of biofilm internal processes. Physical, chemical, and biological properties are dependent upon the environment in which the biofilm was grown. The physical and chemical components of the aquatic and substratum environment affect the predominant biofilm organisms. It is convenient to analyze biofilm as the sum of its constituents. Therefore, a discussion of the physical and biological properties of biofilms will be developed in this section.

2.1.1. Classification and Composition of Bacteria

Bacteria are of primary importance for adequate performance in biological treatment processes (Metcalf and Eddy 2003). Archaea and bacteria are microscopic and prokaryotic. Each lack a nuclear membrane, whereas Eucarya have a nuclear membrane and vary in size from microscopic to macroscopic. Bacteria oxidize dissolved carbonaceous organic matter into simple end products, namely carbon dioxide and water, and additional biological mass, or biomass. The following equation (1), presented by Metcalf and Eddy (2003), describes the aerobic biological oxidation of organic matter.

$$\nu_i\left(organic\ matter\right)+\nu_2O_2+\nu_3NH_3+\nu_4PO_4^{3-}\xrightarrow{microorganisms}\nu_5\left(new\ cells\right)+\nu_6CO_2+\nu_7H_2O \quad (1)$$

Here, ν_i is a stoichiometric coefficient. Oxygen, ammonia, and phosphate are representative nutrients necessary for the conversion of organic matter into the aforementioned simple end products. Usually, bacteria are smaller than 5 μm in diameter. Facultative bacteria decompose organic material in wastewater along with aerobic and anaerobic bacteria. Aerobic bacteria exist near the external surface of the biological film. Dissolved oxygen (DO) consumed in the liquid layer is readily replenished by reoxygenation from ambient air. However, as the microorganisms continue to grow the biological film becomes thicker. Therefore, as the biological film approaches the growth medium, the bacteria may become anaerobic. This is due to the consumption of DO near the biofilm's surface.

Appropriate nutrients must be present in order to sustain microbial growth. An understanding of the composition of bacterial cells provides a basis for the nutrients needed for growth. Prokaryotes are about 80% water and 20% dry material, 90% of the dry material is organic and 10% is inorganic. Major cellular material reported as percent of dry weight is 55% protein, 5% polysaccharide, 9.1% lipid, 3.1% DNA, 20.5% RNA, 20.5% other, and 1% inorganic ions. Cellular elements reported as percent of dry weight is 50% carbon, 22% oxygen, 12% nitrogen, 9% hydrogen, 2% phosphorus, 1% sulfur, 1% potassium, 1% sodium, 0.5% calcium, 0.5% magnesium, 0.5% chlorine, 0.2% iron, and 0.3% other trace elements (Madigan, et al. 1997). A shortage of any of these substances would limit and may alter growth.

In biological wastewater treatment, microorganisms use an electron-donor substrate for synthesis. Initially, a portion of its electron is transferred to the electron acceptor to provide energy for conversion of the other portion of electrons into microbial cells. The portion that is initially converted into cells provides a basis for partitioning the substrate between energy generation and synthesis (Rittmann and McCarty 2001). Aerobic organisms need to send relatively few electrons from their donor to oxygen in order to generate the energy required to synthesize a given amount of new biomass (Rittmann and McCarty 2001).

2.1.2. Extracellular Polymeric Substances (EPS)

Most bacteria produce EPS (Characklis and Marshall, 1990). Bacterial polymers are primarily composed of polysaccharides and protein (Lazarova and Manem 1995). Polysaccharides are carbohydrates that can be decomposed by hydrolysis into two or more molecules of monosaccharides. Exocellular biopolymers are excreted by bacteria and can be attached to the cell in a capsule, or excreted onto surrounding medium as slime (Higgins and Novak 1997). The attachment of microorganisms to surfaces, and other microorganisms, can be found throughout nature and engineered systems (Logan, et al. 1986). Biopolymers provide bacterial microorganisms with a mean of anchoring to medium in order to feed (Zhang, et al. 1999). The interaction between a bacterial cell and the substratum leading to irreversible adhesion is determined by the physical properties of the macromolecules at the cell surface. Furthermore, electron microscopy has revealed that EPS are the extracellular matrix responsible for biofilm integrity. This section will explain the spatial distribution of EPS throughout biofilms, the role of EPS in bioflocculation, and the role of EPS in bacterial attachment and biofilm formation.

2.1.2.1. Physical Properties and Spatial Distribution of EPS in Biofilms

Proteins and polysaccharides are the primary extracellular macromolecules in biofilms (Laspidou and Rittmann 2002). Traditionally, proteins and nucleic acids are termed higher order structures. Physical properties of polymers are greatly influenced by their shape. Alterations to the solvent (in the case of aerobic wastewater treatment, the solvent is water) composition including pH, temperature, or the addition of inorganic salts may alter a polymer's physical properties (Characklis and Marshall 1990). EPS are a primary component of a biofilm's organic mass. Typically, 95% of the mass of a biofilm is water, and 5% is dry material; approximately 90% of a biofilm's organic carbon is comprised of EPS (Characklis and Marshall 1990). During previous kinetic studies (La Motta 1976a; Williamson and McCarty 1976a; Rittmann and McCarty 1978), researchers have assumed that biofilms contain a homogeneous distribution of bacteria. Zhang and Bishop (2001) demonstrated that biofilms are heterogeneous structures. The researchers cut an intact piece of biofilm with a thickness greater than 3500 microns, the biofilm sample was frozen and subjected to "microslicing" (Zhang and Bishop 2001). Subsequently, the researchers divided the sample into 200-micron subdivisions, which were analyzed for EPS. The bacteriological configuration of the biofilm varied along its cross-sectional depth. Zhang and Bishop (2001) demonstrated that anaerobic bacteria replace aerobic bacteria as the organisms approach the growth medium. This is due to transfer limitations in DO and substrate. However, the physical properties of biofilms are dependent upon the conditions under which they are grown. Therefore, specific characteristics vary from treatment system to treatment system. The presence of nutrients and DO promotes the growth of viable biomass (Zhang and Bishop 2001). The outermost layer of a biofilm is subjected to the highest DO and substrate concentrations. Therefore, the highest viable biomass is present in the outermost layer

of the biofilm. Zhang and Bishop (2001) also demonstrated that the EPS yields were directly related to the amount of viable biomass present. Therefore, the most dominant presence of EPS is in the outermost layer of the biological film. This layer has the greatest exposure to organic and inorganic particulates in influent wastewater.

True intrinsic kinetics is masked by thick biological films (the definition of thin and thick biofilms shall be presented in a later section) and has been described by half-order kinetics (La Motta 1976a). In order to observe the intrinsic substrate utilization rate, experiments must be conducted in the absence of external diffusional resistances with thin biological films (La Motta 1976b). A close inspection of Zhang and Bishop's data reveals that EPS yields remain practically constant in the outermost layers (within 500 microns of the biofilm surface).

2.1.2.2. EPS and Biological Flocculation

Bioflocculation promotes physical removal of particulate organics. The EPS on the biofilm's surface act as a flocculating agent for both organic and inorganic particulates (Boltz 2003). Bioflocculation is a physical-chemical process whereby growing and reproducing suspended bacterial cells adhere to each other in a floc formation (Schuyler, et al., 2001). Tenney and Stumm (1965) have described bioflocculation as "an agglomeration of cells resulting from specific adsorption of polymer segments and from bridging of polymers between cells." Friedman, et al., (1969) have presented microscopic evidence that floc-formation of bacteria was caused by exocellular polymers. The aforementioned researchers' data suggested that bacteria that have been selected on the basis of their characteristic flocculent growth habit all possessed exocellular fibrillar polymers. Entanglement of cells among the fibrils, or adsorption of cells to

fibrils is a plausible explanation of the flocculation phenomenon. The physical and chemical properties of the specific exocellular polymer will determine the extent to which water is bound to the polymer and will also determine the solubility properties of the polymer. Liao, et al., (2001) have demonstrated that filamentous microorganisms, in fact, do not control the bioflocculation process. The researchers determined that activated sludge floc formation in laboratory sequential batch reactors, with glucose as the carbon source, was dependent upon inorganic salt concentration, particularly Ca^{2+} and Mg^{2+}. Higgins and Novak (1997) also demonstrated that the addition of divalent cations, Ca^{2+} and Mg^{2+}, to the feed of laboratory activated sludge systems increased the bound protein content, which was also associated with an improvement in settling. The researchers applied a cation bridging model, which explained that divalent cations act as a bridge between negatively charged sites within biopolymers. The interaction between the negatively charged biopolymers and the zeta-potential associated with the surface of organic and inorganic particles provides sufficient explanation for the removal of particulates in fixed-film processes by the bioflocculation phenomenon.

La Motta, et al., (2003) have described bioflocculation as a first-order process in an activated sludge unit operating under optimum environmental conditions. An adaptation of the first-order bioflocculation equation for biofilms is (2):

$$r = -k_p\left(C_e - a\right) \tag{2}$$

where r describes the rate of flocculation (kg/s.m^2), k_p is a first-order rate constant (m/s), C_e is the concentration of particles remaining in the effluent stream after time t (kg/m^3), and a is the

minimum concentration of particles that could be obtained in the effluent by bioflocculation in the reactor (kg/m^3).

Boltz (2003) demonstrated that the removal of organic and inorganic particulate matter, expressed as total suspended solids (TSS) and PCOD, in a pilot-scale TF adheres to equation (2). This consumption in the pilot-scale TF was well described by a dispersion model, whose solution is similar to the one presented by Wehner and Wilhelm (1956). The first-order removal of particulates agrees with the general kinetic behavior of biological flocculation. The presence of EPS explains the removal of particulates by biological flocculation in biological films.

2.1.2.3. EPS and Biofilm Attachment

Biofilm accumulation can be divided into three sequential phases; initial events, exponential accumulation, and steady state (Characklis and Marshall 1990). Various transport, interfacial transfer, and transformation processes contribute to biomass accumulation at a substratum. La Motta, et al., (1982) have described biofilm accumulation as the sum of the following physical, chemical, and biological processes. First, the substratum is conditioned by a series of organic molecules. Next, planktonic microbial cells are transported from the bulk liquid to the conditioned substratum. A portion of the cells that reach the conditioned area is reversibly adsorbed to the substratum. A fraction of the reversibly adsorbed cells remain immobilized and become irreversibly adsorbed. Finally, the irreversibly adsorbed cells utilize substrate and nutrients in the bulk liquid to generate biomass and end products. As additional cells and particulate matter attach to the biofilm, a portion of the gelatinous structure is subject to periodic

sloughing, or rapid, massive loss of biofilm (Atkinson and Howell 1975), from fluid shear stress. The detached material reenters the bulk liquid.

The initial step in biofilm formation is substratum conditioning. The transport of molecules and small particles in laminar flow can be described by molecular diffusion, i.e. Fick's Law (3), (Characklis and Marshall 1990).

$$J_S = D_W \frac{dS_S}{dx} \tag{3}$$

Where,

J_S = mass transfer ($ML^{-3}t^{-1}$)

D_w = diffusivity (Mt^{-1})

$\frac{dS_S}{dx}$ = concentration gradient (ML^{-4})

Biological wastewater treatment systems are generally operated under turbulent flow conditions. Here the diffusion equation (3) must be modified to account for turbulent eddy transport. The diffusion equation (3) is useful in describing the transport of dissolved substrate. However, fluid dynamic forces in a turbulent flow regime transport particles within the bulk liquid to:

(a) the substratum surface during conditioning and film formation, and

(b) the biofilm surface during the bioflocculation of particulates.

The physical-chemical processes associated with each of the aforementioned phenomenon are similar. Therefore, the process will be described at length in later sections to describe the deposition of particles on biofilms.

Marshall and co-workers (1971, 1973, 1976) proposed that the biofilm attachment process occurs in two distinct steps, each of which is controlled by different mechanisms. First, the transport of molecules occurs significantly faster than that of bacterial cells. Therefore, the adsorption of conditioning films is assumed to occur instantaneously. The second stage involves irreversible film attachment and requires an "incubation period" of at least three hours. The lag period allows for the production of EPS necessary for firm attachment.

Adsorption of an organic film is an interfacial transfer process that occurs within minutes of initial exposure (Marshall 1973). This process alters the properties of the wetted surface. Investigators have shown that materials with complex surface properties such as wettability, surface tension, and electrophoretic mobility are readily conditioned by adsorbing organics when exposed to natural waters with low organic concentrations (Characklis and Marshall 1990). The conditioning film is dynamic. Molecular turnover occurs with increasing molecular weight. Polymers adsorb more strongly due to the presence of multiple binding sites, in which they displace molecules of lower molecular weight (Cohen-Stuart, et al. 1980). EPS may have up to 10^5 units per chain. Therefore, each macromolecule may have many bonds to the substratum.

For materials that are not particularly repellent to microorganisms, the surface chemistry of bacteria plays an important role in the adsorption process (Cunliffe, et al., 1999). Several biological studies have been performed on the formation of biological films. Researchers such as Cunliffe, et al. (1999), and Bakker, et al. (2003) have proposed that elimination, or retardation, of bacterial conditioning films is the key to avoiding deleterious biofilm growth. Bakker, et al. (2003) derived a strategy for inhibiting early stages of biofilm formation by utilizing a low

surface-energy polymeric coating. Inversely, La Motta, et al., (1982) proposed that a combination of synthetic and naturally occurring biopolymers, used as surface conditioners, will promote biofilm growth in otherwise slow developing systems such as nitrification and anaerobic carbon removal.

Morphology of the substratum due to the conditioning film, or synthetic polymers, includes a decrease in hydrophobicity. Both positively and negatively charged surfaces acquire net negative charges (Loeb and Neihof 1975), and zeta potentials, contact potentials, and critical surface tensions are increased or decreased (Baier 1975) depending on the initial surface energy. Adsorption of a conditioning film decreases the surface energy of clean, high-energy surfaces (70 dyn cm^{-1}), but has diminutive effects on low energy surfaces (20 dyn cm^{-1}) (Baier 1980).

2.1.3. Soluble Substrate Production from Biodegradable Particulate Organic Matter

The literature describes biological films as being efficient in removing dissolved substrate from wastewaters. There is a paucity of information on the proportion of truly dissolved organic matter in sewage. Metcalf and Eddy (2003) state that only 20-50% of the TCOD in municipal sewage is dissolved and Levine, et al., (1985, 1991) have pointed out that a major fraction of the organic matter in municipal wastewater is in particulate form. The UNO UWMRC has demonstrated that municipal wastewaters in Jefferson Parish, LA, on the west bank of the Mississippi River, contain approximately 15% of DCOD and 85% of PCOD (La Motta, et al., 2003). A review of Figure 1 illustrates that a major fraction of COD in wastewater samples taken from the UNO UWMRC pilot-plant located at the Marrero Wastewater Treatment Plant, Marrero, Louisiana, is in particulate form. Organic particles can be used as a substrate by

biofilms, but bacteria cannot consume particulate substrates directly. The prokaryotic cell wall prevents most bacteria from the uptake and degradation of organic particulates and aqueous polymers by phagocytosis. Organic particulates trapped by biological films are converted to soluble substrate through the excretion of extracellular enzymes before consumption, or removed via secondary settling after sloughing. The decomposition process is referred to as hydrolysis. This section will discuss the method by which particles (organic and inorganic) are transported to the biofilm surface, the method of entrapment (namely bioflocculation), hydrolysis of organic particulates, and the rate of production.

2.1.3.1. Deposition of Particulates on Biological Films

Dynamic forces govern transport and interfacial processes in a turbulent flow regime. The particle flux to the surface increases with increasing particle concentration. However, the particle flux is dictated by the particle characteristics (e.g., size, shape, density, etc.) (Characklis and Marshall 1990). Particles (inorganic or organic) in turbulent flow are transported to within a short distance of the biofilm surface by eddy diffusion and are propelled into the laminar sublayer (a detailed definition of bulk liquid and the laminar sublayer will be presented in a later section) by their acquired momentum. When evaluating the mode of particle transport, it is convenient to consider two cases:

(a) particles that are retained in suspension, and

(b) particles that, either because density or size, are subject to settling.

For soluble matter and colloidal particulates (case *a*), diffusion can adequately describe transport in the laminar layer (Lister 1981, Lin, et al., 1953, Wells and Chamberlain 1967).

Microbial cells and macrocolloidal particulates ranging in size form 0.5 to 10 microns can be transported from the bulk liquid to the biofilm surface by several mechanisms including diffusion (Brownian and non-Brownian), gravity, fluid dynamic forces, and thermophoresis. The latter is only significant when particles are being transported through a temperature gradient (Lister 1981).

In the case of particle density greater than that of the surrounding liquid (case *b*), the particle will travel along the wetted surface faster than the liquid in the region of the surface. Lift forces will direct the particles to the surface (Rouhiainen and Stachiewicz 1970). If the mass density of the particle is substantially different from that of the surrounding liquid, then gravity forces govern particle transport.

2.1.3.2. Hydrolysis of Organic Particulates

Hydrolysis refers to the breakdown of complex organic particles into smaller soluble products that can be utilized by bacteria. However, the strict definition of hydrolysis is the breakdown of a polymer into smaller units by the addition of water (Brock and Madigan 1991). When analyzing hydrolysis in aerobic wastewater treatment systems, two categories can be differentiated. First, the hydrolysis of primary substrate, where organic particulates within the wastewater are degraded, and second, the hydrolysis of secondary substrate, i.e. hydrolysis of bacterial cell's internal storage products, of substances released during normal metabolism, or of particles produced during bacteria decay (Morgenroth, et al., 2002). The latter case is a complex study in itself, and the removal of COD from domestic and industrial wastewaters is of primary concern to sanitation engineers. Therefore, primary hydrolysis will be the focus of the

discussion. In wastewater treatment applications, the processes of hydrolysis includes all mechanisms that make slowly biodegradable substrate available for biomass production (Gujer, et al., 1999).

Hydrolysis is diverse and is influenced not only by the properties of the particle, but with the type of organisms involved in the process. Degradation is dependent upon extracellular depolymerization followed by cellular uptake and subsequent metabolization (Chróst 1991). There are two mechanisms of depolymerization, exo- and endo-enzymes. Exo-enzymes attack the integrity of a specific bond upstream of the end (normally the non-reducing end). Endo-enzymes act randomly on internal polymer bonds away from the terminal monomers (Morgenroth, et al., 2002). The Enzyme Handbook (Schomburg, et al., 1997) identifies 197 extracellular enzymes, 145 of which are hydrolytic.

Morgenroth, et al., (2002) claims, "The substrate specific activity is thought to follow traditional Michaelis-Menten kinetics." Other factors affecting the rate of reaction for the degradation of organic particulates and polymers by extracellular hydrolysis include local concentration of enzymes, location of the enzymes, and product transport mechanisms. Existing models explain the uptake of soluble substrate present in the wastewater and available after the hydrolysis process. There is a general agreement throughout the literature that it is necessary to differentiate between readily biodegradable (dissolved) and not readily biodegradable (particulate) substrates (Dold, et al., 1980, Henze, et al., 1987, Orthon, et al., 1994). The rate of hydrolysis is much slower than that of the utilization of the dissolved substrate the process

generates (Okutman, et al., 2001). Hydrolysis is typically described by means of a surface limited type of reaction kinetics (4) (Henze, et al., 1987)

$$\frac{dX_S}{dt} = -k_h \frac{X_S / X_H}{K_X + X_S / X_H} X_H \quad (4)$$

Where,

X_S = Slowly biodegradable PCOD (mg/L)

k_h = Overall rate constant for hydrolysis (day^{-1})

X_H = Active heterotrophic biomass (mg/L)

K_X = Overall saturation coefficient for hydrolysis (mg COD/mg cell COD)

A simple approach to expressing the rate of hydrolysis has been described (5):

$$r_{hyd} = -k_h X_S \quad (5)$$

Where,

r_{hyd} = first-order hydrolysis rate coefficient (day^{-1})

Principally, the rate coefficient is proportional to the hydrolytic enzyme concentration, as well as the intrinsic hydrolysis kinetics of the enzymes (Rittman and McCarty 2001). Some researchers include the active biomass concentration within k_h, this approach is convenient in that the hydrolysis rate reduces to zero when there is no biomass present. However, this also implies that the extracellular enzymes are linearly proportional to the biomass. This researcher was not able to locate proof of this assertion.

2.1.4. Biofilm Thickness

Biofilm thickness, δ, is an important characteristic in the analysis of biofilm processes. Thickness defines diffusional length and is necessary for determining fluid frictional and heat transfer resistances. Biofilm thickness varies over a given substratum due to the morphological features of the biofilm. The nonuniform thickness of biofilms increases fluid frictional resistances and advective mass transfer at interfaces (Picologlou, et al., 1980). In slow moving, nutrient rich water δ may exceed 30 mm. There is an absence of research pertinent to the thickness of biofilms found in fixed film wastewater treatment systems, but Table 1 lists δ and densities reported by several researchers for laboratory studies. There are three methods utilized to measure δ,

(1) light microscopy

(2) *in situ* light microscopy, and

(3) confocal microscope imaging.

The light microscopy method described by La Motta (1976b) was used in this investigation. Due to the disruptive effects of this method, Bakke and Ollson (1986) developed a nondestructive method to measure the thickness *in situ*. The physical process is similar to that described for light microscopy, but a correction factor of 1.36 must be applied to δ to account for light refraction through a glass cover. Confocal microscope imagery allows for the time series production of a digital three-dimensional image of a biofilm by utilizing a high speed camera coupled to a piezoelectric actuator mounted on the microscope's objective lens. When using light microscopy, δ is determined as the difference between a reference plane and the mean surface height at time *t*.

Table 1. Reported Biofilm Thickness and Density (adapted from Characklis and Marshall 1990)

Reference	Thickness, δ (μm)	Density (kg/m^3)	Biofilm Type[a]
Kornegay and Andrews, 1967	160-210	66-130	A
Hoehn and Ray, 1973	30-1300	20-105	B
Williamson and McCarty, 1976b	150-580	42-109	C
La Motta, 1976a	0-600	-	A
Rittmann and McCarty, 1978	100	50[b]	A
Rittmann and McCarty, 1980	119-126	5[c]	B
Rittmann and McCarty, 1981	0-125	5[c]	B
Trulear and Characklis, 1982	10-124	65	B
Trulear, 1983	36-47	17-47[d]	D
Bakke, 1986	0-60	27	D

a A-steady state, heterotrophic, mixed population; B-heterotrophic, mixed population; C-steady state, nitrifying; D-steady state; E-steady state, *Psuedomonas aeruginosa*

b calculated assuming biofilm is 80% volatile solids

c calculated assuming biofilm is 50% carbon

d calculated from measured thickness corrected for refractive index of biofilm

2.1.5. Biofilm Density

Biofilm density and porosity vary with cross-sectional depth (Characklis and Marshall 1990; Zhang and Bishop 1994; Zhang and Bishop 2001). Zhang and Bishop (1994) measured a porosity of 84 to 93% in the outermost layers, and a porosity of 58 to 67% in the innermost layers of biofilm grown from a 350-700 mg COD/L feed (the feed was composed of meat extract, yeast extract, peptone, trout chow, and nutrients). Consequently, biofilm becomes denser and the pore volume becomes smaller along the biofilm depth. These researchers used a modification of a microprobe designed by Fu (1993) to measure biofilm density *in situ* and make inferences about density along a biofilm's cross-sectional depth. However, to determine the density of a biofilm sample of thickness δ, the dry biofilm mass on a known substratum area is divided by the measured biofilm thickness. The term can be expressed (6):

$$\rho = \frac{X_f^{"}}{\delta} \tag{6}$$

Where,

ρ = biofilm mass density (ML^{-3})

$X_f^{"}$ = area biofilm concentration(ML^{-2})

Recall a discussion of the Zhang and Bishop's (2001) techniques in section 2.1.2.1. Density varies significantly in biofilms approaching 3000-micron δ, and no research was identified by this investigator pertaining to biofilm thicknesses found in actual aerobic wastewater treatment systems. However, Characklis and Marshall (1990) claims that biofilm density increases with initial fluid shear stress. Biofilm density can be significantly higher in environments containing suspended particulates and inorganic salts with low solubility that become integrated in the biofilm (Characklis and Marshall 1990). The density, ρ, of a biofilm containing organic and inorganic components can be expressed by (16).

$$\rho = \frac{\rho_0 V_0 + \rho_i V_i}{V_0 + V_i} \tag{7}$$

Where,

ρ_o, ρ_i = wet density of organic and inorganic compounds, respectively (ML^{-3})

V_0, V_i = volume of each component (L^3)

The water content in biofilms containing organic and inorganic constituents may be affected since the inorganic fraction immobilizes less water than the inorganic fraction. Trulear (1980)

observed increasing biofilm density with time. This was attributed to EPS accumulation since the cell mass remained constant.

2.2. DISSOLVED SUBSTRATE UTILIZATION BY BIOLOGICAL FILMS

When analyzing the rate of dissolved substrate utilization by biological films, it is convenient to consider the process as three components:

(a) diffusion of substrate from the bulk of the liquid to the wastewater/biofilm interface,

(b) diffusion of the substrate within the porous EPS matrix, and

(c) biochemical reaction, or substrate consumption, by the bacterial cells (La Motta 1976a).

Several researchers have proposed models describing dissolved substrate utilization in biofilms including La Motta (1974), Williamson (1973), Harremoës (1978), and Rittmann and McCarty (1980). A detailed evaluation of the nomenclature and approach taken by each of the aforementioned researchers will be discussed in this section.

In order to establish concentration gradients due to transport and biochemical reaction, an "idealized biofilm" (Rittmann and McCarty 2001) with the following properties is analyzed

(a) the biofilm has a uniform biomass density, ρ (ML^{-3})

(b) the biofilm has a locally uniform thickness, δ (L)

(c) due to mass-transport resistance, the dissolved substrate concentration available at the biofilm surface (S_s) is less than that in the bulk liquid (S_b), unless external mass transfer resistances are eliminated.

Finally, it is necessary to consider two special biofilm cases. Figure 2 is a useful companion to the following discussion. The first case is that of a fully penetrated, or thin, biofilm. Thin biofilms allow for complete substrate penetration, i.e., at $x = 0$, $S = S_s$, and at $x = \delta$, $\frac{dS}{dx} = 0$ (no substrate penetration at the wall). The second case is that of thick biofilms. In thick biofilms, dissolved substrate is depleted within a distance δ_c, which is less than the film thickness δ, i.e., $x = \delta_c$, $\frac{dS}{dx} = 0$ (no mass transport beyond $x = \delta_c$) (La Motta 1976a).

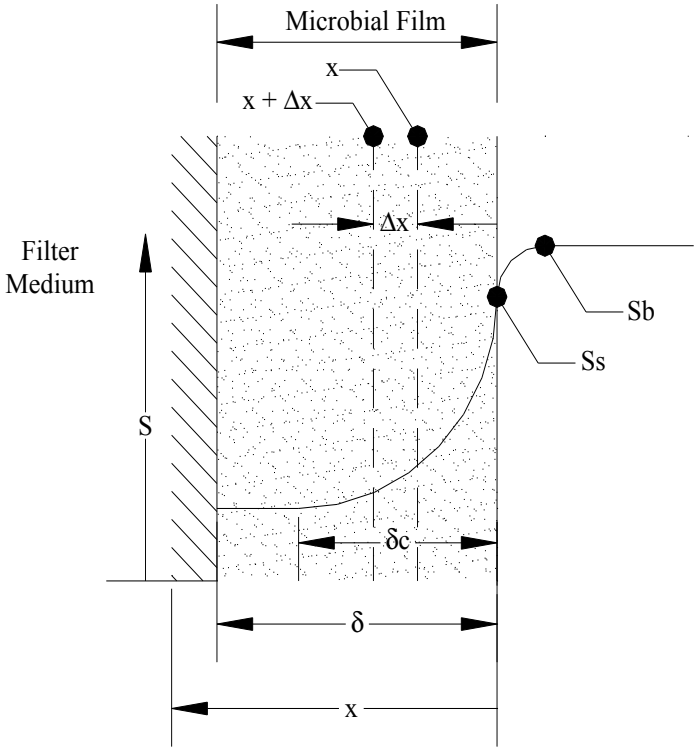

Figure 2. Biofilm Dissolved Substrate Concentration Profile

2.2.1. External Diffusion and its Influence on Reactions at the Biofilm Surface

Several investigations have concluded that mass transfer resistances, external to the biofilm, limit the rate of dissolved substrate removal by biofilm (Tomlinson and Snaddon 1966; Kornegay and Andrews 1967; Maier, et al., 1967; La Motta 1976b; Trulear 1980; Siegrist and Gujer 1985). Physical processes such as mass and energy transfer affect the overall rate of substrate (dissolved and particulate) utilization in biofilm systems. The extent of this influence depends on the characteristics of the system and must be evaluated for rational biofilm reactor design (La Motta 1976b). The discussion contained within this section will describe the external mass transfer process. Although aerobic wastewater treatment systems are operated under a turbulent flow regime, biofilms have a thin laminar sublayer. Williamson and McCarty (1976a) account for the nonplanar nature of biofilms by dividing the laminar sublayer into two portions. The first is the thickness required to fill the nonplanar surface of the biofilm and the second is an external laminar layer. The researchers delineate the layers L_1 and L_2, respectively. The sum of the two thicknesses describes total thickness, L, of the laminar sublayer (i.e., $L = L_1 + L_2$).

Trulear (1980) observed an increase in glucose removal rate with an increased rotational speed in a concentric cylinder reactor, typically referred to as a RotoTorque system. The noteworthy portion of Trulear's (1980) experiments was that the external mass transfer study was carried out on biofilms with 110-micron δ. Trulear and Characklis (1982) also observed an increase in glucose removal rate with an increased rotational speed in a RotoTorque reactor (δ = 112 microns). La Motta (1976b) conducted experiments with biofilm thicknesses ranging from 5 to 8 microns so that the influence of pore diffusion was negligible. Therefore, resistance to external diffusion can be determined with biofilms exceeding La Motta's (1976b) experimental δ

by two orders of magnitude. This is important to the results contained herein because exceedingly thin δ may result in poor bioflocculation.

The transport of dissolved substances across an interface, especially in turbulent flow, can be described by the empirical external mass transfer equation (8).

$$N = k_L \left(S_b - S_s \right) \tag{8}$$

Where,

N = the rate of mass transfer, or flux ($ML^{-2}t^{-1}$)

k_L = mass transfer coefficient (Lt^{-1})

Two extreme conditions can be created based on the magnitude of the mass transfer coefficient (Frank-Kamenetskii 1969). Large values of k_L allow the microorganisms forming the film to receive the maximum concentration available in the bulk liquid (S_b). Here, the rate of dissolved substrate disappearance is dependant upon the rate at which the microorganisms can utilize the substrate. This limiting regime is the only case (assuming internal diffusional resistances have been minimized) in which the intrinsic biofilm kinetics can be measured. Small values of k_L lead to a negligible S_s. In the ladder case, the rate of dissolved substrate disappearance is dependant upon the rate at which substrate diffuses across the laminar sublayer from the bulk of the liquid to the biofilm surface. La Motta (1976b) presented a mass conservation equation (9).

{S consumed in reactor} = {S transported to biofilm surface} = {S consumed by biofilm} (9)

The amount of dissolved substrate consumed in the laboratory reactor can be obtained from a mass balance on the substrate. In the case of a completely mixed reactor, such a balance produces (10):

$$N = \frac{Q}{A}\left(S_i - S_e\right) \tag{10}$$

Where,

N = rate of substrate consumption per unit film area ($ML^{-2}t^{-1}$)

Q = volumetric flow rate of substrate solution (L^3t)

A = total biofilm surface area (L^2)

S_i = concentration of substrate in the influent stream (ML^{-3})

S_e = concentration of substrate in the effluent stream (ML^{-3})

The amount of substrate transported to the film surface is defined by (8). In a completely mixed reactor, the substrate concentration in the effluent stream is equal to the bulk substrate concentration. Therefore, combining of equations (8) and (10) yields (11):

$$k_L = \frac{\frac{Q}{A}\left(S_i - S_e\right)}{S_e - S_s} \tag{11}$$

A detailed description of internal diffusion and reaction in biofilms will be discussed in the next section. However, a brief analysis of the subject is necessary to develop the discussion of resistance to external mass transfer. Frank-Kamenetskii (1969) presented a solution to the problem of diffusion and reaction within a porous catalytic slab (12), which can be utilized to analyze internal diffusion and biochemical reaction in biofilms.

$$N = \left[\frac{2}{n+1} D_{eff} k_v S_s^{(n+1)} \right]^{\frac{1}{2}} \tag{12}$$

Where,

N = rate of reactant disappearance in the slab ($Mt^{-1}L^{-2}$)

n = intrinsic reaction order

D_{eff} = effective diffusivity of reactant through the slab (L^2t^{-1})

k_v = dissolved substrate kinetic constant ($Mt^{-1}L^{-3}$)

La Motta (1976a), Harremoës (1978), and Trulear and Characklis (1982) have observed zero-order removal kinetics in biofilm reactors with glucose (dissolved substrate) being consumed by an undefined multispecies biofilm. Applying zero-order kinetics to (12), the macroscopic, or observed, rate of substrate uptake rate will be given by (13).

$$N = \left[2 D_{eff} k_v S_s \right]^{\frac{1}{2}} \tag{13}$$

Equating (10) and (13) produces the concentration of substrate at the film surface (14).

$$S_s = \frac{\left[\frac{Q}{A} \left(S_i - S_e \right) \right]^2}{2 D_{eff} k_v} \tag{14}$$

Applying this equation to experimental results La Motta (1976b) proposed the following empirical correlation (15).

$$k_L = 5.33 \times 10^{-4} \Omega^{0.657} \quad (15)$$

Where, Ω is the external cylinder speed in a RotoTorque type reactor (rev/s). Therefore, increasing velocity to a sufficiently high value will bring the reactor operation to the kinetic regime.

2.2.2. Internal Diffusion and Reaction of Substrate in a Biological Film

There is an agreement throughout the literature attributing dissolved substrate concentration reduction within a biofilm to molecular diffusion through the porous film matrix and biochemical reaction within the biofilm. Diffusion is usually described by Fick's first law (3). Two methods have been used to describe the rate of dissolved substrate utilization by biological films. Firstly, Williamson and McCarty (1976a) proposed Monod type saturation kinetics (16) to describe the rate of dissolved substrate utilization by biofilms. Subsequently, the researchers developed a "biofilm model" and sought verification empirically (Williamson and McCarty 1976b). Extensive research efforts have been performed (Rittman and McCarty 1978; Rittman and McCarty 1980a; Rittman and McCarty 1980b; Rittman and McCarty 1981) to elaborate upon the dissolved substrate "biofilm model". However, the procedure offers no basis for the recognition of substrates that exhibit different kinetic characteristics.

$$r_{ut} = -\frac{\hat{q} X_f S_f}{K + S_f} \quad (16)$$

Where,

r_{ut} = "biofilm model" rate of substrate utilization

q = maximum specific substrate removal rate ($M_s M_x^{-1} t^{-1}$)

X_f = active biomass density within the biofilm ($M_x L^{-3}$)

S_f = substrate concentration at that point in the film ($M_s L^{-3}$)

K = half-velocity coefficient ($M_s L^{-3}$)

Secondly, empirical observations were used to characterize the rate of glucose, dissolved substrate, utilization by an undefined multispecies biofilm. Such efforts were carried out by La Motta (1976a) and Harremoës (1978). These studies revealed the rate of glucose removal can be accurately described by zero-order kinetics, which disagrees with the general first-order expression describing bioflocculation (2). A preceding description of diffusion and reaction in a porous catalyst (12) has been applied to portray diffusion and reaction of dissolved substrates within a biofilm (La Motta 1976a). Consider the continuity equation (17), neglecting the convective terms:

$$\frac{\partial S_f}{\partial t} = D_{eff} \frac{\partial^2 S_f}{\partial x^2} + r \tag{17}$$

Where,

D_{eff} = effective diffusivity of substrate in the film ($L^2 t^{-1}$)

r = rate of substrate utilization per unit film volume ($M_s L^{-3} t^{-1}$)

x = depth dimension normal to the biofilm surface (L)

This equation (17) assumes microorganisms are uniformly dispersed throughout the biofilm matrix, which implies that the film volume is directly proportional to the film active biomass. Despite recent research indicating that biofilms are heterogeneous structures, the assumption is realistic for thin (fully penetrating), steady state, heterotrophic, mixed population biofilms. An assumption of an "idealized biofilm" is that there is uniform local δ. Therefore, only diffusion normal to the biofilm surface is considered. After a stationary concentration profile is established, steady state conditions can be assumed. Applying zero-order kinetics, the balance can be reduced to (18).

$$\frac{k_v}{D_{eff}} = \frac{d^2 S_f}{dx^2} \tag{18}$$

Integrating (18) with the boundary conditions separating thick and thin biofilms yields the concentration gradient. The rate expression can be determined by recognizing that the reaction rate equals the rate of mass transfer across the film surface (La Motta 1976a). The rate corresponding to thin films, r, (complete substrate penetration) can be described by (19),

$$r = A k_v \delta \tag{19}$$

and the rate corresponding to thick films, r_T, (incomplete substrate penetration) can be described by (20).

$$r_T = A\left(2 D_{eff} k_v\right)^{\frac{1}{2}} S_s^{\frac{1}{2}} \tag{20}$$

The effect of thick films is to mask the intrinsic reaction rate, as indicated by (20) the half-order reaction rate.

2.2.3. Growth Kinetics in a Biofilm System

The studies of Monod (1949) have been used extensively in environmental engineering. The resulting empirical equation (21) relates growth rate to the concentration of dissolved substrate remaining in the system.

$$\mu = \mu_{\max} \frac{S}{K_s + S} \tag{21}$$

Where,

μ = specific growth rate

μ_{max} = asymptote representing maximum attainable growth rate

S = substrate concentration at time t in a batch reactor

K_s = half-velocity coefficient

However, several investigators including Gaudy, et al. (1967), Gaudy and Gaudy (1971), Gaudy, et al. (1971), and Gaudy, et al. (1973) has concluded that the specific growth rate in a batch reactor is controlled by the initial concentration of dissolved substrate. La Motta (1976c) proposed a similar approach for biofilms, where the resulting function applied to a continuous flow reactor was (22).

$$k_v = k_{v_{\max}} \frac{S_i}{K_s + S_i} \tag{22}$$

Here, $k_{v_{\max}}$ is an asymptote representing the maximum attainable intrinsic uptake rate coefficient, and S_i is the influent dissolved substrate concentration.

2.3. A COMPARISON OF BENCH SCALE REACTORS

When analyzing biofilm kinetics, several factors must be considered prior to the selection of the experimental apparatus. The reactor must allow for the differentiation of each step in the biofilm substrate consumption process, namely external diffusion of dissolved and particulate substrate to the wastewater/biofilm interface, determination of a rate expression describing dissolved substrate internal diffusion and biochemical reaction, and determination of a rate expression describing bioflocculation. Ideally, the reactor will:

(a) be constructed of a material with adequate surface energy to promote biofilm growth,

(b) minimize suspended microorganism growth so the observed uptake rate can be attributed to the biofilm,

(c) allow isothermal substrate utilization over a wide range of concentrations under clearly defined residence time conditions and facilitate direct intrinsic rate measurements (Carberry 1964),

(d) control fluid velocity in a sufficiently wide range to evaluate external diffusional resistances (La Motta 1974),

(e) promote relatively uniform biofilm thickness,

(f) provide continuous biofilm growth to avoid undesirable change in environment (which may affect the behavior of the microorganisms), and

(g) be hydrodynamically simple (i.e., completely submerged and mixed) so that the theoretical solution of the combination of mass- and momentum balance equations is possible.

Several laboratory reactors have been used in biofilm studies including inclined plates (Maier, et al., 1967; Maier 1973; Logan 1987). A theoretical solution of diffusion and reaction at the plate surface indicates that a diffusion boundary layer forms. The boundary layer thickness starts at zero on the leading edge of the plate and increases proportionally to the square root of the distance along the plate; the implications of this variation are a change in the reaction regime from one end of the plate to the other. Chambré and Acrivos (1956) demonstrated that at the leading edge the reaction is chemically controlled, and at the latter end the reaction is controlled by mass transport. The intermediate portion is influenced by mixed chemical reaction and mass transport. While the flat plate is an attractive alternative for modeling trickling filters constructed of plastic modules, the apparatus complicates analysis when developing biofilm kinetic models. Recent research efforts have utilized the radial flow reactor, RotoTorque reactor, tubular reactor, and submerged rotating disc reactor, and this section will discuss each of these reactors.

2.3.1. The Radial Flow Reactor

The radial flow reactor, as described by Fowler and McCay (1980), contains two parallel discs separated by a narrow gap. Typically, there is a 500-micron gap. The test liquid is pumped in at the center of one of the discs and flows out radially between the discs to a collection manifold (Characklis and Marshall 1990). As the cross-sectional area available for flow increases with increasing radius, the linear velocity and fluid shear stress decrease. Therefore,

high shear stress occurs near the inlet and lowers near the outlet. There is tendency to plug flow in the gap, which may influence the spatial colonization pattern on the substratum. Detached cells have the opportunity to colonize the substratum downstream, which affect the desirable characteristics (*e*, *f*, and *g*) of a biofilm reactor. Deficiencies in the calculation of shear stress within this type of reactor may have influenced earlier interpretation of data (Fryer, et al., 1984).

2.3.2. The RotoTorque

The RotoTorque (IPA, Montana State University), or rotating annular reactor, is a popular laboratory system for monitoring biofilm development and reaction kinetics because of its sensitivity to changes in fluid frictional resistances. This type of reactor satisfies all of the desirable characteristics (*a-f*) of a biofilm reactor. The reactor consists of two concentric cylinders, a stationary outer cylinder and a rotating inner cylinder. However, La Motta (1974) chose to rotate the external cylinder in an effort to avoid the formation of Taylor vortices. As for any biofilm reactor, removable slides are an integral part of the laboratory process. In the case of the rotating annular reactor, removable slides are placed on the inside wall of the outer cylinder to permit biofilm sampling. Subsequently, the samples may be analyzed for thickness, mass, and for biofilm chemical and microbial composition. Turbulence is induced to a degree that promotes complete mixing. A complete description and theoretical analysis of the rotating annular reactor are presented elsewhere (Kornegay 1969, La Motta 1974, Characklis and Marshall 1990).

2.3.3. The Submerged Rotating Disc Reactor: Theory and Analysis

The submerged rotating disc biofilm reactor, the RDBR, was used in this study. The apparatus is an attractive alternative to evaluate the kinetics of particulate and dissolved substrate disappearance in biofilms. The reactor was initially used by Gulevich (1967) to analyze the role of diffusion in wastewater treatment processes. The reactor has also been used in the chemical engineering literature to study the kinetics of heterogeneous catalysis and electrochemical reaction (La Motta 1974). According to several investigators (Frank-Kamenetskii 1969; Levich 1962; Satterfield 1968) the equations describing the hydrodynamics and mass transfer under laminar conditions are the simplest. The three-dimensional flow pattern causes the mass transfer coefficient to be the same at all points on the surface, and the surface is uniformly accessible. If the reactor is constructed with sufficiently small gaps between the rotating disc and the chamber walls suspended growth can be minimized, and a completely mixed flow regime is easily attained. La Motta, et al., (1982) successfully applied a RDBR to evaluate the effect of synthetic polymers on biofilm formation. For the purpose of this investigation, it was necessary to evaluate the effect of the ratio of biofilm surface area to liquid volumetric flow rate on the concentration of substrate (dissolved or particulate) and inorganic particles remaining in the effluent stream. The RDBR allowed for the construction of multiple chambers that could be operated in parallel with variable liquid volumetric flow rates, while maintaining identical influent substance concentrations. A detailed presentation of the experimental apparatus is presented in later sections. However, material balances appropriate to the reactor shall be presented here.

The RDBR is a steady-state mixed flow reactor. The substance concentration is uniform throughout and the following general mass balance is applicable:

input = output + reaction

In the RDBR, the influent and effluent liquid volumetric flow rate, Q, are equal due to continuity. The influent dissolved substrate concentration, S_i, (C_i in the case of particles) is reduced by a reaction of rate, r (kg/s.m^3 of film for dissolved substrates and kg/s.m^2 of film for particles). The concentration of the substance remaining in the effluent stream is denoted S_e (C_e in the case of particles). Applying zero-order kinetics to the general form of the RDBR mass balance (recognizing that dissolved substrate consumption is dependent upon δ when working with thin biofilms). The mass balance on such a reactor yields (23) for dissolved substrate removal in thin biofilm systems.

$$S_e = S_i - k_v \delta \left(\frac{A}{Q} \right) \tag{23}$$

Recall the equation describing bioflocculation (2) and the assertion that bioflocculation is a surface phenomenon, independent of film thickness. Appling this term to the general mass balance equation describing the RDBR yields an expression that describes the disappearance of particles by bioflocculation (24).

$$C_e = \frac{C_i + k_p\left(\frac{A}{Q}\right)a}{1 + k_p\left(\frac{A}{Q}\right)} \tag{24}$$

Here, C_i is the particle concentration suspended in the influent stream (mg/L).

2.4. EXISTING SUBSTRATE UTILIZATION MODELS

Biofilm models have commonly been used as simulation tools in engineering applications and as research tools to identify and fill gaps in our knowledge of biofilm process (Noguera, et al., 1999). Generally, engineering models incorporate simplifying assumptions to make them practical. Biofilm models are perceived as complicated mathematical entities. Typically, simplifications and assumptions used in one-dimensional models are not supported by experimental observation. An International Association on Water Quality (IAWQ) specialist meeting on biofilm modeling (Lake Bluff, IL, USA, 09-11-98) identified specific areas of concern, including but not limited to, the fate of particulate substrates. Since this time, efforts have been made to describe the role of EPS production (Boltz and La Motta, submitted for publication 2005) on the removal of PCOD in fixed film processes. However, research to date has attributed the mechanism of PCOD removal to hydrolysis. These projects further complicate the biofilm analytical process and falsely describe the actual PCOD removal mechanism, bioflocculation.

3. RESISTANCE TO EXTERNAL MASS TRANSFER OF MACROCOLLOIDAL PARTICULATES IN A BIOLOGICAL FILM REACTOR

The environmental engineering literature has described operational definitions for size categories of contaminants as: dissolved (< 0.001 μm), colloidal (0.001 – 1 μm), supracolloidal (1 – 100 μm), and settleable (> 100 μm). To describe size ranges in biological systems more specifically, a subset of supracolloidal particles, macrocolloidal particles, has been used to describe particles ranging in size from 1 to 10 μm (Levine, et al., 1991). Colloids can accumulate hydrophobic organic trace compounds and heavy metals onto their surface and work as carriers of these pollutants (Schmid, et al., 2003). Bouwer (1987) presented theoretical work describing the impact of particle size on biological film treatment process efficiency. His investigation concluded that removal of particles larger than 10 μm is controlled by sedimentation and filtration, and that diffusion describes the transport of submicron particulates. However, based on theoretical considerations, macrocolloidal particles are the most difficult size range to remove in biofilm reactors (Levine, et al., 1991). Since a small fraction of the TCOD in raw sewage and primary effluents is dissolved and macrocolloidal particulates are the most difficult constituent of PCOD to remove in biofilm wastewater treatment processes, efficient removal of macrocolloids will improve system performance.

Elucidation of bioflocculation as a physical-chemical, surface phenomenon that is independent of biofilm thickness implies that particles are detained on the biofilm surface prior to removal. Therefore, additional active biofilm sites are generated by two mechanisms: organic particle hydrolysis and periodic sloughing whereby flocculated particulates are carried by

detached biofilm and removed in secondary settling. It is not very well understood which proportion of the flocculated particulates are removed by hydrolysis and sloughing. Although it is generally accepted that physical-chemical processes, such as bioflocculation, have a substantially greater rate than purely chemical processes, such as hydrolysis, there is no substantiation of this claim. Therefore, inorganic particulates (Min-U-Sil 10) were used in this investigation to avoid disappearance by hydrolysis.

There is a well-known laminar liquid sublayer blanketing biofilms. Particles (inorganic or organic) in turbulent flow are transported to within a short distance of the biofilm surface by eddy diffusion and are propelled into the laminar sublayer by momentum acquired from dynamic forces. Macrocolloidal particulates are transported through the laminar layer by turbulent diffusion. La Motta (1976b) provided the theoretical and experimental framework for the external mass transfer of glucose in a RotoTorque type biofilm reactor. His study concluded that the laminar sublayer could be eliminated by external cylinder rotational speeds exceeding 100 rpm. This is a higher velocity than can be expected in trickling filters, a typical fixed film biological reactor (Särner 1986). Therefore, the removal rate is most likely affected by external diffusional resistances. However, this investigator could not locate any literature on the resistance to external mass transfer of macrocolloidal particulates in a biofilm reactor.

3.1. EXPERIMENTAL DESIGN AND SETUP

The RDBR was used in this investigation to evaluate the resistance to external mass transfer of macrocolloidal particles in a biological film reactor. The reactor is similar to the one

used by Gulevich (1967) to analyze the role of diffusion in wastewater treatment processes and is schematically represented in Figure 3.

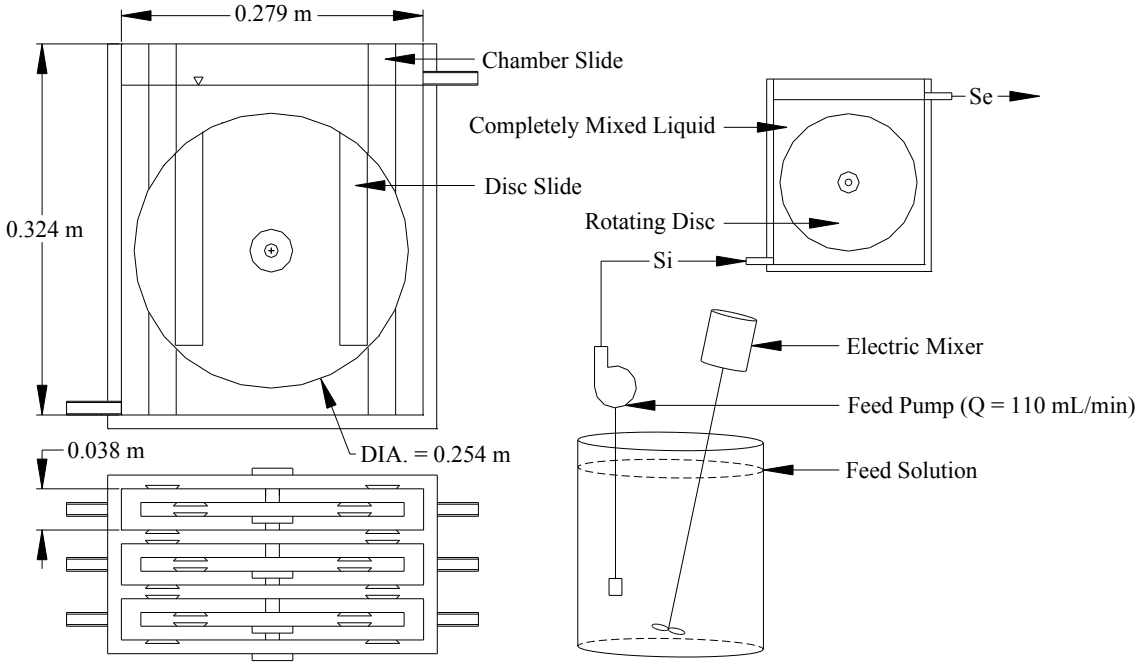

Figure 3. RDBR Schematic

The reactor was constructed with sufficiently small gaps between the rotating disc and the chamber walls to avoid suspended bacterial growth, and a completely mixed flow regime was easily attained, as demonstrated by a tracer test whose results will be presented in a later section. In order to evaluate the effect of various ratios of total film area to flow rate, *A/Q*, the RDBR was constructed with three chambers that could be operated in parallel with variable liquid volumetric flow rates, while maintaining an identical influent particle concentration. Photographs of the experimental apparatus and setup can be seen in Appendix A.

The volume available for solution inside each of the reactor chambers is 2.8 L (volume of the chamber less the volume displaced by the disc, disc support, and shaft), and the water depth is 0.3 m. The RDBR is constructed of acrylic, and each chamber has a width of 0.038 m, length of 0.279 m, and height of 0.324 m. A 0.254-m diameter, 0.013-m thick disc that is supported by a 0.051-m diameter, 0.013-m thick plate, is rotated around a 0.013-m diameter stainless steel shaft. A variable speed controlled motor drives the shaft. The area within the chamber available for biofilm growth is 0.313 m^2 (internal chamber walls, disc, disc support, and shaft). The reactor was seeded with wastewater containing heterotrophic bacteria from an aeration basin at the Marrero Wastewater Treatment Plant, Marrero, LA, and the reactor was continuously fed a synthetic wastewater solution with DCOD and TSS.

The composition of the feed was the following: methanol, 20 mg COD/L; Min-U-Sil 10, 20 mg TSS/L; NH_4Cl, 1.3 mg/L; $NaHCO_3$, 62.6 mg/L; K_2HPO_4, 13.8 mg/L; KH_2PO_4, 5.3 mg/L; $MgSO_4.7H_2O$, 13.8 mg/L; $FeCl_2.4H_2O$, 0.2 mg/L; $CaCl_2.2H_2O$, 18.4 mg/L; and $Na_2HPO_4.7H_2O$, 20.7 mg/L. Methanol served as the electron donor and DO as the electron acceptor. A pH of 7.2 was maintained and the DO concentration within the reactor was kept between 2-4 mg/L. A constant temperature ranging between 21°C and 23°C was maintained in the bulk of the liquid. Biofilm thickness was measured (as described by La Motta, 1976a) by light microscopy on removable slides located on the interior of the chamber walls and on the discs. Min-U-Sil 10 was used as the inorganic particles. Here, by volume, 95% of the particles were less than a 11.1-micron equivalent spherical diameter, and the median particle diameter was 4.1 microns. Only 5% of the Min-U-Sil particles were less than 0.6 microns. Particle size distributions were determined using a Coulter particle characterization machine (Model LS200, Ser. No.

AC26661). Prior to sample analysis, the particle samples were submersed in an ultrasonic bath for 30 seconds. While the strict definition of macrocolloidal particulates describes sizes ranging from 1–10 microns, particles considered in this investigation were collected on a 0.45-μm pore size filter.

Influent and effluent 600-mL samples were collected for various rotational speeds and allowed to settle for 15 minutes to remove any detached biofilm or loose polymers. A range of rotational speeds from 14-250 rev/min was analyzed in this investigation. Table 2 lists the rotational speeds along with the test results. From the samples, 300 mL of supernatant was extracted and analyzed for TSS. The TSS test was performed according to Method 2540 D of the *Standard Methods for the Examination of Water and Wastewater* (APHA 1998). After filtration, the solids retained on a 0.45-μm pore size filter paper were dried at 103 $\pm$ 1 °C. A control experiment (20 mg/L Min-U-Sil 10) was conducted to insure that none of the sample would be lost to settling. The 20-mg/L control reported perfectly. To avoid sedimentation, the feed solution was continuously mixed and pumped by a diaphragm pump at a 110-cm^3/min flow rate. For each revolutional speed analyzed, the reactor was operated during 4 theoretical detention times to obtain hydrodynamic steady state conditions prior to sample extraction. Three samples were extracted during a single sampling event and the average of the analytical results are reported as an observation.

3.2. THE TRACER TEST

A tracer test was performed to determine the hydrodynamic properties of the RDBR during experimentation. The tracer test was conducted with a flow rate and disc rotational speed

of 110 cm^3/min per chamber and 120±1 rpm, respectively. Sodium chloride (NaCl), table salt, was used as the tracer material.

A step input tracer test was conducted. The tracer solution was mixed with dissolved substrate, methanol, in the feed stock. The feed stock was prepared with 1472 g NaCl per 55 gal of deionized (DI) water. However, for a period of 12 hours preceding the test a stock solution of 736 g NaCl per 55 gal DI water was fed to the reactor. The saturation was necessary to prevent NaCl absorption by the biological film during the test. A chemical feed pump introduced the solution at a continuous and constant flow rate directly preceding the RDBR influent. A salinity meter, YSI model 85, was used to record the tracer concentration in the RDBR.

Table 2. External Mass Transfer Data

Rotational Speed (rpm)	C_i (mg/L)	C_e (mg/L)	Conversion (unitless)	Average δ (μm)
14.4	20.0	17.9	0.105	51
23.1	20.0	16.7	0.165	51
37.7	20.0	15.0	0.250	51
55.1	20.0	13.3	0.335	51
68.9	20.0	14.7	0.265	51
85.5	20.0	12.7	0.365	51
97.0	20.0	12.3	0.385	51
109.9	20.0	11.7	0.415	51
120.0	20.0	10.7	0.465	51
131.1	20.0	11.0	0.450	51
142.6	20.0	10.7	0.465	51
168.4	20.0	11.0	0.450	51
190.0	20.0	11.0	0.450	51
201.3	20.0	10.7	0.465	51
220.4	20.0	10.7	0.465	51
249.1	20.0	11.0	0.450	51

Note:
1. Each reactor chamber has 3130.70 cm^2 available for biofilm growth (including interior walls, disc, disc edge, disc support, and disc support edge)
2. Q = 110 cc/min

A cumulative residence time distribution (F curve), defined by (25), was observed for the step input tracer test performed on the RDBR.

$$F = \left(\frac{C}{C_o} \right)_{step} \tag{25}$$

Where, C is the concentration of the tracer in the reactor at time t (ppt) and C_0 is the initial concentration of the tracer in the reactor (ppt). Differentiation of the cumulative residence time distribution function yields the E function, or the residence time distribution function. To facilitate differentiation of the F curve, a best-fit polynomial was adjusted to the experimental data. Differentiation of this polynomial yields (26).

$$E(t) = 3at^2 + 2bt + c \tag{26}$$

The values of the constants in the best-fit function are; a = 0.000002, b = -0.00002, c = 0.0004, d = 0.0344, and t is the time in minutes corresponding to the concentration measurement. The nonlinear regression analysis produced a coefficient of multiple determination (R^2) equal to 0.999. Figure 4 illustrates the observed tracer response curve. The volume available for water inside each chamber is 2.8 L. Therefore, the theoretical detention time is 25 minutes. The detention time determined from the tracer test conducted on one of the chambers is 25 minutes. This demonstrates that NaCl is an effective tracer. The increased density of the solution due to the NaCl does not result in density currents. The tracer test provides sufficient proof that the RDBR is operating under a completely mixed condition, which is apparent from the small

deviation from the ideal complete-mix reactor F curve, which is also depicted in Figure 4. The response for a continuous step input of tracer which is instantaneously mixed, i.e. ideally mixed, can be described by (27).

$$C = C_0\left(1 - e^{-\theta}\right) \tag{27}$$

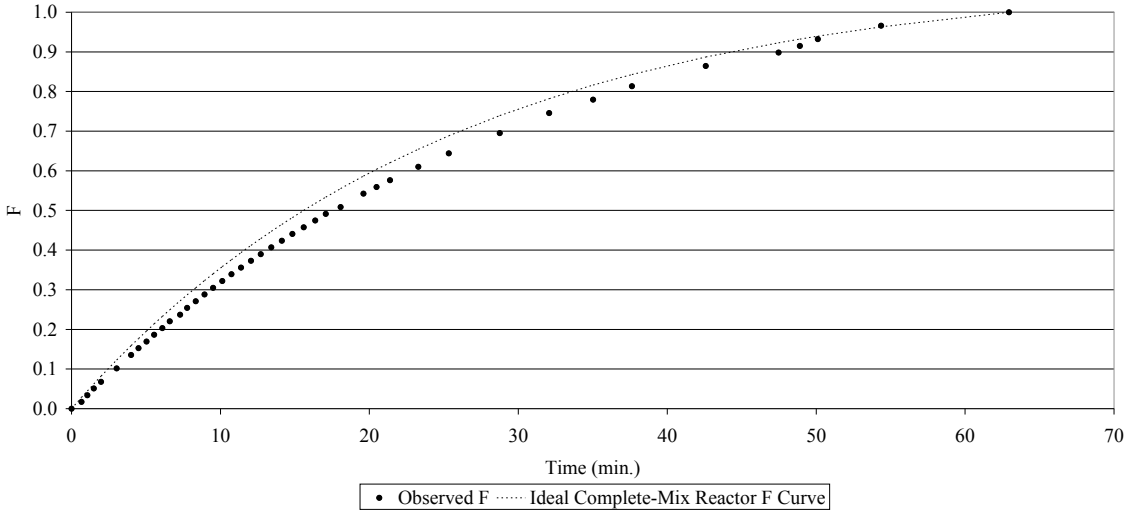

Figure 4. F Curve for RDBR Step Input Tracer Test

Where, θ is the normalized detention time (unitless). The RDBR reaches hydrodynamic steady-state conditions after approximately 63 minutes when Q = 110 cm^3/min. The tracer test worksheet can be reviewed in Appendix B.

3.3. CONFIRMATION OF STEADY STATE

Strictly speaking, the criteria for the steady state conditions in an ideal biofilm reactor are evenly distributed biofilm with constant thickness, pH, COD remaining in the effluent, DO, and negligible suspended growth. Realistically, these variables fluctuate slightly. However, in the

laboratory reactor it was possible to obtain a quasi-steady state with respect to effluent particle concentration during experimentation. This is illustrated in Figure 5, and the test data is listed in Table 3.

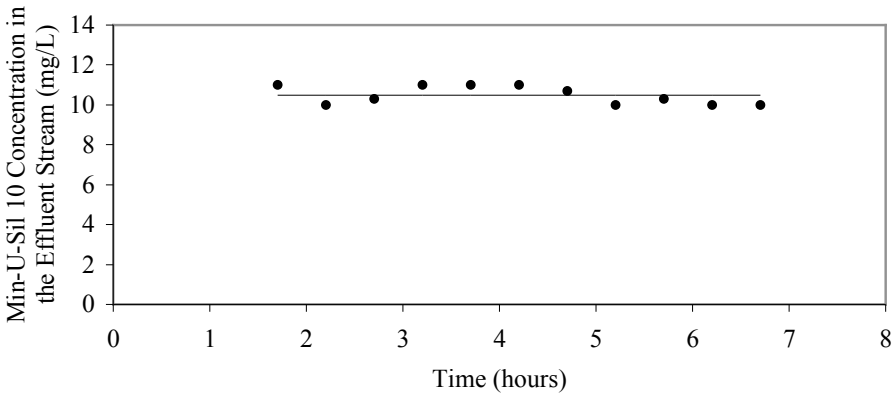

Figure 5. Effluent Min-U-Sil 10 Concentration as a Function of Time

Table 3. Steady State Assumption Confirmation

Rotational Speed (rpm)	Time (mins.)	TSS-C_i (mg/L)	TSS-C_e (mg/L)	Average δ (μm)
120.0	102.0	20.0	11.0	51
120.0	132.0	20.0	10.0	51
120.0	162.0	20.0	10.3	51
120.0	192.0	20.0	11.0	51
120.0	222.0	20.0	11.0	51
120.0	252.0	20.0	11.0	51
120.0	282.0	20.0	10.7	51
120.0	312.0	20.0	10.0	51
120.0	342.0	20.0	10.3	51
120.0	372.0	20.0	10.0	51
120.0	402.0	20.0	10.0	51

3.4. RESULTS AND DISCUSSION

Min-U-Sil 10, inorganic macrocolloidal particles, is affected by laminar sublayer diffusivity. Figure 6 illustrates the effect of disc rotational speed on the removal of the inorganic particles in the RDBR.

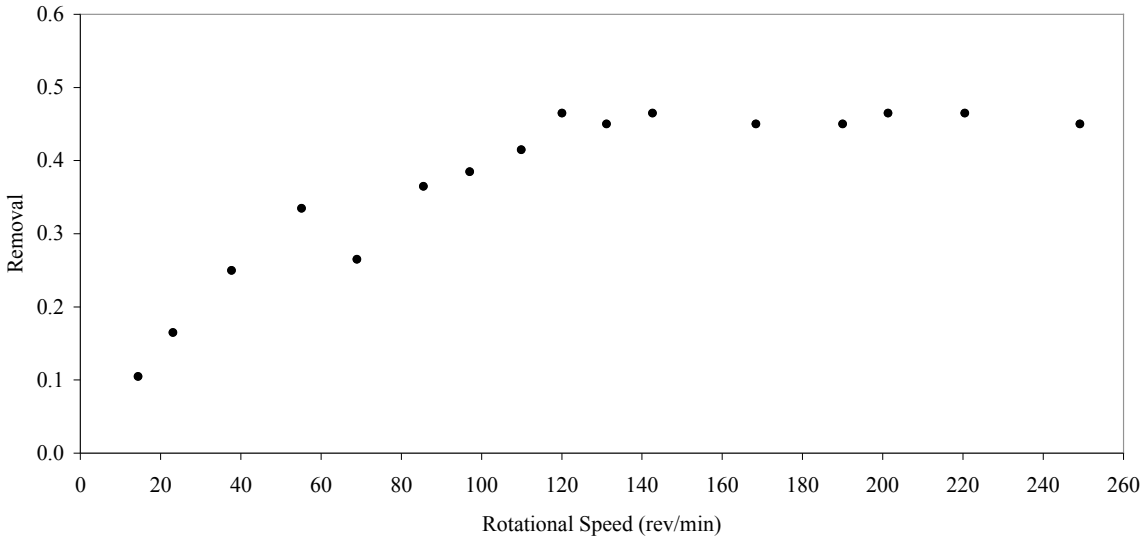

Figure 6. Min-U-Sil 10 Removal vs. Rotational Speed

La Motta (1976b) conducted experiments with biofilm thicknesses ranging from 5 to 8 microns so that the influence of pore diffusion was negligible. Trulear (1980) observed an increase in glucose removal rate with an increased rotational speed in a concentric cylinder reactor with 110-micron thick biofilms. Trulear and Characklis (1982) also observed an increase in glucose removal rate with an increased rotational speed in a concentric cylinder reactor with 112-micron thick biofilms. Therefore, biofilm accumulation is negligible and resistance to external diffusion can be determined with biofilms exceeding La Motta's (1976b) experimental biofilm thickness by two orders of magnitude. This is important to the results contained herein because

exceedingly thin biofilms may result in poor bioflocculation. Therefore, the experiments were run with biofilms 50-53 μm thick. The removal became insensitive when the rotational speed exceeded 100 rev/min. Thus, indicating that the kinetic regime of bioflocculation had been attained. At, or in excess of, this rotational speed the turbulence is sufficient to reveal the intrinsic rate of bioflocculation.

4. KINETICS OF PARTICULATE AND DISSOLVED SUBSTRATE REMOVAL BY AEROBIC FIXED-FILMS

Several mechanistic models have been developed to describe the kinetics of dissolved substrate utilization by biological films. These models, however, have limited application when the primary constituent of COD in domestic wastewaters is organic particulates. Recent research has demonstrated that frequently a small fraction of the TCOD in raw sewage and primary effluents is dissolved, as depicted in Figure 1. Therefore, there is a need to develop a kinetic expression capable of describing the removal of PCOD from wastewaters by biological film reactors. Independent experiments were conducted on dissolved and particulate substrates in order to demonstrate that they can be separated by their reaction kinetics. For each substrate analyzed, removal at four volumetric flow rates (30, 44, 60, and 110 cm^3/min) was studied. For each experiment, the RDBR was operated during four theoretical detention times to obtain hydrodynamic steady state conditions. Dividing the external biofilm area by each of the volumetric flow rates allowed for the description of the substance remaining in the effluent stream as a function of A/Q. Furthermore, EPS were extracted for each substance studied to make inferences on their role in the bioflocculation process.

4.1. EXPERIMENTAL SETUP AND DESIGN

The RDBR was used in this investigation to evaluate the effect of various ratios of total film area to flow rate, A/Q, on the concentration of dissolved and particulate substrates remaining in the effluent stream. The RDBR was constructed with three chambers that could be operated in parallel with variable liquid volumetric flow rates, while maintaining an identical influent substrate concentration. The volume available for solution inside each of the reactor chambers is

2.8 L (volume of the chamber less the volume displaced by the disc, disc support, and shaft), and the water depth is 0.3 m. The RDBR is constructed of acrylic, and each chamber has a width of 0.038 m, length of 0.279 m, and height of 0.324 m. A 0.254-m diameter, 0.013-m thick disc that is supported by a 0.051-m diameter, 0.013-m thick plate, is rotated around a 0.013-m diameter stainless steel shaft. A variable speed controlled motor drives the shaft.

La Motta (1976b) demonstrated that resistance to external mass transfer of the dissolved substrate glucose can be eliminated at rotational speeds in excess of 100 rpm. The preceding section presents evidence that inorganic macrocolloidal particulates are also subject to external diffussional resistances. During these experiments, the discs were rotated at 120 rpm to eliminate resistance to external mass transfer and observe intrinsic reaction kinetics. The area within the chamber available for biofilm growth is 0.313 m^2 (internal chamber walls, disc, disc support, and shaft). The reactor was seeded with wastewater containing heterotrophic bacteria from an aeration basin at the Marrero Wastewater Treatment Plant, Marrero, LA, and the reactor was continuously fed a synthetic wastewater solution with DCOD or PCOD. The composition of the feed was methanol (dissolved substrate), or native corn starch (particulate substrate), variable concentrations; NH_4Cl, 1.3 mg/L; $NaHCO_3$, 62.6 mg/L; K_2HPO_4, 13.8 mg/L; KH_2PO_4, 5.3 mg/L; $MgSO_4.7H_2O$, 13.8 mg/L; $FeCl_2.4H_2O$, 0.2 mg/L; $CaCl_2.2H_2O$, 18.4 mg/L; and $Na_2HPO_4.7H_2O$, 20.7 mg/L. Methanol, or corn starch, served as the electron donor and DO as the electron acceptor. By volume, 95% of the native corn starch particles were less than a 23.9-micron equivalent spherical diameter, and the median particle diameter was 14.1 microns. Only 5% of the native corn starch particles were less than 1.4 microns. Particle size distributions were determined using a Coulter particle characterization machine (Model LS200, Ser. No.

AC26661). Prior to sample analysis, the particle samples were submersed in an ultrasonic bath for 30 seconds. A pH of 7.2 was maintained and the DO concentration within the reactor was kept between 2-4 mg/L. A constant temperature ranging between 21°C and 23°C was maintained in the bulk of the liquid. Biofilm thickness was measured (as described by La Motta 1976a) by light microscopy on removable slides located on the interior of the chamber walls and on the discs. Each chamber housed four slides on the interior chamber walls and four on the disc. Two measurements were performed on each slide and the average biofilm thickness was reported. Strictly speaking, the criteria for the steady state conditions in an ideal biofilm reactor should include the following conditions: evenly distributed biofilm with constant thickness, pH, COD remaining in the effluent, DO, and negligible suspended growth. Realistically, these variables fluctuate slightly. However, in the laboratory reactor it was possible to obtain a quasi-steady state with respect to effluent substrate, particulate and dissolved, concentration during experimentation. For each substance analyzed, three samples were extracted during a single sampling event and the average of the analytical results are reported as an observation.

During the analysis of methanol (dissolved substrate) removal, 100-mL influent and effluent samples were collected and filtered through a washed 0.45-µm pore size filter paper. Filtration was applied to remove any loose polymers or sloughed biofilm. The filtered samples were analyzed for total organic carbon (TOC) (Tekmar Dohrmann Apollo 9000 TOC combustion analyzer). The results are reported as dissolved organic carbon (DOC).

During native corn starch (organic particulates) analysis, 100-mL influent and effluent samples were collected and analyzed. Organic carbon analyses were performed directly (without

previous filtration) despite the fact that polymeric substances and sloughed biofilm may cause interference. Filtration, however, removes part of the substrate and, therefore, is not possible. The results are reported as particulate organic carbon (POC).

Finally, when extracting EPS from biofilm samples, the steaming method described by Zhang, et al., (1999) was applied. During this procedure, a combined sample, succeeding a washing and stripping step, is steamed at 80ºC and 1 bar of pressure for 10 min and then centrifuged while still hot at 8000*g* for 10 min. In this study, the TOC of the supernatant is reported as the total exocellular polymeric carbon (TEPC). A detailed explanation of the procedure is:

1. Washing: Mix 1 g of biofilm with 25 mL of DI water and gently shake the mixture. Centrifuge the sample for 10 minutes at 3500 rpm. Decant the liquid.
2. Stripping: Add 25 mL of DI water to the biofilm pellets and blend the mixture in a high speed, vortex blender for 1 min. Combine 25 mL from the washing step with 25 mL from the stripping step for extraction.
3. Extraction: Steaming extraction requires that 50 mL of the combined sample is autoclaved at 80ºC and 1 bar for 10 minutes. Normal autoclaving forces cell lyses and may lead to measurement of the cells' internal carbon. Centrifuge the hot sample for 10 minutes at 5500 rpm.
4. Collection: Filter the supernatant from the extraction method through a washed 0.45-µm filter, the TOC of the supernatant is reported as the TEPC.

4.2. CONFIRMATION STUDIES ON DISSOLVED SUBSTRATE REMOVAL

The effect of several different influent methanol concentrations (S_i = 4.41, 9.91, 17.93, 60.00, and 128.13 mg DOC/L) on removal rates was investigated. In each case, the concentration of methanol remaining in the effluent stream as a function of A/Q adjusts well to (23). Table 5 lists the coefficient of determination, R^2, best-fit dissolved substrate rate coefficient, k_v, (obtained form a linear regression analysis) and experimental biofilm thickness, δ, associated with each of the aforementioned influent methanol concentrations. Figure 7 is a representative graph that illustrates the application of (23) to the observed concentration of methanol remaining in the effluent stream. Here, the influent methanol concentration is 4.41 mg DOC/L. The remaining graphs can be seen in Appendix C.

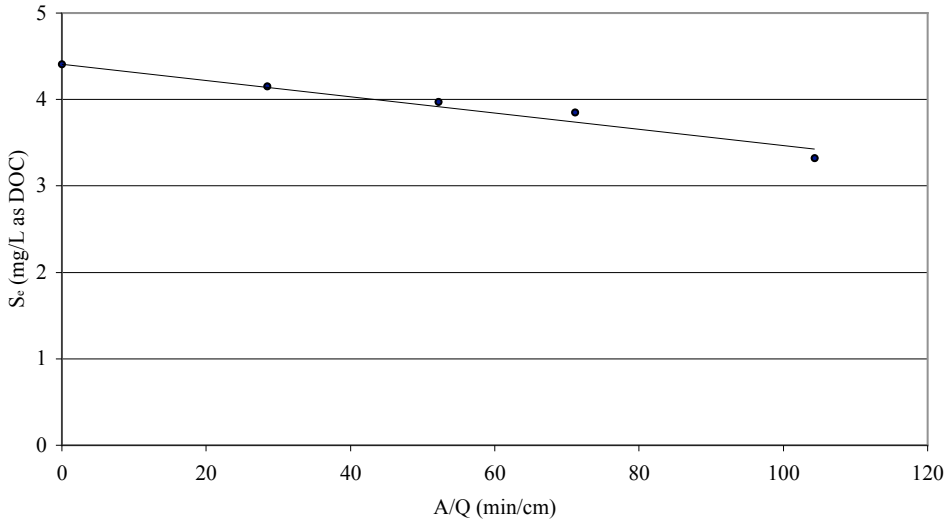

Figure 7. Effluent Methanol Concentration vs. A/Q, S_i = 4.41 mg DOC/L, δ = 40 μm

Evidence will be presented that demonstrates the experiments were conducted within the intrinsic, or kinetic, regime. Therefore, the actual rate of methanol utilization is described.

Table 4. Methanol Experimental Data Linear Regression Analysis

S_i (mg DOC/L)	k_v (mg/min.cm^3)	δ (μm)	R^2
4.41	2.36	40	0.9601
9.91	7.89	38	0.9846
17.93	9.19	41	0.9771
60.00	15.20	41	0.9563
128.13	16.88	44	0.9827

The intrinsic methanol uptake rate coefficient, k_v, is a function of the influent methanol concentration and is well described by (22). Application of the aforementioned saturation function (22) is illustrated in Figure 8. Here, the R^2 is 0.9753, and the best-fit coefficients, $k_{v\text{-}max}$ and K_s, are 19.65 and 19.04, respectively.

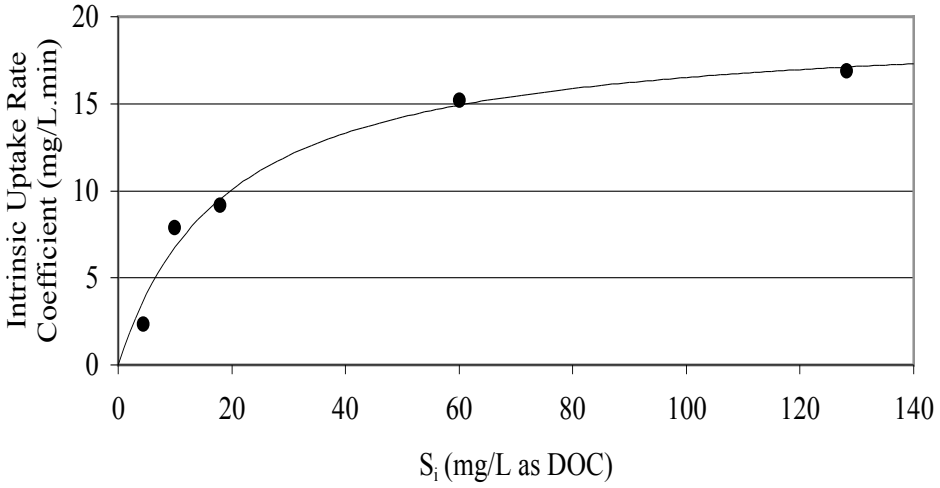

Figure 8. Methanol Uptake Rate Coefficient vs. Influent Methanol Concentration

An alternate procedure used to check the applicability of zero-order kinetics to DOC consumption is to test the effect of biofilm thickness on intrinsic methanol uptake rate in the RDBR. Figure 9 illustrates the said relationship.

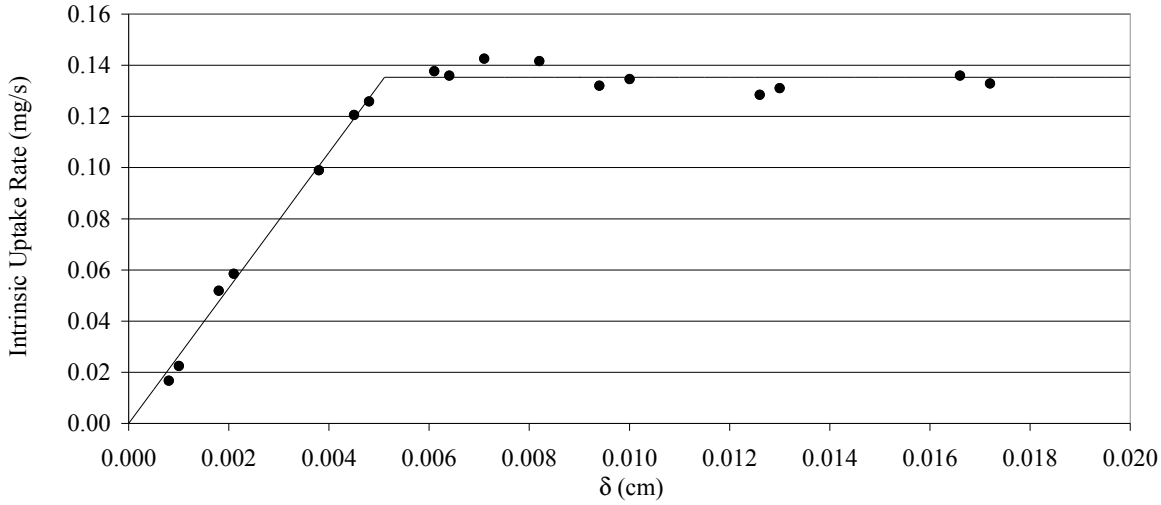

Figure 9. Intrinsic Methanol Uptake Rate vs. Biofilm Thickness

Applying zero-order reaction kinetics, the increasing rate is described by (19). The coefficient of determination, R^2, for the application of (19) to the increasing portion is 0.9942. A linear regression analysis produced a dissolved substrate rate coefficient, k_v, of 8.459 x 10^{-3} mg/s.cm^3 of biofilm. After a biofilm thickness approximately equal to 55 microns has been obtained, the intrinsic rate of methanol uptake is unaffected by biofilm thickness. An F-test on the remaining points indicated independence at the 95% confidence level. During this experiment, the RDBR was operated at 120 rpm with a flow rate, Q, of 44 cm^3/min, and an influent methanol concentration, S_i, of 10.27 mg DOC/L. Raw data can be viewed in Appendix D.

4.3. KINETICS OF ORGANIC PARTICLE REMOVAL IN THE RDBR

Similar to the methanol experiments, the effect of several different influent native corn starch concentrations (C_i = 21.43, 48.88, 101.32, 196.00, and 401.79 mg POC/L) was investigated. In each case, the concentration of native corn starch remaining in the effluent stream as a function of A/Q adjusts well to (24). Table 5 lists the coefficient of determination, R^2, best-fit particulate substrate rate coefficient, k_p, best-fit asymptote, a, (obtained form a nonlinear regression analysis) and experimental biofilm thickness, δ, associated with each of the aforementioned influent native corn starch concentrations. Figure 10 is a representative graph that illustrates the application of (24) to the observed concentration of native corn starch remaining in the effluent stream. Here, the influent methanol concentration is 21.43 mg POC/L. The remaining graphs can be seen in Appendix E.

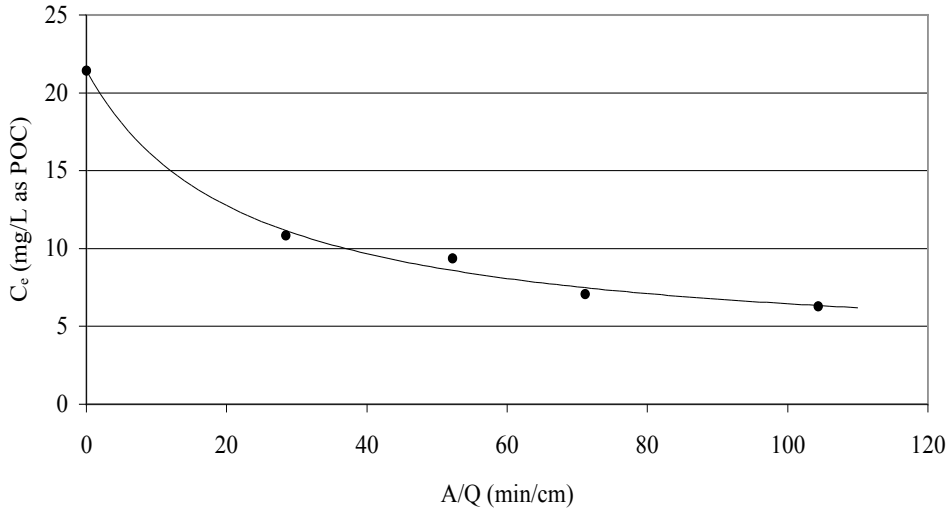

Figure 10. Effluent Corn Starch Concentration vs. A/Q when C_i = 21.43 mg POC/L

Although it is proposed that bioflocculation is a physical process occurring at the biofilm surface, when conducting experiments designed to measure the kinetics of simultaneous POC and DOC removal it is necessary to operate in the kinetic regime to eliminate the effect of pore diffusion on DOC consumption. Therefore, the experiments designed to evaluate the kinetics of particle removal were conducted in the dissolved substrate kinetic regime.

Table 5. Corn Starch Nonlinear Regression Analysis Parameters

C_i (mg/L as POC)	k_p (mg/min.cm^2)	a (mg POC/L)	δ (μm)	R^2
21.43	0.044930	3.12	54	0.9943
48.88	0.014590	3.00	55	0.9957
101.32	0.008575	10.67	55	0.9834
196.00	0.008674	123.10	43	0.9433
401.79	0.005311	265.90	57	0.9822

A further demonstration that biofilm thickness does not affect the rate of bioflocculation, i.e., bioflocculation is a physical process that occurs at the biofilm surface. An experiment was implemented that varied biofilm thickness while the influent native corn starch concentration remained constant. Appendix F contains the experiment's data, and Figure 11 illustrates this relationship. An F-test indicated the independence is accepted with 95% confidence.

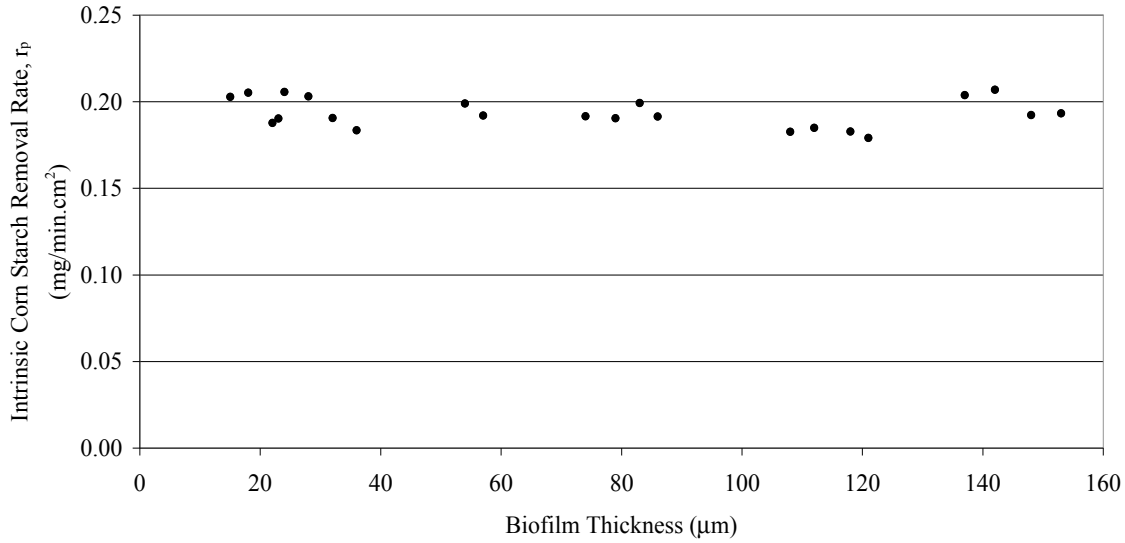

Figure 11. Intrinsic Corn Starch Removal Rate vs. Biofilm Thickness

The data demonstrates that the rate of dissolved substrate consumption is less than the rate of bioflocculation. Särner and Marklund (1984) claims that particulate hydrolysis may take up to 10 days and is influenced by the physical properties of the organic particulates. In any case, there is an agreement throughout the literature that the rate of hydrolysis is less than the rate of soluble substrate utilization. Despite the fact that healthy biofilms are subject to periodic sloughing, Bakke (1986) demonstrated that biofilm thickness is steady state in a tubular biofilm reactor. Therefore, high influent particulate concentrations lead to particulate accumulation. Figure 12 illustrates this phenomenon. A one-phase exponential decay equation (28) can be applied to express this relationship.

$$k_p = k_{p_{\max}} e^{(-K \cdot C_i)} + k_{p_{\min}} \tag{28}$$

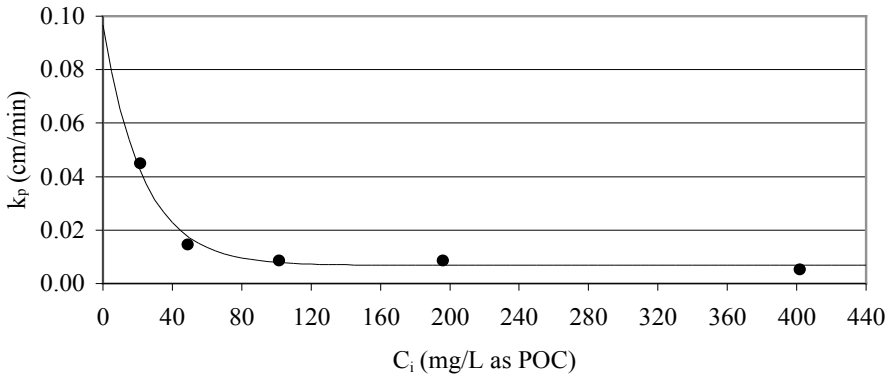

Figure 12. Bioflocculation Rate Coefficient vs. Influent Corn Starch Concentration

Here, k_{pmax} is the maximum attainable bioflocculation rate coefficient (cm/min), K is a constant (cm^3/mg), and k_{pmin} is a plateau representing a minimum rate coefficient as the available biofilm sites that promote bioflocculation are depleted (cm/min). A nonlinear regression analysis produced an R^2 of 0.9794, k_{pmax} value of 0.09 cm/min, K value of 0.04325 cm^3/mg, and a k_{pmin} value of 0.006776 cm/min.

The minimum concentration of particles that can be removed by flocculation, or the asymptote a, is also a function of the influent particle concentration, C_i. This relationship is well described by a Boltzmann sigmoidal function (29).

$$a = a_0 + \frac{(a_1 - a_0)}{1 + \exp\left(\frac{C_{50} - C_i}{\lambda}\right)} \tag{29}$$

The function has two asymptote plateau regions, with a transitional asymptote range in between. A best-fit curve is represented in Figure 13 with the Boltzmann sigmoidal function (29) drawn

through the organic particle asymptote data. The asymptote values before and after the transition, a_o and a_1, are 2.094 mg POC/L and 266.2 mg POC/L, respectively. The constant governing the slope of the rise during the transition, λ, is 29.24 mg POC/L. The coefficient of determination, R^2, equals 1, indicating a perfect fit. The initial concentration corresponding to 50% transition completion, C_{50}, is 200.9 mg POC/L and C_i is the variable initial native corn starch concentration. The bottom plateau, a_o, represents the lowest attainable particle concentration in the RDBR, which corresponds to the lowest possible influent concentration. As particle concentration increases, heightened particle activity increases particle flux to the biofilm surface. This is marked by a rapid increase in the minimum concentration of particles that can be obtained by flocculation. However, since bioflocculation is dependent upon external biofilm surface area, high particle concentrations may lead to an exhaustion of available active sites. Thus, despite increased particle flux, there is a relaxation prior to reaching the maximum attainable particle concentration by flocculation. This relationship implies that a maximum attainable removal per unit biofilm area may be applied to the design of biofilm reactors. Figure 14 shows the flocculated native corn starch particles on the biofilm under 4x magnification.

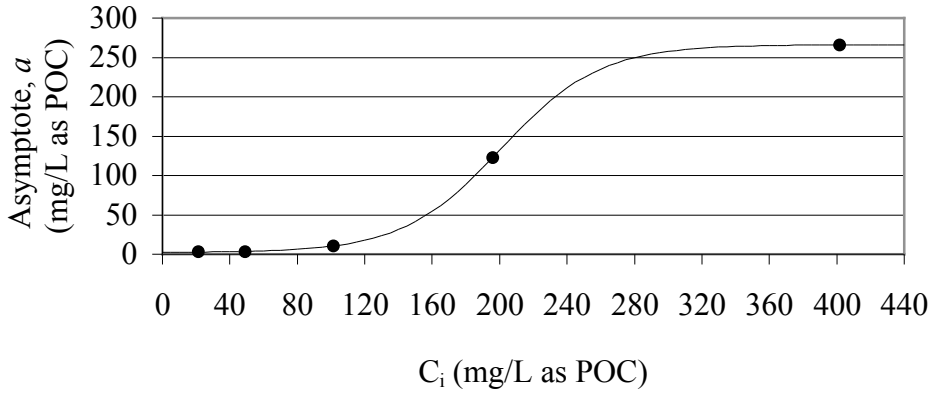

Figure 13. Organic Particle Asymptote, *a*, vs. Influent Corn Starch Concentration

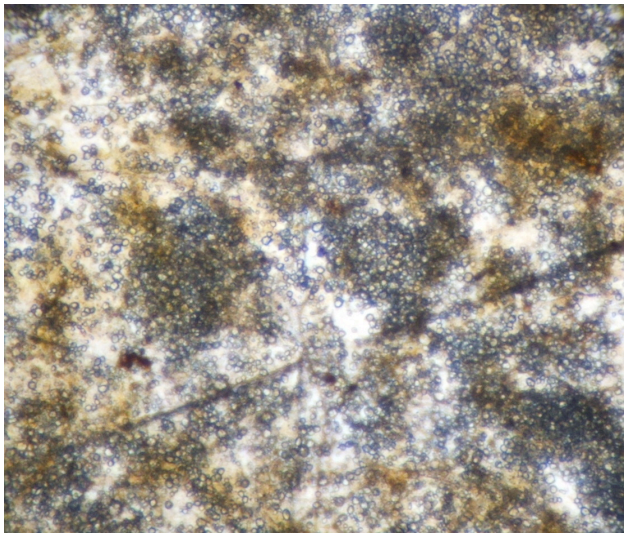

Figure 14. Flocculated Native Corn Starch Particles at the Biofilm Surface (4x)

Figure 15 is another photograph showing the flocculated native corn starch particles at 10x magnification.

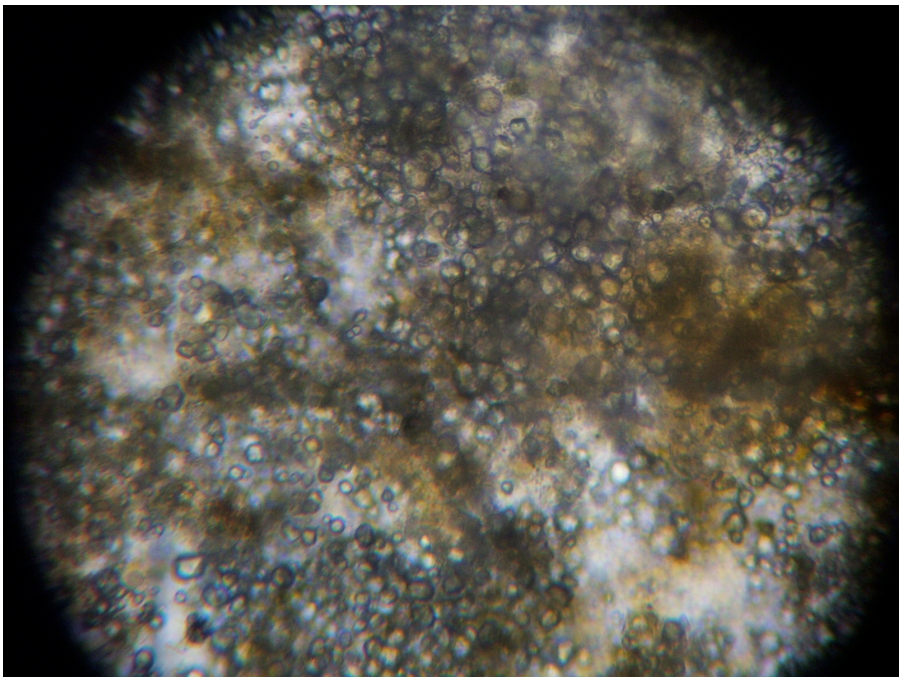

Figure 15. Flocculated Native Corn Starch Particles at the Biofilm Surface (10x)

4.4. KINETICS OF INORGANIC PARTICLE REMOVAL IN THE RDBR

In an effort to further demonstrate the validity of the assertion that bioflocculation is a physical, surface dependent process, an experiment was conducted in the same manner as that for the native corn starch, but with inorganic particles, the Min-U-Sil 10. The effect of several different influent Min-U-Sil 10 suspensions (C_i = 20, 50, 100, 200, and 400 mg TSS/L) was investigated. In each case, the concentration of Min-U-Sil 10 remaining in the effluent stream as a function of A/Q adjusts well to (24). Table 6 lists the coefficient of determination, R^2, best-fit bioflocculation rate coefficient, k_p, (obtained form a nonlinear regression analysis), best-fit asymptote, a, and experimental biofilm thickness, δ, associated with each of the aforementioned influent Min-U-Sil 10 concentrations. Figure 16 is a representative graph that illustrates the application of (24) to the observed concentration of Min-U-Sil 10 remaining in the effluent

stream. Here, the influent methanol concentration is 20 mg TSS/L. The remaining graphs can be seen in Appendix G.

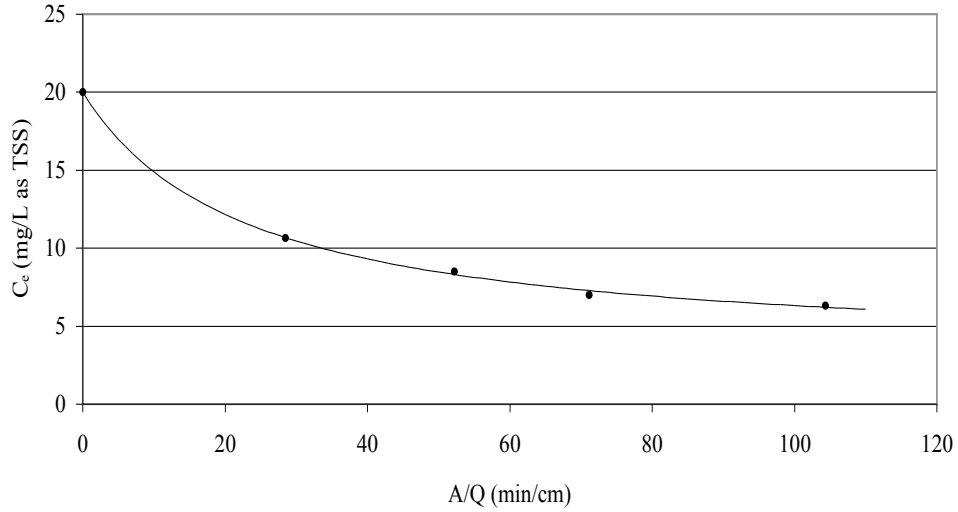

Figure 16. Effluent Min-U-Sil 10 Concentration vs. A/Q when C_i = 20 mg TSS/L

Table 6. Min-U-Sil 10 Nonlinear Regression Analysis Parameters

C_i (mg/L as TSS)	k_p (mg/min.cm^2)	a (mg TSS/L)	δ (μm)	R^2
20	0.043640	3.19	51	0.9990
50	0.018890	11.75	52	1.0000
100	0.013336	38.37	50	0.9968
200	0.012215	130.80	52	0.9841
400	0.008079	308.90	52	0.9931

Another demonstration that biofilm thickness does not affect the rate of bioflocculation, i.e., bioflocculation is a physical process that occurs at the biofilm surface, took the form of an experiment that varied biofilm thickness while the influent Min-U-Sil 10 concentration remained

constant. Appendix D contains the experiment's data, and Figure 17 illustrates this relationship. An F-test indicated the independence is accepted with 95% confidence.

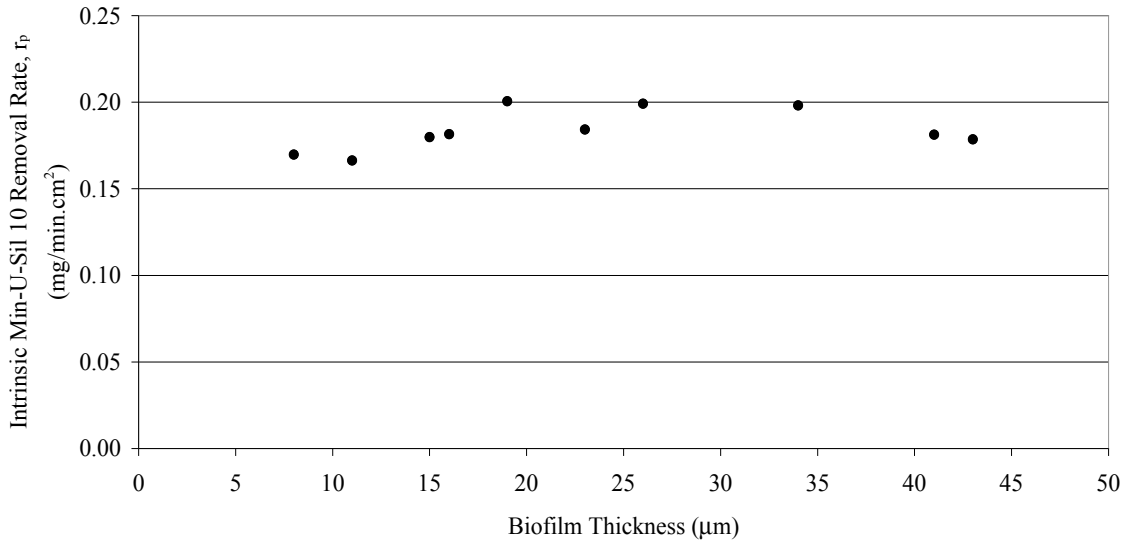

Figure 17. Intrinsic Min-U-Sil 10 Removal Rate vs. Biofilm Thickness

Due to the inorganic composition of the Min-U-Sil 10, the only way to create active biofilm sites is sloughing. Therefore, the presence of high particulate concentrations forces accumulation, which interferes with the rate of bioflocculation. Figure 18 illustrates the best-fit one-phase exponential decay equation (28) relative to the inorganic particle bioflocculation rate coefficient obtained from the nonlinear regression analyses on the concentration profiles.

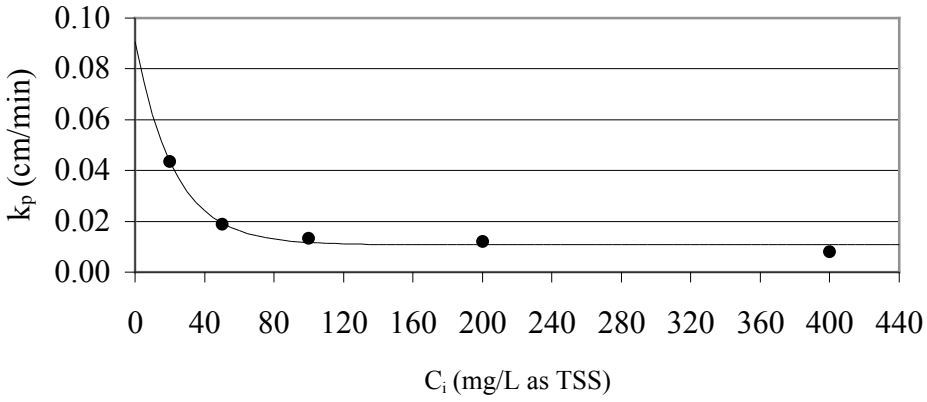

Figure 18. Bioflocculation Rate Coefficient vs. Influent Min-U-Sil 10 Concentration

A nonlinear regression analysis produced an R^2 of 0.9850, k_{pmax} value of 0.08001 cm/min, K value of 0.004457 cm^3/mg, and a k_{pmin} value of 0.01075 cm/min.

A best-fit curve is represented in Figure 19 with the Boltzmann sigmoidal function (29) drawn through the inorganic particle asymptote data. The asymptote values before and after the transition, a_o and a_1, are 0.0000001 mg TSS/L and 321.8 mg TSS/L, respectively. The constant governing the slope of the rise during the transition, λ, is 56.55 mg TSS/L. The initial concentration corresponding to 50% transition completion, C_{50}, is 220.6 mg TSS/L and C_i is the variable initial Min-U-Sil 10 concentration. The coefficient of determination, R^2, is 0.9990. Since bioflocculation is physical and dependent upon external biofilm surface area, inorganic particles exhibit the same kinetic behavior as organic particles. Additionally, although there is a 10-micron difference between the mean diameter of individual corn starch and Min-U-Sil 10 particles, the kinetic coefficients (asymptote, a, and bioflocculation rate coefficient, k_p) remain practically constant. A review of Tables 5 and 6 confirms this assertion, which indicates that the

biofilm is capable of flocculating all suspended particles exposed to the biofilm's surface.

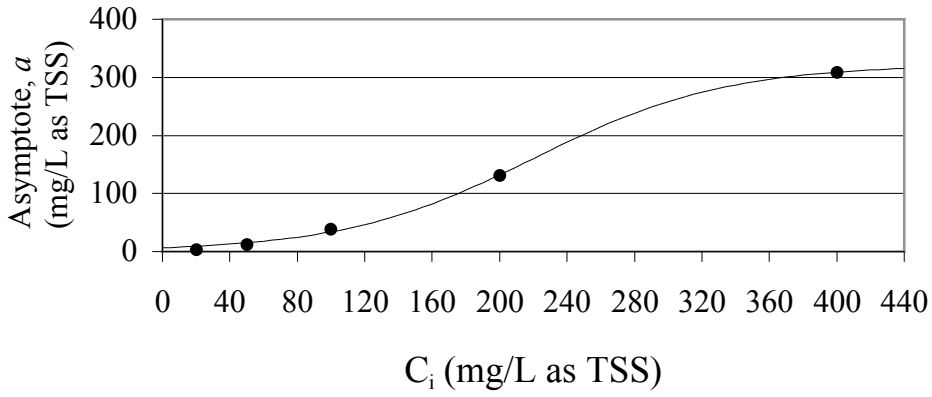

Figure 19. Inorganic Particle Asymptote, *a*, vs. Influent Min-U-Sil 10 Concentration

4.5. THE ROLE OF EPS IN THE BIOFLOCCULATION PROCESS

Most bacteria produce EPS, which participate in the formation of microbial aggregates and bioflocculation. By definition, EPS are located at or outside the cell wall, and are biopolymers excreted by bacteria that can be attached to the cell in a capsule, or excreted onto surrounding medium as slime (Higgins and Novak 1997). Electron microscopy has revealed that EPS are the gelatinous structure responsible for biofilm formation and integrity, and provide bacterial microorganisms with a mean of anchoring to medium in order to feed (Zhang, et al., 1999). Several researchers, including Wanner and Gujer (1986) and Laspidou and Rittmann (2002), have agreed that EPS can trap, bind, and concentrate organic particles.

EPS are a primary component of the biofilm organic mass, to the extent that approximately 90% of the biofilm organic carbon is comprised of EPS (Characklis and Marshall

1990). Typically, 95% of the mass of a biofilm is water, and 5% is dry material. For thick biofilms, the bacteriological configuration varies along its cross-sectional depth. Due to transfer limitations of DO and substrate, aerobic bacteria may be replaced by anaerobic bacteria as the organisms approach the growth medium. In addition to the type of bacteria present in thick biofilms, the porosity changes along the biofilm profile. Consequently, biofilms become denser and the pore volume becomes smaller through the biofilm depth. However, the physical properties of biofilms are dependent upon the conditions under which they are grown. Therefore, specific characteristics vary from treatment system to treatment system. The presence of nutrients and DO promotes the growth of viable biomass (Zhang and Bishop 2001). La Motta, et al., (2003) observed that EPS production in suspended growth reactors is very low at low DO concentrations. Since the outermost layer of a biofilm is subjected to the highest DO and substrate concentrations, the highest concentration of viable biomass and EPS is expected to occur in the outermost layer of the biofilm, which has the greatest exposure to organic and inorganic particles suspended in influent wastewater. The distribution of EPS in thin biofilms is indicative of the EPS located along the surface of biofilms of any thickness. This region is significant for adequate reactor performance considering bioflocculation as the principle particulate removal mechanism.

Bioflocculation is inherent in the presence of bacteria and the process is mediated by EPS. Figure 20 illustrates the linear relationship between TEPC due to EPS extracted from biofilms grown in this investigation on dissolved substrate, methanol. The linear regression analysis produced an R^2 of 0.9899.

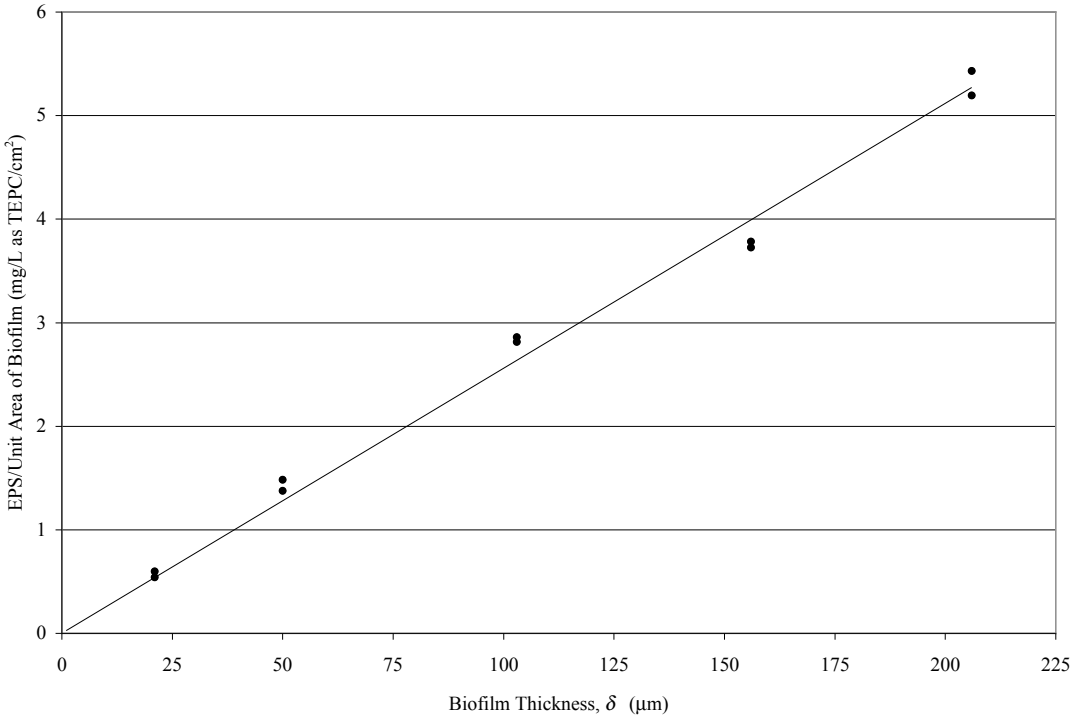

Figure 20. TEPC/Unit Biofilm Area vs. Biofilm Thickness Grown from Methanol

Figure 21 illustrates the linear relationship between TEPC due to EPS extracted from biofilms grown on particulate substrate, native corn starch. The linear regression analysis produced an R^2 of 0.9809. The linear relationship indicates that the EPS are uniformly distributed throughout the biofilm thickness, and are proportional to the film's biomass. The slopes of the best-fit lines for the EPS extracted from biofilm grown on methanol and native corn starch are 0.0256 and 0.0285, respectively. This indicates that there were slightly more EPS produced from particulate substrates. This is consistent with Morgenroth's (2002) claim that additional extracellular polymers and enzymes are produced in the presence of organic particulates. Worksheets related to polymer extraction can be seen in Appendix H.

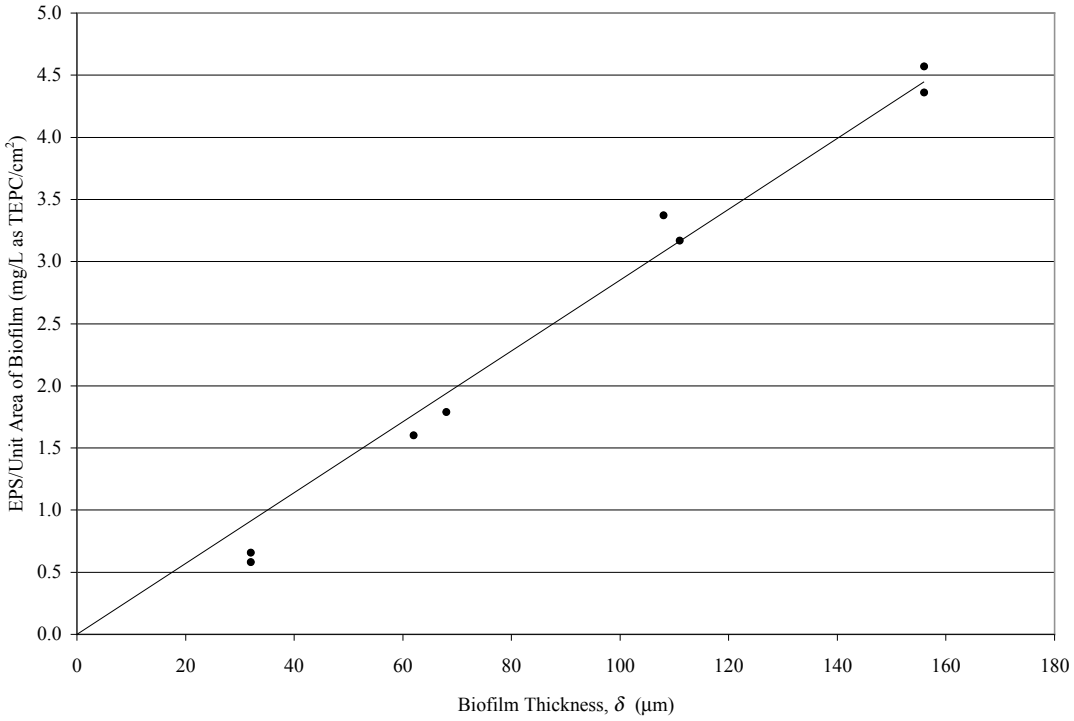

Figure 21. TEPC/Unit Biofilm Area vs. Biofilm Thickness Grown from Corn Starch

5. A MODEL FOR SIMULTANEOUS PARTICULATE AND DISSOLVED SUBSTRATE REMOVAL BY BIOLOGICAL FILMS

The general form of the bioflocculation equation (11) provides for an asymptote representing the minimum concentration of particles that could be achieved by flocculation in the reactor. In reality, biological wastewater treatment systems are dynamic, and responsible for the sanitation of complex solutions containing dissolved and particulate substrates. Therefore, there is a need to develop an expression capable of predicting simultaneous dissolved and particulate substrate removal. Larson and Harremoës (1994) claim that an experimental/theoretical approach must be taken to model the removal of particulate substrate from a laboratory biofilm reactor because there is no method to separate the rate of hydrolysis from dissolved substrates.

In chapter 4, it was demonstrated that dissolved and particulate substrates can be separated by their reaction kinetics, and bioflocculation controls the removal of particles in fixed-film reactors. The general bioflocculation equation must be modified to account for the presence of dissolved substrates. The modified bioflocculation equation takes the form (30):

$$r_p = -k_p\left(C_e' - m\right) \tag{30}$$

Here, C_e' is the concentration of particles in the effluent stream when readily biodegradable (dissolved) substrates are available and m is the minimum concentration that could be achieved in the reactor when readily biodegradable (dissolved) and nonreadily biodegradable (particulate) substrates are available (mg/L). The research presented herein demonstrates that for the range of A/Q studied, the rate of dissolved substrate removal can be adequately described by zero-order

reaction kinetics. Similarly, the rate of particulate (organic and inorganic) removal is described by first-order reaction kinetics. Domestic sewage (and laboratory solutions designed to emulate domestic sewage) can be readily analyzed to determine the proportion of dissolved and particulate substrates. The proportions can then be described as percents of TCOD. Modification of the general mass-balance on the RDBR to incorporate two reaction rates, namely those of dissolved substrate utilization and the modified bioflocculation equation (30), and influent and effluent concentrations expressed as TCOD, or TOC, produces the following equation (31).

$$S_{T_e} = S_{T_i} - k_v \delta \left(\frac{A}{Q} \right) + r_p \left(\frac{A}{Q} \right) \tag{31}$$

Here, S_{Te} and S_{Ti} are the concentrations of TCOD in the effluent and influent streams, respectively, in the case of complete dissolved substrate penetration. The equation functions under the premise:

$$PCOD = f \cdot TCOD + d \tag{32}$$

In this equation, f is a multiplier representing the fraction of TCOD due to PCOD, and d/f is a baseline DCOD concentration, which is schematically represented in Figure 1 as the x-intercept. Applying the aforementioned reaction kinetics and (32) produces an equation capable of describing simultaneous dissolved and particulate substrate disappearance by biofilms in the RDBR, a mixed-order model (33).

$$S_{T_e} = \frac{S_{T_i} + \left(\frac{A}{Q}\right)\left(k_p m - k_v \delta - k_p d\right)}{1 + k_p f\left(\frac{A}{Q}\right)} \tag{33}$$

5.1. EXPERIMENTAL SETUP AND DESIGN

The experimental apparatus was operated as described in preceding chapters, but when analyzing simultaneous methanol and native corn starch removal, 200-mL influent and effluent samples are analyzed. The samples are divided into equivalent proportions. For the first proportion, organic carbon analyses were performed directly (without previous filtration) despite the fact that polymeric substances and sloughed biofilm may cause interference. Filtration, however, removes part of the substrate and, therefore, is not possible. The results are reported as POC.

The other portion is analyzed for dissolved organic carbon by a physical-chemical method described by Mamais, et al., (1993). This method can be described as follows: First, 100 mL of the sample is isolated in a 125-mL flask. Next, the pH of the sample is adjusted to approximately 10.5 with a 6 M sodium hydroxide solution. Then, the sample is flocculated by adding 1 mL of a 100 g/L zinc sulfate solution to the 100 mL sample. The sample is vigorously mixed with a magnetic stirrer for approximately 1 min, and is allowed to settle quiescently for approximately 3 min (Standard Methods, Section 417 B, 1998). Depending on the degree of settling of the flocculated solids, 20-30 mL of the clear supernatant are carefully withdrawn with a pipette and passed through a 0.45-μm pore size filter paper. Due to the presence of starch in

the filters, it is necessary to wash them with DI water prior to filtration. The organic carbon of the supernatant filtrate was taken as the truly dissolved organic carbon, or DOC of the sample. The TOC less the DOC defines the POC.

A control experiment was conducted to insure that the procedure was not solublizing any of the particulates. Native corn starch/methanol solutions containing 90%-10%, 80%-20%, 70%-30%, 60%-40%, and 50%-50% (mg/L POC-mg/L DOC) of each substance were prepared and analyzed by the above described procedure. Each control behaved perfectly.

5.2. MIXED-ORDER MODEL CONFIRMATION STUDIES

Native corn starch/methanol solutions containing approximately 90%-10%, 80%-20%, 70%-30%, 60%-40%, 50%-50%, 40%-60%, and 30%-70% (mg/L POC-mg/L DOC) of each substance were prepared and introduced to the RDBR. Table 7 summarizes the influent concentrations according to the above-described proportionality.

Table 7. Influent Parameters for Mixed-Order Model Conformation Studies

Proportionality (% POC-% DOC)		TOC (mg/L)	DOC (mg/L)	POC (mg/L)	δ (μm)
90	10	39.61	4.11	35.50	45
79	21	40.26	8.65	31.61	45
70	30	40.02	11.91	28.11	46
61	39	39.21	15.15	24.06	47
49	51	40.71	20.62	20.09	49
40	60	40.04	23.99	16.05	45
30	70	40.20	28.23	11.97	47

Figures 22 is a representative illustration, and depicts the effluent TOC as a function of *A*/*Q* when there is 90% POC and 10% DOC. Figures for the remaining proportionalities can be seen in Appendix I.

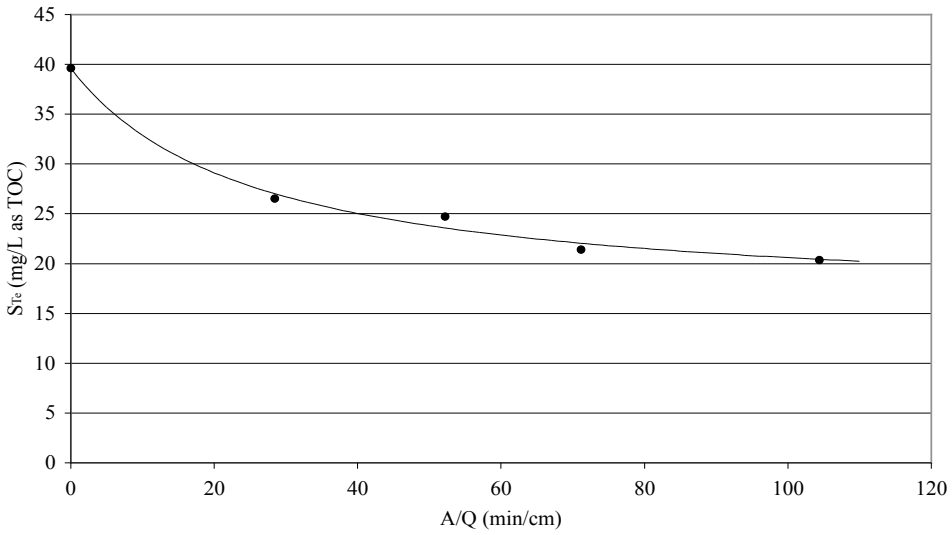

Figure 22. Effluent TOC vs. A/Q with 90% POC-10% DOC

Table 8 lists the coefficient of determination, R^2, best-fit bioflocculation rate coefficient, k_p, (obtained from a nonlinear regression analysis), best-fit asymptote, *m*, best-fit dissolved substrate rate coefficient, k_v, and fraction of TOC due to POC, *f*, associated with each of the aforementioned proportionalities. By experimental design, $d = 0$. Figure 23 is a plot of the dissolved substrate rate coefficient, k_v, versus the fraction of TOC due to DOC, f_d. The best-fit curve is described by equation (34), which follows traditional Michaelis-Menten kinetics.

$$k_v = k_{v_{\max}} \frac{f_d}{K_{f_d} + f_d} \tag{34}$$

Here, K_{fd} is a half-rate constant. A nonlinear regression analysis produced a coefficient of determination, R^2, equal to 0.9466, a best-fit k_{vmax} of 13.02 mg/min.cm^3, and a best-fit K_{fd} of 0.5296.

Table 8. Nonlinear Regression Parameters for Mixed-Order Model Confirmation

Proportionality (% POC-% DOC)		f	f_d	m (mg/L)	k_p (mg/min.cm^2)	k_v (mg/min.cm^3)	R^2
90	10	0.8962	0.1038	14.26	0.0439	1.128	0.9839
79	21	0.7851	0.2149	13.22	0.0437	4.000	0.9873
70	30	0.7024	0.2976	12.64	0.0544	5.069	0.9835
61	39	0.6136	0.3864	11.74	0.0889	5.720	0.9969
51	49	0.4935	0.5065	11.87	0.0967	6.431	0.9917
60	40	0.4008	0.5992	9.88	0.1123	6.982	0.985
71	29	0.2978	0.7022	8.22	0.1301	7.057	0.9102

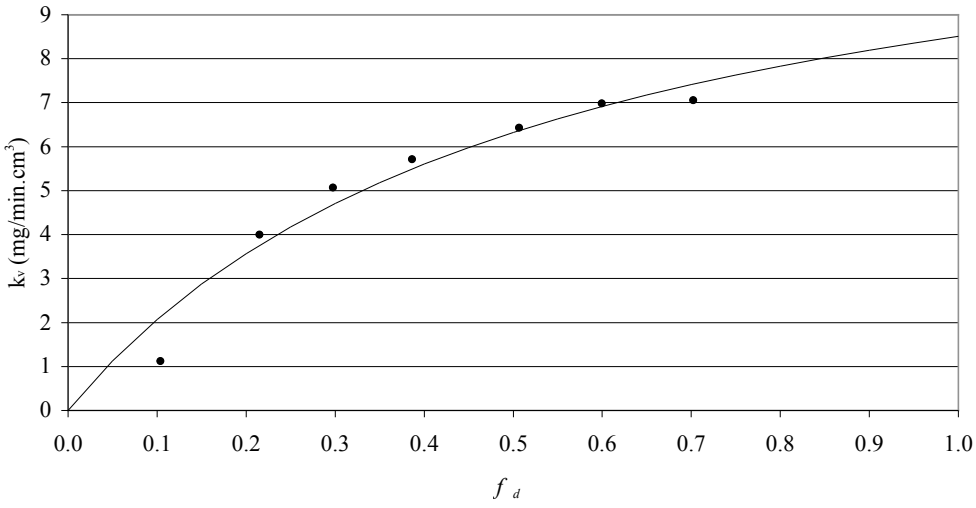

Figure 23. Dissolved Substrate Rate Coefficient, k_v, vs. f_d

The asymptote, m, has been described as a function of the influent particle concentration using a Boltzmann sigmoidal equation (29). A modification of the aforementioned function to be applicable in the presence of dissolved and particulate substrates is shown by (35).

$$m = m_0 + \frac{(m_1 - m_0)}{1 + \exp\left(\frac{f_{50} - f}{\lambda}\right)} \tag{35}$$

The function has two asymptote plateau regions, with a transitional asymptote range in between. There are two asymptote values, before and after the transition, m_o and m_1 (mg TOC/L), respectively. The constant governing the slope of the rise during the transition is λ. The fraction, f, corresponding to 50% transition completion is denoted by f_{50}, and f is the variable fraction of TOC due to POC. This relationship is illustrated in Figure 24, but the range of influent concentrations applied during mixed-order model confirmation studies only represents a small portion of the Boltzmann sigmoidal curve. Therefore, it appears that the function is not applicable.

Finally, the bioflocculation rate coefficient, k_p, is illustrated against the fraction of TOC due to POC in Figure 25. The bioflocculation rate coefficient, k_p, has been described as a function of the influent particle concentration using a one-way exponential decay equation (28). A modification of the aforementioned function to be applicable in the presence of dissolved and particulate substrates is shown by (36). The range of influent concentrations applied during mixed-order model confirmation studies only represents the decreasing portion of curve, which can be seen in Figure 25. However, the function can not be fully developed due to the narrow

range of influent concentration represented. The worksheet pertaining to the mixed-order model confirmation studies can be reviewed in Appendix J.

$$k_p = k_{p_{\max}} e^{(-K \cdot f)} + k_{p_{\min}} \tag{36}$$

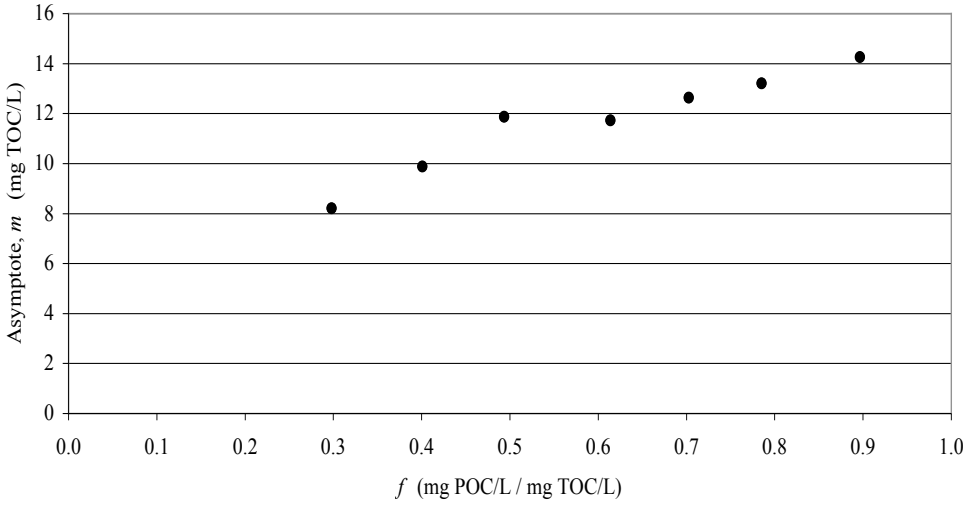

Figure 24. Asymptote, *m* vs. *f*

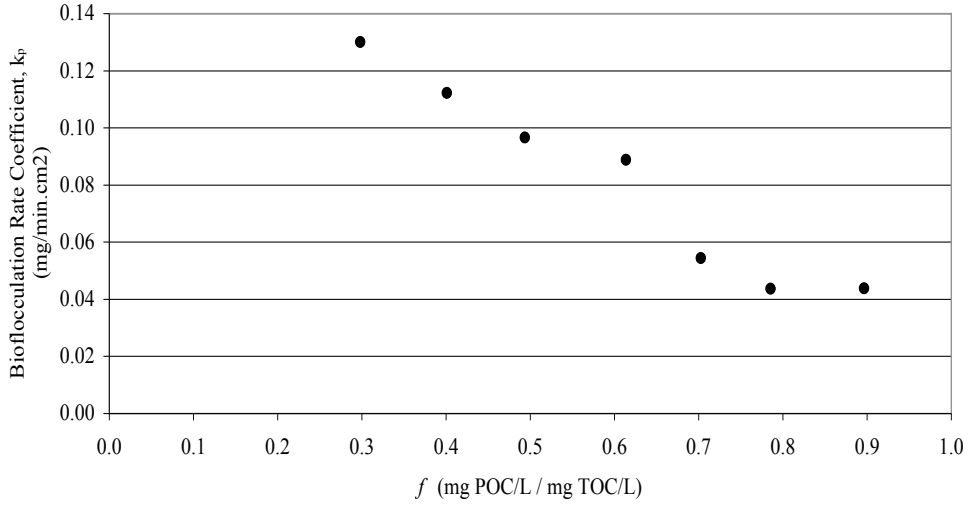

Figure 25. k_p vs. *f*

6. CONCLUSIONS AND RECOMMENDATIONS

The following conclusions can be derived from the research presented in this dissertation:

1. Conversion of inorganic particle removal became insensitive to the rotational speed when the speed exceeded 100 rev/min. Thus, indicating that the kinetic regime of bioflocculation had been attained. At, or in excess of, this rotational speed the fluid velocity is sufficient to reveal the intrinsic rate of bioflocculation.
2. Macrocolloidal particulates are affected by external diffusion, very similar to the demonstration using glucose (dissolved substrate) conducted by La Motta (1976b). Therefore, external diffusional resistances should be considered when designing biofilm reactors to remove the particulate fraction of chemical oxygen demand.
3. For the range of A/Q investigated, the removal of methanol (dissolved substrate) in the RDBR adheres to zero-order reaction kinetics, which agrees with the observations of La Motta (1976a), Harremoës (1978), and Trulear and Characklis (1982) when removing glucose, another dissolved substrate.
4. The removal of Maizena native corn starch (organic particles), and Min-U-Sil 10 (inorganic particles) is rapid in comparison to the removal of methanol, and is well-described by the first-order bioflocculation rate equation.
5. Bioflocculation is a physical process dependent upon external biofilm surface area, which is demonstrated by the removal of organic and inorganic particles.
6. The dissolved substrate rate coefficient, k_v, is a function of the influent dissolved substrate concentration and follows traditional Michaelis-Menten kinetics.

7. The bioflocculation rate coefficient, k_p, is a function of the influent particle concentration and follows a one-way exponential decay equation. The decrease can be attributed to accumulation of particles on the biofilm surface when there are high particle concentrations.
8. The asymptote, a, in the bioflocculation rate equation can be described by a Boltzmann sigmoidal function. As the particle concentration increases, heightened particle activity increases particle flux to the biofilm surface. This is marked by a rapid increase in the minimum concentration of particles that can be obtained by flocculation. However, since bioflocculation is dependent upon external biofilm surface area, high particle concentrations lead to an exhaustion of available active biofilm sites. Thus, despite increased particle flux, there is a relaxation prior to reaching the maximum attainable particle concentration by flocculation.
9. EPS were successfully extracted and quantified in thin biological films. The linear relationship between the TEPC/unit biofilm area and the biofilm thickness implies that EPS are evenly distributed along the biofilm thickness. When external diffusional resistances have been eliminated, the biofilm surface exposes an equal distribution of EPS to particles suspended in the bulk of the liquid.
10. Since dissolved and particulate substrates can be differentiated by their reaction kinetics, a mixed-order model can be used to describe the removal of TCOD in the RDBR. The mixed-order model considers a first-order bioflocculation of particulate organic carbon and zero-order consumption of dissolved organic carbon. Such a model was developed for the RDBR and experimentally verified.

The following are recommendations for future research projects:

1. A survey of biofilm thickness typical to operational wastewater treatment systems should be conducted and a database should be initiated.
2. Pulsed field gradient nuclear magnetic resonance should be applied to an operational, full-scale biofilm wastewater treatment system in order to trace particulate matter in an effort to determine the fraction of organic particles removed by hydrolysis, and the fraction removed by secondary clarification.
3. The effect entrapped particles have on the settleability of sloughed biofilm should be evaluated. The properties of the particulate fraction of the wastewater are likely to fluctuate from treatment system to treatment system, and secondary clarifier design should incorporate the settling properties of fixed-film reactor effluent based on the composition of the settleable material.

7. REFERENCES

APHA, AWWA, and WEF (1998). *Standard Methods for the Examination of Waste and Wastewater*. 20th ed. Baltimore: American Public Health Association.

Atkinson, B., and Howell, J.A., (1975). Slime holdup, influent BOD, and mass transfer in trickling filters. *J. Env. Engr.* 11, 585-605.

Baier, R.E., (1980). "Substrata influences on adhesion of microorganisms and their resultant new surface properties," in G. Bitton and K.C Marshall (eds.), *Adsorption of Microorganisms to Surfaces,* Wiley, New York, pp. 59-104.

Baier, R.E., "Applied chemistry at protein interfaces," in R.E. Baier (ed.), *Applied Chemistry at Protein interfaces,* Advances in Chemistry Series, 145, ACS, Washington, pp. 1-25.

Bakke, R. (1986). Ph.D. Dissertation. Montana State University, Bozeman, MT.

Bakke, R., and Ollson, P.Q., (1986). *J. Microbiol. Meth.,* 5, 93-98.

Bakker, D. P., van der Plaats, A., Verkerke, G. J., Busscher, H. J., and van der Mei, H. C. (2003). Comparison of velocity profiles for different flow chamber designs used in studies of microbial adhesion to surfaces. *Appl. Environ. Microbiol.* 69, 6280-6287

Boltz, J.P. (2003). "The Kinetics of PCOD Removal in the Trickling Filter Process". Master's Degree Thesis. University of New Orleans, New Orleans, LA.

Bouwer, E.J. (1987). Theoretical investigation of particle deposition in biofilm systems. *Wat. Res.* 21, 1489-1498.

Brock, T.D., and Madigan, M.T., (1991). *Biology of Microorganisms* Prentice Hall, New Jersey.

Buydos, J.F. (1980). "The Effect of Polyelectrolytes on the Attached Growth of Bacteria". Master's Degree Thesis. University of Massachusetts, Boston, Mass.

Cambré, P.L., and Acrivos, A., (1956). On chemical surface reactions in laminar boundary-layer flow. *J. App. Physics,* vol. 27 (11), 1322-1328.

Carberry, J.J., (1964). Designing laboratory catalytic reactors. *Industrial and Engineering Chemistry*, vol. 56, 39-46.

Characklis, W.G., Marshall, K.C., (1990). *Biofilms*, Wiley, New York.

Chróst, R.J. (1991). 'Environmental control of the synthesis and activity of aquatic microbial ectoenzymes," in R.J. Chróst (ed.), *Microbial Enzymes in Aquatic Environments,* pp. 29, Springer Verlag, New York.

Cohen-Stuart, M.A., Scheutjens, and Fleer, G.J., (1980). *J. Polymer Sci.* (Part B), 18, 559.

Cunliffe, D., Smart, C.A., Alexander, C., and Vulfson, E.N., (1999). Bacterial adhesion at synthetic surfaces. *Applied and Environmental Microbiology,* vol. 65 (11), 4995-5002.

Dold, P.L., Ekama, G.A., Marais, G., (1980). A General Model for the Activated Sludge Process. *Prog. Water Technology.* Vol. 12, 47-77.

Fowler, H.W., and McKay, A.J., (1980). "Measurement of Microbial Adhesion," in R.W. Berkley, J.M. Lynch, J. Melling, P.R. Rutter, and B. Vincent (eds.), *Microbial Adhesion to Surfaces*, Ellis Horwood, Chichester, U.K. p. 143.

Frank-Kamenetskii, D.A. (1969) *Diffusion and Heat Transfer in Chemical Kinetics*. 2nd ed. Transl. By J.P. Appleton, Plenum Press, New York.

Friedman, B., Dugan, P., Pfister, R., Remsen, C., (1969). "Structure of Exocellular Polymers and Their Relationship to Bacterial Flocculation." *Journal of Bacteriology. American Society of Microbiology,* June, 1328-1334.

Fryer, P.J., Slater, N.K.H., and Duddridge, J.E., (1984). "On the analysis of biofouling data with radial flow shear stress cells, " AERE-R11295, United Kingdom Atomic Energy Authority, Harwell.

Fu, Y.-C., (1993). "Characterizing oxygen profiles and determining oxygen diffusivity in biofilm during biodegradation of azo dye." Ph.D. thesis, University of Cincinnati, Cincinnati, Ohio.

Gaudy, A.F., Ramanathan, M., and Rao, B.S., (1967). Kinetic behavior of heterogeneous populations in completely mixed reactors. *Biotech. Bioengr.,* vol. 9, 387-411.

Gaudy, A.F., and Gaudy, E.T., (1971). *Biological concepts for design and operation of the activated sludge process,* Water Pollution Control Research Series.17090 FQJ 09/71.

Gaudy, A.F., Obayashi, A., and Gaudy, E.T., (1971). Control of growth rate by initial substrate concentration at values below maximum rate. *Applied Microbiology,* vol. 22, 1041-1047.

Gaudy, A.F., Yang, P.Y., Bustamante, R., and Gaudy, E.T., (1973). Exponential growth in systems limited by substrate concentration. *Biotech. Bioengr.*, vol. 15, 589-596.

Grady, L.C.P., Daigger, G.T., and Lim, H.C., (1999). *Biological Wastewater Treatment.* 2nd ed. Marcel Dekker, New York.

Gujer, W., Henze, M., Mino, T., and Loosdrecht, M.C.M. (1999). Activated sludge model No. 3. *Wat. Sci. Tech.*, 39(1), 183-193.

Gulevich, W., (1967). "The role of diffusion in biological waste treatment," Ph.D. Dissertation. The Johns Hopkins University, Baltimore, Maryland.

Harremoës, P. (1978) Biofilm Kinetics. *Water Pollution Microbiology* (Edited by Mitchell R.), Vol. 2. Wiley, New York.

Henze, M., Grady Jr., L., Gujer, W., Marais, G., Matsuo, T., (1987). A General Model for Single-Sludge Wastewater Treatment Systems. *Water Resources,* Vol. 21, 505-515.

Higgins, M.J., Novak, J.T., (1997). Characterization of Exocellular Protein and Its Role in Bioflocculation. *Journal of Environmental Engineering,* Vol. 123, No. 5, May, 479-485.

Jiménez, J.A. (2002), "Kinetics of COD Removal in the Activated Sludge Process, Including Bioflocculation," Ph.D. Dissertation, University of New Orleans.

Kornegay, B.H., and Andrews, J.H. (1967). *Characteristics and Kinetics of Fixed-Film Biological Reactors*, Final report, Grant WP-01181, Federal Water Pollution Control Administration, U.S. GPO, Washington.

La Motta, E., Jimenez, J., Parker, D. and McManis, K., (2003). Removal of Particulate COD by Bioflocculation in the Activated Sludge Process. *Water Pollution VII.* ISBN: 1-85312-976-3, 349-358.

La Motta, E.J., Hickey, R.F., and Buydos, J.F., (1982). Effect of polyelectrolytes on biofilm growth. *J. Env. Engr.*, Vol. 108, 1326-1341.

La Motta, E.J. (1976a) Internal diffusion and reaction in biological films. *Envir. Sci. Technol.* 10, 765-769.

La Motta, E.J. (1976b) External mass transfer in a biological film reactor. *Biotechnol. Bioengng.* XVIII, 1359-1370.

La Motta, E.J. (1976c) Kinetics of growth and substrate uptake in a biological film system. *Appl. Envir. Microbiol.* 31, 286-293.

La Motta, E.J. (1974) Ph.D. Dissertation, University of North Carolina at Chapel Hill, Chapel Hill, N.C.

Larsen, T.A. and Harremoës, P. (1994). Modeling experiments with colloidal organic matter in biofilm reactors. *Wat. Sci. Tech.* 29, 479-486.

Laspidou, C.S., and Rittmann, B.E., (2002). A unified theory for extracellualr polymeric substances, soluble microbial products, and active and inert biomass. *Wat. Sci. Tech.* 36, 2711-2720.

Lazarova, V., and Manem, J., (1995). "Biofilm characterization and activity analysis in water and wastewater treatment." *Water Res.* 29 (10), 2227-2245.

Levich, V.G. (1962). Physiochemical Hydrodynamics, translated by Scripta Technica, Inc., Prentice Hall, Englewood Cliffs, New Jersey.

Levine, A.D., Tchobanoglous G., and Asano, T. (1991). Size Distribution of Particulate Contaminants in Wastewater and Their Impact on Treatability. *Water Research.* 25(8), 911-922.

Liao, B.Q., Allen, D.G., Droppo, I.G., Leppard, G.G., and Liss, S.N., (2001). Surface properties of sludge and their role in bioflocculation and settleability. *Water Research,* 35 (2). 339-350.

Lin, C.S., Moulton, R.W., and Putnam, G.L. (1953). *Ind. Eng. Chem.,* 45, 636-640.

Lister, D.H. (1981) "Corrosion products in power generating systems," in E.F.S. Somerscales and J.G.Knudsen (eds.), *Fouling of Heat Transfer Equipment*, Hemisphere, Washington, pp. 135-200.

Loeb, G.I., and Neihof, R.A., (1975). "Marine conditioning films," in R.E. Baier (ed.), *Applied Chemistry at Protein interfaces,* Advances in Chemistry Series, 145, ACS, Washington, pp. 319-335.

Logan B., Hermanowicz, S., Parker, D., (1987). A Fundamental Model for Trickling Filter Process Design. *Journal of Water Pollution Control Federation,* Vol. 59, No. 2, 1029-1043.

Logan, B., Hunt, J.R., (1986). Bioflocculation as a Microbial Response to Substrate Limitation. *Biotechnology and Bioengineering,* Vol. 31, 91-101.

Luque, Jackeline (2005), "Exocellular Polymeric Substances, Bioflocculation, and Sludge Settling Properties in a Combined Anaerobic/ Activated Sludge Process," Ph.D. Dissertation Proposal, University of New Orleans.

Madigan, M.T., Martinko, J.M., and Parker, J., (1997). *Brock Biology of Microorganisms,* 8th ed., Prentice-Hall, Upper Saddle River, NJ.

Maier, W.J., (1973). "Biological removal of colloidal matter from wastewater," *Environmental Protection Technology Series,* EPA, EPA-R2-73-147.

Maier, W.J., Behn, V.C., and Gates, C.D., (1967). *J. San. Eng. Div. ASCE*, 93, 91.

Mamais, D., Jenkins, D., and Pitt, P., (1993). A Rapid Physical Chemical Method for the Determination of Readily Biodegradable Soluble COD in Municipal Wastewaters. *Water Res.* Vol. 22, 195-197.

Marshall, K.C., Stout, R., and Mitchell, R., (1971). Selective sorption of bacteria from sea water. *Canadian Journal of Microbiology*, Vol. 17, 1413-1416.

Marshall, K.C., and Cruickshank, R.K., (1973). Cell surface hydrophobicity and the orientation of certain bacteria at interfaces. *Archives of Microbiology,* Vol. 91, 29-40.

Marshall, K.C., (1976). *Interphases in Microbial Ecology,* Harvard University Press, Cambridge, Mass.

Metcalf and Eddy, (2003). *Wastewater Engineering Treatment and Reuse 4th ed.* McGraw Hill, New York.

Monod, J., (1949). The growth of bacterial cultures. *Annual Review of Microbioloogy*, vol. 3, pp. 371-394.

Morgenroth, E., Kommedal, R., and Harremoës, P., (2002). Processes and modeling of hydrolysis of particulate organic matter in aerobic wastewater treatment – a review. *Wat. Sci. Tech.* Vol. 45, No. 6, pp. 25-40.

Nogura, D.R., Okabe, S., and Picioreanu, C, (1999). Biofilm modeling: present status and future directions. *Wat. Sci Tech.*, vol. 39 (7), 273-278.

Ohron, D., Artan, N., (1994). *Modeling of Activated Sludge Systems.* Technomic Press, Lancester, PA.

Okutman, D., Övez, S, and Orhon, D., (2001). Hydrolysis of settleable substrate in domestic sewage. *Biotech. Letters.* 23, 1907-1914.

Picologlou, B.F., Zelver, N., and Characklis, W.G., (1980). *J. Hyd. Div. ASCE*, 106, 733-746.

Rittmann, B.E. and McCarty, P.L., (2001). *Environmental Biotechnology: Principles and Applications*, McGraw Hill, New York.

Rittmann, B.E. and McCarty, P.L., (1981). Substrate flux into biofilms of any thickness. *J. Env. Eng*. 107, 831-849.

Rittmann, B.E. and McCarty, P.L., (1980a). Model of steady state biofilm kinetics. *Biotechnol. Bioengr*. 22, 2343-2357.

Rittmann, B.E. and McCarty, P.L., (1980b). Evaluation of steady state biofilm kinetics. *Biotechnol. Bioengr*. 22, 2359-2373.

Rittmann, B.E. and McCarty, P.L., (1978). Variable-order model of bacterial film kinetics. *J. Env. Eng*. 104, 889-900.

Rojas, J.A. (2004), "Relationship Between the Sludge Settling Characteristics and the Parameters of the Activated Sludge System," Master's Thesis, University of New Orleans.

Rouhiainen, P.O., and Stachiewicz, (1970), *J. Heat Transfer* (Trans. ASME), 92, 169-177.

Särner, E. (1986). Removal of particulate and dissolved organics in aerobic fixed-film biological processes. *J. Wat. Poll. Contr. Fed*. 58, 165-172.

Särner, E. and Marklund, S. (1984). Influence of particulate organics on the removal of dissolved organics in fixed-film biological reactors. *Wat. Sci. Tech*. 17, 15-26.

Satterfield, C.N. (1968). Mass Transfer in Heterogeneous Catalysis, MIT Press, Cambridge, Mass.

Schmid, T., Helmbrecht, C., Panne, U., Haisch, C., and Niessner, R. (2003). Process analysis of biofilms by photoacoustic spectroscopy. *Anal. Bioanal. Chem.* 375, 1124-1129.

Schomburg, D., Saltzmann, M., Stephan, D., (1997). *The Enzyme Handbook*. Springer Verlag, Berlin.

Schuyler, R., Weigand, R., Stover, E., (2001). "Wastewater Microbiology." 75th Annual Conference and Exposition of the Water Environmental Federation, Georgia, October.

Siegrist, H. and Gujer, W., (1985). *Wat. Res.*, 19, 1369.

Smidsrod, O., and Haug, A., (1971). *Biopolymers*, 10, 1213.

Tanford, C., (1961). *Physical Chemistry of Macromolecules,* Wiley, New York.

Tenney, M.W., Stumm, W., (1965). Chemical Flocculation of Microorganisms in Biological Waste Treatment. *Journal of Water Pollution Control Federation,* Vol. 37, 1370-1388.

Tomlinson, T.G. and Snaddon (1966). *Int. J. Air Wat. Poll.,* 10, 865.

Trulear, M.G. and Characklis, W.G., (1982). *J. Wat. Poll. Contr. Fed.*, 54, 1288.

Trulear, M.G., (1980). "Dynamics of Biofilm Processes in an Annular Rotating Reactor". Master's Degree Thesis. Rice University, Houston, TX.

Tsibouklis, J., Graham, P., Eaton, P.J., Smith, J.R., Nevell, T.G., Smart, J.D., and Ewen, R.J., (2000).

Wanner, O., and Gujer, W., (1986). A multispecies biofilm model. *Biotechnol. Bioengr.* Vol. XXVIII. Pp. 314-328.

Wehner, J.F., Wilhelm, R.H., (1956). Boundary Conditions of Flow Reactor. *Chemical Engineering Science,* Vol. 6, February, 89-93.

Wells, A.C. and Chamberlain, A.C., (1967). *Br. J. Appl. Physiol.,* 18, 1793-1799.

Williamson, K. and McCarty, P.L., (1976a). A model of substrate utilization by bacterial films. *J. Wat. Poll. Contr. Fed.* 48, 9-24

Williamson, K. and McCarty, P.L., (1976b). Verification studies of the biofilm model for bacterial substrate utilization. *J. Wat. Poll. Contr. Fed.* 48, 281-289.

Williamson, K. (1973) Ph.D. Dissertation, Stanford University, Stanford, CA.

Zhang, X., Bishop, P.L., (2001). Spatial Distribution of Extracellular Polymeric Substances in Biofilms. *Journal of Environmental Engineering,* Vol. 127, No. 9, September, 850-856.

Zhang, X., Bishop, P., Kinkle, B., (1999). Comparison Methods for Quantifying Extracellular Polymers in Biofilms. *Water Science Technology,* Vol. 39, No. 7, 211-218.

Zhang, T.C., Bishop, P.L., (1994). Density, Porosity, and Pore Structure of Biofilms. *Water Res.* Vol. 28, No.11, 2267-2277.

APPENDIX A

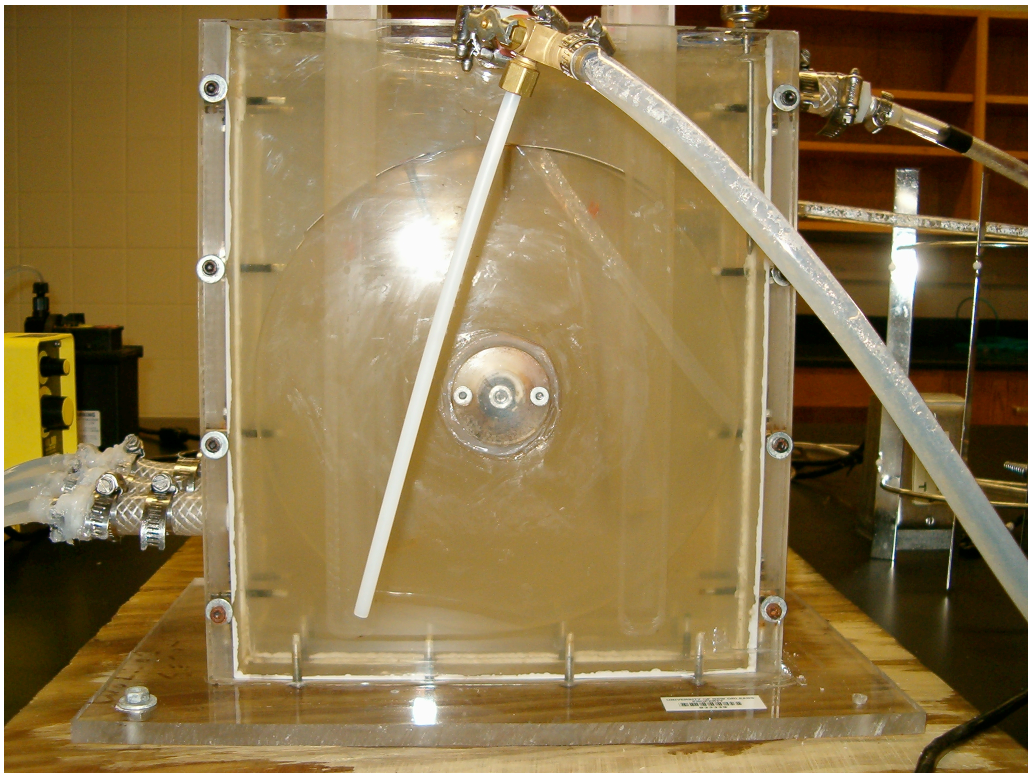

Appendix A-1. RDBR Profile

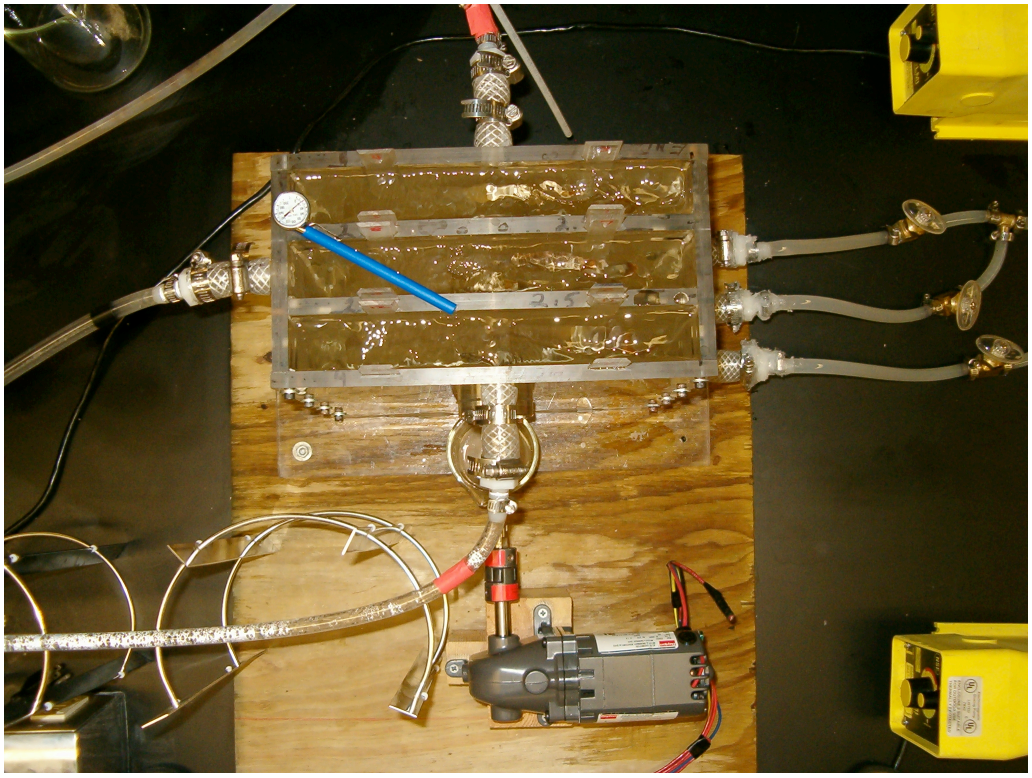

Appendix A-2. RDBR Plan

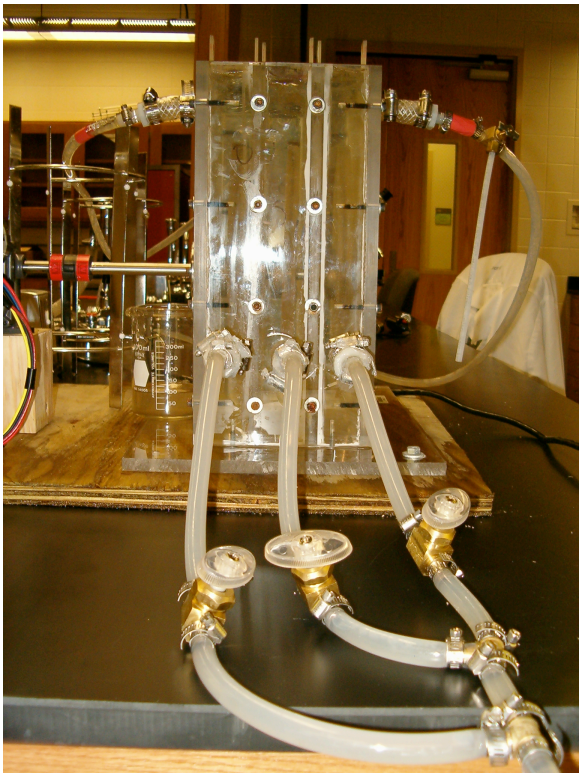

Appendix A-3. RDBR Elevation

Appendix A-4. Experimental Setup

APPENDIX B

Appendix B. Tracer Test Data

Time, t (min.)	Concentration, C (ppt)	1 C Adjusted (ppt)	2 F_t (unitless)	3 E_t ($min.^{-1}$)	4 $E_t \times \Delta t$ (unitless)	5 $E_t \times t$ (unitless)	6 $t \times E_t \times \Delta t$ (min.)	7 $t^2 \times E_t$ (min.)	8 $t^2 \times E_t \times \Delta t$ (min.)
0.00	0.1	0.0	0.0000	0.0344	0.0000	0.0000	0.00	0.00	0.00
0.67	0.2	0.1	0.0169	0.0339	0.0228	0.0226	0.01	0.02	0.01
1.07	0.3	0.2	0.0339	0.0336	0.0135	0.0358	0.01	0.04	0.01
1.50	0.4	0.3	0.0508	0.0332	0.0145	0.0498	0.02	0.07	0.02
1.98	0.5	0.4	0.0678	0.0328	0.0160	0.0651	0.03	0.13	0.05
3.03	0.7	0.6	0.1017	0.0320	0.0341	0.0972	0.09	0.29	0.22
4.00	0.9	0.8	0.1356	0.0313	0.0306	0.1252	0.11	0.50	0.38
4.50	1.0	0.9	0.1525	0.0309	0.0156	0.1391	0.07	0.63	0.28
5.03	1.1	1.0	0.1695	0.0305	0.0164	0.1536	0.08	0.77	0.37
5.55	1.2	1.1	0.1864	0.0301	0.0157	0.1673	0.08	0.93	0.44
6.10	1.3	1.2	0.2034	0.0297	0.0165	0.1814	0.10	1.11	0.56
6.60	1.4	1.3	0.2203	0.0294	0.0148	0.1939	0.09	1.28	0.60
7.28	1.5	1.4	0.2373	0.0289	0.0199	0.2104	0.14	1.53	0.96
7.77	1.6	1.5	0.2542	0.0285	0.0139	0.2217	0.10	1.72	0.79
8.33	1.7	1.6	0.2712	0.0281	0.0161	0.2346	0.13	1.95	1.04
8.93	1.8	1.7	0.2881	0.0277	0.0168	0.2477	0.14	2.21	1.25
9.50	1.9	1.8	0.3051	0.0273	0.0156	0.2597	0.14	2.47	1.33
10.12	2.0	1.9	0.3220	0.0269	0.0167	0.2723	0.16	2.76	1.61
10.73	2.1	2.0	0.3390	0.0265	0.0165	0.2845	0.17	3.05	1.79
11.38	2.2	2.1	0.3559	0.0261	0.0171	0.2968	0.19	3.38	2.09
12.05	2.3	2.2	0.3729	0.0256	0.0172	0.3089	0.20	3.72	2.37
12.70	2.4	2.3	0.3898	0.0252	0.0165	0.3201	0.20	4.07	2.53
13.42	2.5	2.4	0.4068	0.0247	0.0179	0.3320	0.23	4.45	3.05
14.12	2.6	2.5	0.4237	0.0243	0.0172	0.3431	0.24	4.84	3.25
14.83	2.7	2.6	0.4407	0.0239	0.0173	0.3538	0.25	5.25	3.62
15.58	2.8	2.7	0.4576	0.0234	0.0177	0.3645	0.27	5.68	4.10
16.37	2.9	2.8	0.4746	0.0229	0.0181	0.3750	0.29	6.14	4.63
17.07	3.0	2.9	0.4915	0.0225	0.0159	0.3839	0.27	6.55	4.44
18.07	3.1	3.0	0.5085	0.0219	0.0222	0.3958	0.39	7.15	6.85
19.60	3.3	3.2	0.5424	0.0210	0.0329	0.4121	0.62	8.08	11.67
20.48	3.4	3.3	0.5593	0.0205	0.0184	0.4205	0.37	8.61	7.37
21.38	3.5	3.4	0.5763	0.0200	0.0183	0.4285	0.38	9.16	8.00
23.28	3.7	3.6	0.6102	0.0190	0.0371	0.4430	0.83	10.31	18.50
25.33	3.9	3.8	0.6441	0.0180	0.0379	0.4556	0.92	11.54	22.40
28.75	4.2	4.1	0.6949	0.0164	0.0587	0.4703	1.58	13.52	42.82
32.07	4.5	4.4	0.7458	0.0149	0.0519	0.4783	1.57	15.34	47.86
35.02	4.7	4.6	0.7797	0.0137	0.0423	0.4813	1.42	16.85	47.48
37.63	4.9	4.8	0.8136	0.0128	0.0347	0.4814	1.26	18.12	45.75
42.58	5.2	5.1	0.8644	0.0112	0.0594	0.4775	2.37	20.33	95.09
47.47	5.4	5.3	0.8983	0.0099	0.0517	0.4721	2.32	22.41	104.50
48.90	5.5	5.4	0.9153	0.0096	0.0140	0.4708	0.67	23.02	32.48
50.11	5.6	5.5	0.9322	0.0094	0.0115	0.4699	0.57	23.55	28.17
54.36	5.8	5.7	0.9661	0.0086	0.0383	0.4698	2.00	25.54	104.31
62.94	6.0	5.9	1.0000	0.0078	0.0706	0.4920	4.13	30.97	242.40
Total	-	-			1.08	-	25.21	330.05	907.46

t-bar =	**25.21**	**minutes**	**0.42**	**hours**	Mean residence time
Pe =	**∞**				Peclet number
d =	**∞**				Dispersion number

APPENDIX C

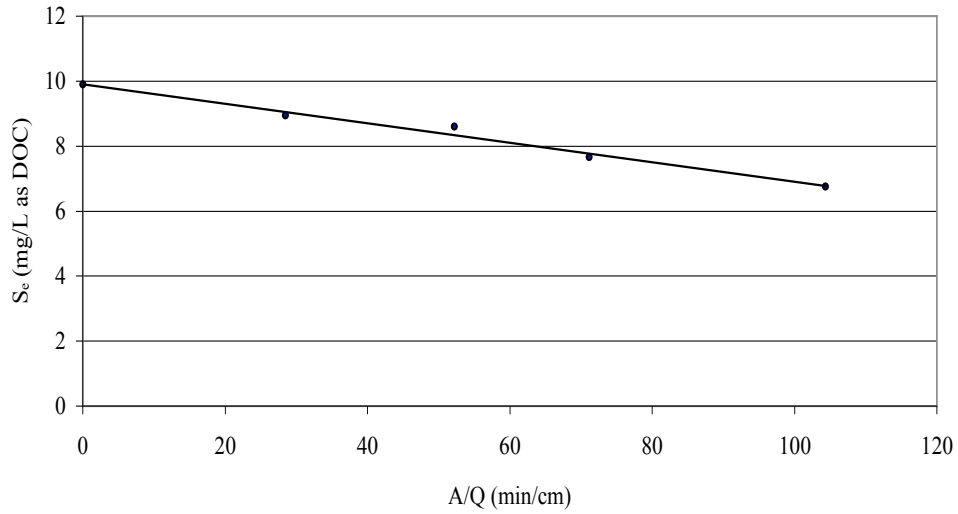

Appendix C-1. Effluent Methanol Concentration vs. A/Q when S_i = 9.91 mg DOC/L

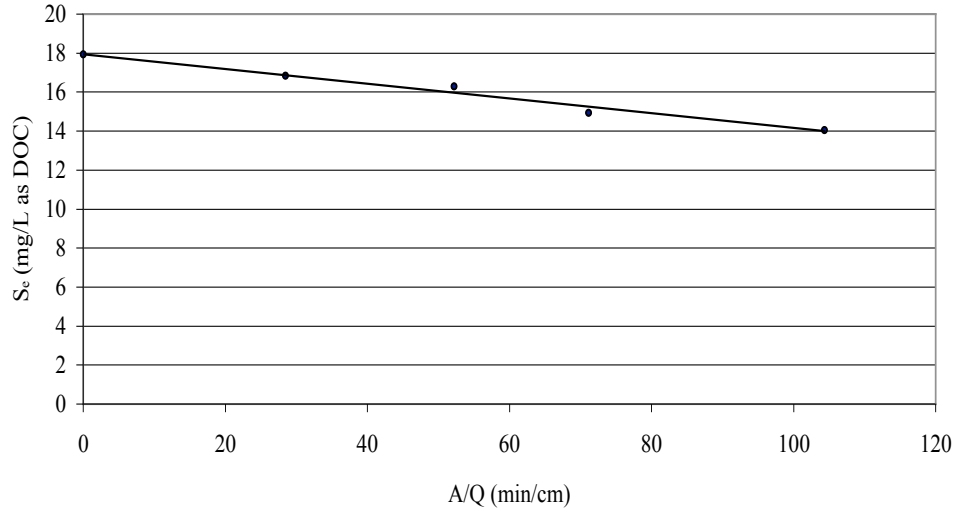

Appendix C-2. Effluent Methanol Concentration vs. A/Q when S_i = 17.93 mg DOC/L

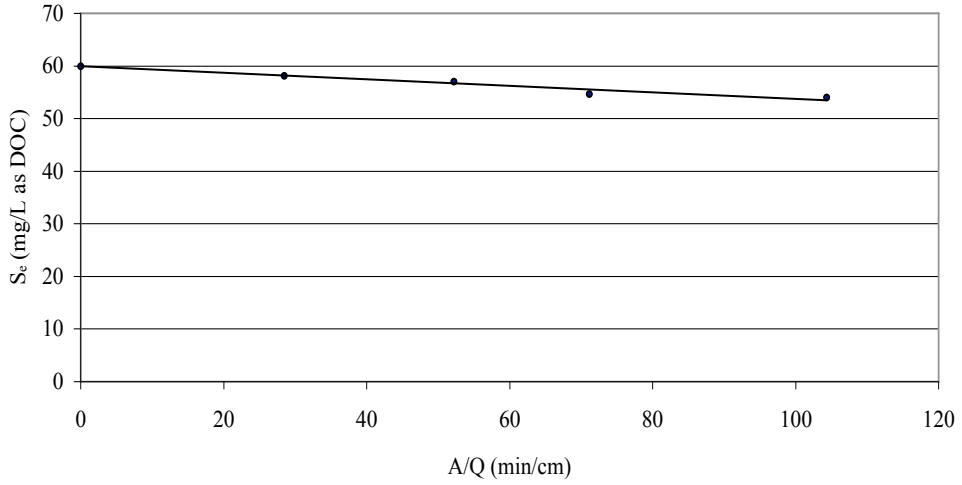

Appendix C-3. Effluent Methanol Concentration vs. A/Q when S_i = 60.00 mg DOC/L

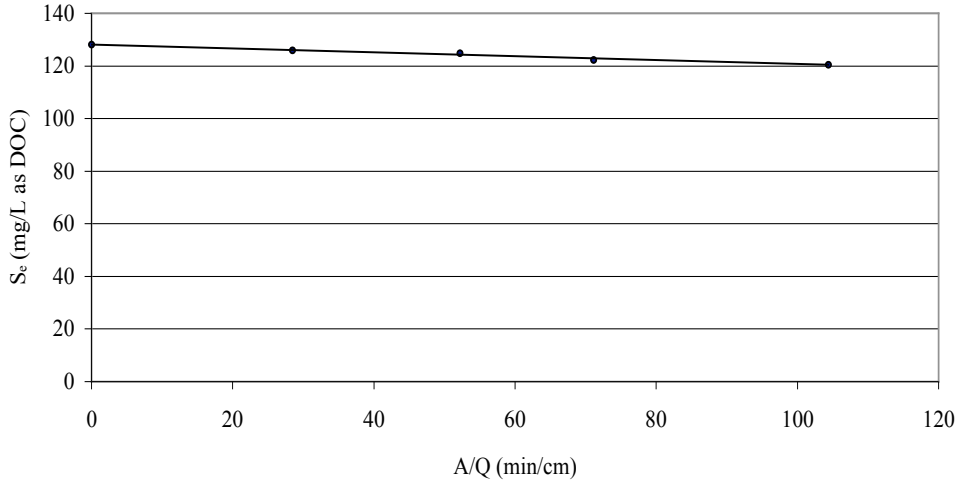

Appendix C-4. Effluent Methanol Concentration vs. A/Q when S_i = 128.13 mg DOC/L

APPENDIX D

Appendix D-1. Methanol Internal Diffusion

Date	S_i (ppm as TOC)	S_e (ppm as TOC)	Conversion (X)	δ (μm)	Consumption Rate (mg/s)	r (rpm)
11/3/08	9.91	7.66	0.2270	38	0.0990	120
11/9/08	10.30	9.79	0.0495	10	0.0224	120
11/9/08	10.30	9.92	0.0369	8	0.0167	120
11/11/08	10.26	9.08	0.1150	18	0.0519	120
11/11/08	10.26	8.93	0.1296	21	0.0585	120
11/14/08	10.16	7.42	0.2697	45	0.1206	120
11/14/08	10.16	7.30	0.2815	48	0.1258	120
11/16/08	10.29	7.16	0.3042	61	0.1377	120
11/16/08	10.29	7.20	0.3003	64	0.1360	120
11/18/08	10.49	7.25	0.3089	71	0.1426	120
11/18/08	10.49	7.27	0.3070	82	0.1417	120
11/20/08	10.31	7.31	0.2910	94	0.1320	120
11/20/08	10.31	7.25	0.2968	100	0.1346	120
11/22/08	10.13	7.21	0.2883	126	0.1285	120
11/22/08	10.13	7.15	0.2942	130	0.1311	120
11/24/08	10.38	7.29	0.2977	166	0.1360	120
11/24/08	10.38	7.36	0.2909	172	0.1329	120

Appendix D-2. Native Corn Starch as a Function of Biofilm Thickness Worksheet

Date	S_i (ppm as TOC)	S_e (ppm as TOC)	Conversion (X)	δ (μm)	Biofilm's Consumption Rate mg/(s.cm^2)	r (rpm)
1/11/05	20.55	6.12	0.7022	15	0.2028	120
1/11/05	20.55	5.94	0.7109	18	0.2053	120
1/13/05	20.32	6.77	0.6668	23	0.1904	120
1/13/05	20.32	6.96	0.6575	22	0.1878	120
1/15/05	19.86	5.41	0.7276	28	0.2031	120
1/15/05	19.86	5.22	0.7372	24	0.2058	120
1/17/05	20.82	7.76	0.6273	36	0.1836	120
1/17/05	20.82	7.25	0.6518	32	0.1907	120
1/19/05	19.99	5.83	0.7084	54	0.1990	120
1/19/05	19.99	6.32	0.6838	57	0.1921	120
1/22/05	20.45	6.81	0.6670	74	0.1917	120
1/22/05	20.45	6.89	0.6631	79	0.1906	120
1/23/05	20.00	5.82	0.7090	83	0.1993	120
1/23/05	20.00	6.37	0.6815	86	0.1916	120
1/25/05	20.14	7.14	0.6455	108	0.1827	120
1/25/05	20.14	6.98	0.6534	112	0.1850	120
1/27/05	19.54	6.53	0.6658	118	0.1828	120
1/27/05	19.54	6.79	0.6525	121	0.1792	120
1/29/05	20.66	5.93	0.7130	142	0.2070	120
1/29/05	20.66	6.15	0.7023	137	0.2039	120
1/30/05	20.07	6.31	0.6856	153	0.1934	120
1/30/05	20.07	6.38	0.6821	148	0.1924	120
2/1/05	19.64	7.96	0.5947	185	0.1642	120
2/1/05	19.64	8.12	0.5866	181	0.1619	120
2/3/05	19.89	6.58	0.6692	193	0.1871	120
2/3/05	19.89	7.44	0.6259	204	0.1750	120

Appendix D-3. Min-U-Sil 10 as a Function of Biofilm Thickness Worksheet

Date	S_i (mg/L as TSS)	S_e (mg/L as TSS)	Conversion (X)	δ (μm)	Biofilm's Consumption Rate mg/(s.cm^2)	r (rpm)
3/4/09	19.21	7.37	0.6163	11	0.1664	120
3/4/09	19.21	7.13	0.6288	8	0.1698	120
3/6/09	19.83	6.91	0.6515	16	0.1816	120
3/6/09	19.83	7.03	0.6455	15	0.1799	120
3/7/09	19.81	5.54	0.7203	19	0.2006	120
3/7/09	19.81	6.70	0.6618	23	0.1843	120
3/9/09	20.01	5.91	0.7046	34	0.1982	120
3/9/09	20.01	5.84	0.7081	26	0.1992	120
3/12/09	19.72	6.82	0.6542	41	0.1813	120
3/12/09	19.72	7.01	0.6445	43	0.1786	120

APPENDIX E

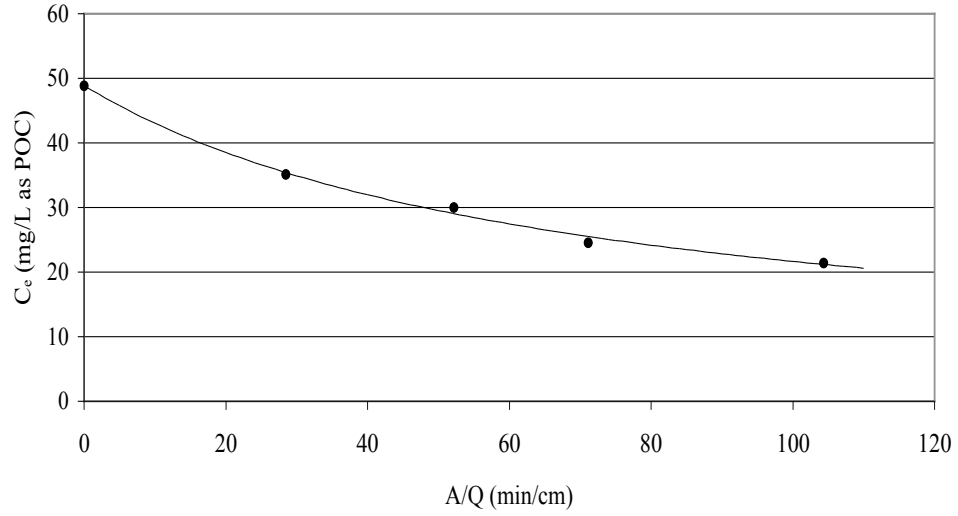

Appendix E-1. Effluent Corn Starch Concentration vs. A/Q when C_i = 48.88 mg POC/L

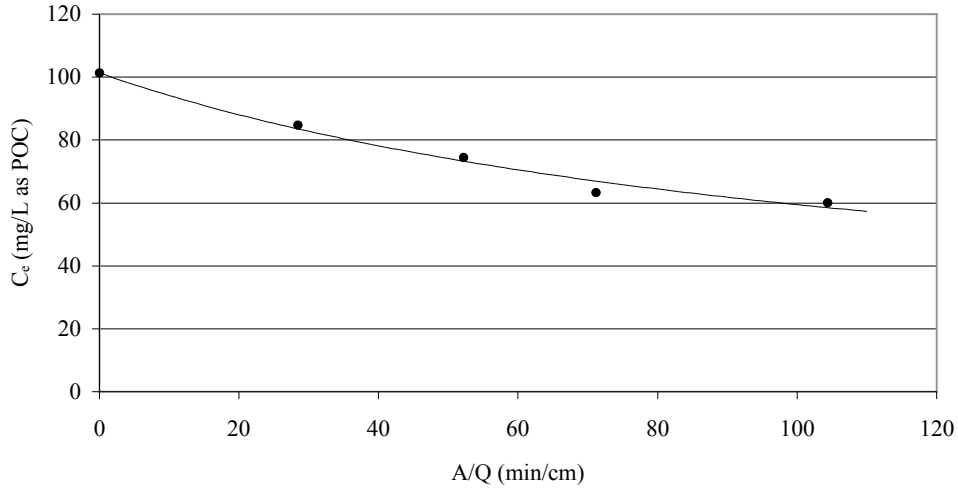

Appendix E-2. Effluent Corn Starch Concentration vs. A/Q when C_i = 101.32 mg POC/L

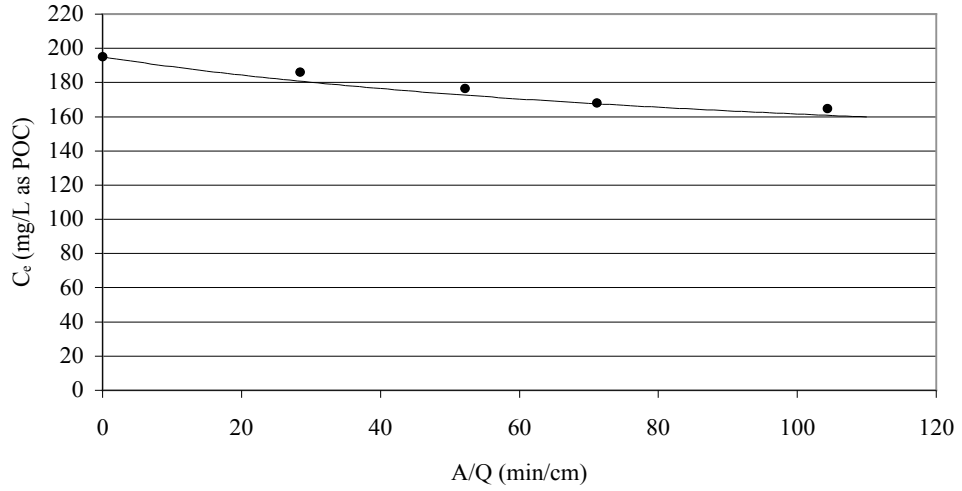

Appendix E-3. Effluent Corn Starch Concentration vs. A/Q when C_i = 196.00 mg POC/L

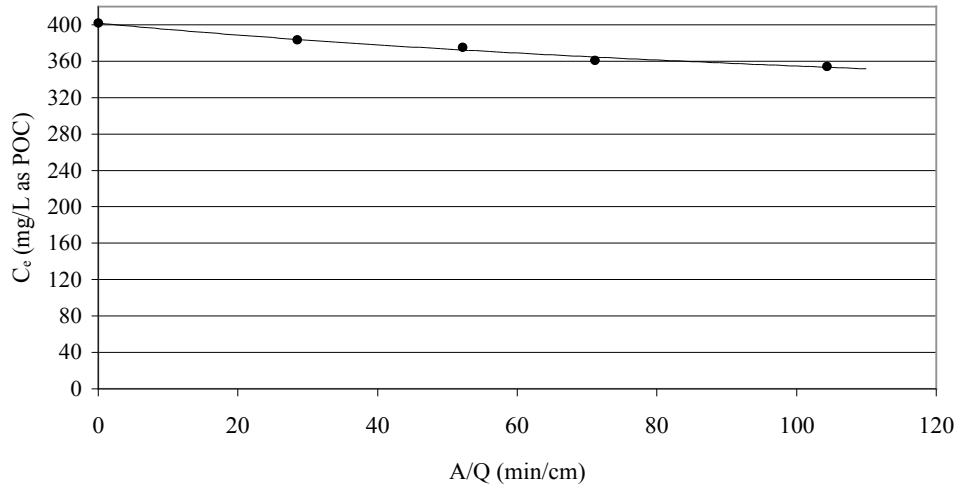

Appendix E-4. Effluent Corn Starch Concentration vs. A/Q when C_i = 401.79 mg POC/L

APPENDIX F

Appendix F-1. Bioflocculation Rate Data – Organic Particles

Date	Q (cm^3/min)	A (cm^2)	C_i (mg/L as POC)	C_e (mg/L as POC)	Conversion (X)	δ (μm)	Removal Rate (mg/min)	Removal Rate mg/(min.cm^2)	r (rpm)
12/20/04	30.00	3130.70	21.43	6.28	0.7070	54	0.4545	0.145175	120.0
12/20/04	44.00	3130.70	21.43	7.08	0.6696	54	0.6314	0.201680	120.0
12/20/04	60.00	3130.70	21.43	9.36	0.5632	54	0.7242	0.231322	120.0
12/20/04	110.00	3130.70	21.43	10.84	0.4942	54	1.1649	0.372089	120.0
12/21/04	30.00	3130.70	48.88	21.43	0.5616	55	0.8235	0.263040	120.0
12/21/04	44.00	3130.70	48.88	24.56	0.4975	55	1.0701	0.341802	120.0
12/21/04	60.00	3130.70	48.88	30.03	0.3856	55	1.1310	0.361261	120.0
12/21/04	110.00	3130.70	48.88	35.12	0.2815	55	1.5136	0.483470	120.0
12/21/04	30.00	3130.70	101.32	60.11	0.4067	55	1.2363	0.394896	120.0
12/21/04	44.00	3130.70	101.32	63.34	0.3749	55	1.6711	0.533785	120.0
12/21/04	60.00	3130.70	101.32	74.52	0.2645	55	1.6080	0.513623	120.0
12/21/04	110.00	3130.70	101.32	84.77	0.1633	55	1.8205	0.581499	120.0
2/28/05	30.00	3130.70	196.00	164.78	0.1593	43	0.9366	0.299166	120.0
2/28/05	44.00	3130.70	196.00	167.98	0.1430	43	1.2329	0.393803	120.0
2/28/05	60.00	3130.70	196.00	176.43	0.0998	43	1.1742	0.375060	120.0
2/28/05	110.00	3130.70	196.00	186.15	0.0503	43	1.0835	0.346089	120.0
12/22/04	30.00	3130.70	401.79	354.37	0.1180	57	1.4226	0.454403	120.0
12/22/04	44.00	3130.70	401.79	360.84	0.1019	57	1.8018	0.575526	120.0
12/22/04	60.00	3130.70	401.79	375.52	0.0654	57	1.5762	0.503466	120.0
12/22/04	110.00	3130.70	401.79	383.45	0.0456	57	2.0174	0.644393	120.0

Appendix F-2. Bioflocculation Rate Data – Inorganic Particles

Date	Q (cm^3/min)	A (cm^2)	C_i (ppm as TSS)	C_e (ppm as TSS)	Conversion (X)	δ (μm)	Removal Rate (mg/min)	Removal Rate mg/(min.cm^2)	r (rpm)
12/14/04	30.00	3130.70	20.00	8.33	0.5835	52	0.3501	0.111828	120.0
12/14/04	44.00	3130.70	20.00	9.00	0.5500	52	0.4840	0.154598	120.0
12/14/04	60.00	3130.70	20.00	9.50	0.5250	52	0.6300	0.201233	120.0
12/14/04	110.00	3130.70	20.00	10.70	0.4650	52	1.0230	0.326764	120.0
12/15/04	30.00	3130.70	50.00	28.00	0.4400	53	0.6600	0.210815	120.0
12/15/04	44.00	3130.70	50.00	31.00	0.3800	53	0.8360	0.267033	120.0
12/15/04	60.00	3130.70	50.00	31.00	0.3800	53	1.1400	0.364136	120.0
12/15/04	110.00	3130.70	50.00	36.70	0.2660	53	1.4630	0.467308	120.0
12/16/04	30.00	3130.70	100.00	63.70	0.3630	50	1.0890	0.347846	120.0
12/16/04	44.00	3130.70	100.00	71.30	0.2870	50	1.2628	0.403360	120.0
12/16/04	60.00	3130.70	100.00	74.00	0.2600	50	1.5600	0.498291	120.0
12/16/04	110.00	3130.70	100.00	83.00	0.1700	50	1.8700	0.597311	120.0
12/17/04	30.00	3130.70	200.00	159.57	0.2022	52	1.2129	0.387421	120.0
12/17/04	44.00	3130.70	200.00	171.00	0.1450	52	1.2760	0.407577	120.0
12/17/04	60.00	3130.70	200.00	172.33	0.1384	52	1.6602	0.530297	120.0
12/17/04	110.00	3130.70	200.00	181.00	0.0950	52	2.0900	0.667582	120.0
12/18/04	30.00	3130.70	400.00	358.00	0.1050	52	1.2600	0.402466	120.0
12/18/04	44.00	3130.70	400.00	366.33	0.0842	52	1.4815	0.473210	120.0
12/18/04	60.00	3130.70	400.00	375.00	0.0625	52	1.5000	0.479126	120.0
12/18/04	110.00	3130.70	400.00	381.33	0.0467	52	2.0537	0.655987	120.0

Appendix F-3. Methanol Rate Data – Reactors in Parallel

Date	Q (cm^3/min)	A (cm^2)	S_i (ppm as TOC)	S_e (ppm as TOC)	Conversion (X)	δ (μm)	Consumption Rate (mg/min)	Biofilm's Consumption Rate mg/(min.cm^3)	r (rpm)
11/3/04	30.00	3130.70	4.41	3.32	0.2472	40	0.0327	0.002611	120.0
11/3/04	44.00	3130.70	4.41	3.90	0.1156	40	0.0224	0.001792	120.0
11/3/04	60.00	3130.70	4.41	3.97	0.0998	38	0.0264	0.002219	120.0
11/3/04	110.00	3130.70	4.41	4.15	0.0590	38	0.0286	0.002404	120.0
11/2/04	30.00	3130.70	9.91	6.76	0.3179	38	0.0945	0.007943	120.0
11/2/04	44.00	3130.70	9.91	7.66	0.2270	38	0.0990	0.008322	120.0
11/2/04	60.00	3130.70	9.91	8.60	0.1322	40	0.0786	0.006277	120.0
11/2/04	110.00	3130.70	9.91	8.95	0.0969	40	0.1056	0.008433	120.0
11/4/04	30.00	3130.70	17.93	14.05	0.2164	43	0.1164	0.008647	120.0
11/4/04	44.00	3130.70	17.93	14.93	0.1673	41	0.1320	0.010284	120.0
11/4/04	60.00	3130.70	17.93	16.30	0.0909	41	0.0978	0.007619	120.0
11/4/04	110.00	3130.70	17.93	16.85	0.0602	41	0.1188	0.009255	120.0
11/5/04	30.00	3130.70	128.13	120.53	0.0593	44	0.2280	0.016552	120.0
11/5/04	36.00	3130.70	128.13	122.27	0.0457	45	0.2110	0.014974	120.0
11/5/04	60.00	3130.70	128.13	124.77	0.0262	45	0.2016	0.014310	120.0
11/5/04	110.00	3130.70	128.13	125.97	0.0169	45	0.2376	0.016865	120.0
11/6/04	30.00	3130.70	60.00	53.99	0.1002	48	0.1803	0.011998	120.0
11/6/04	36.00	3130.70	60.00	54.71	0.0882	48	0.1904	0.012673	120.0
11/6/04	60.00	3130.70	60.00	57.00	0.0500	48	0.1800	0.011978	120.0
11/6/04	110.00	3130.70	60.00	58.09	0.0318	48	0.2101	0.013981	120.0

APPENDIX G

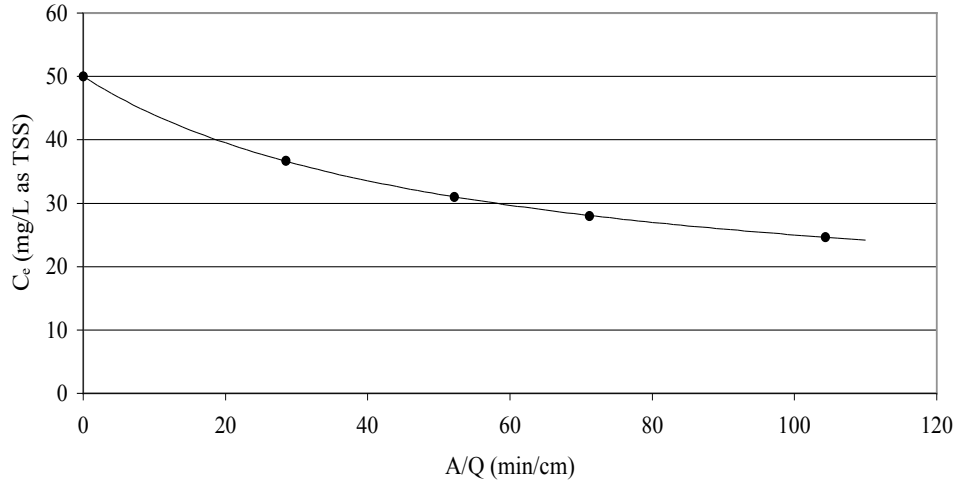

Appendix G-1. Effluent Min-U-Sil 10 Concentration vs. A/Q when C_i = 50 mg TSS/L

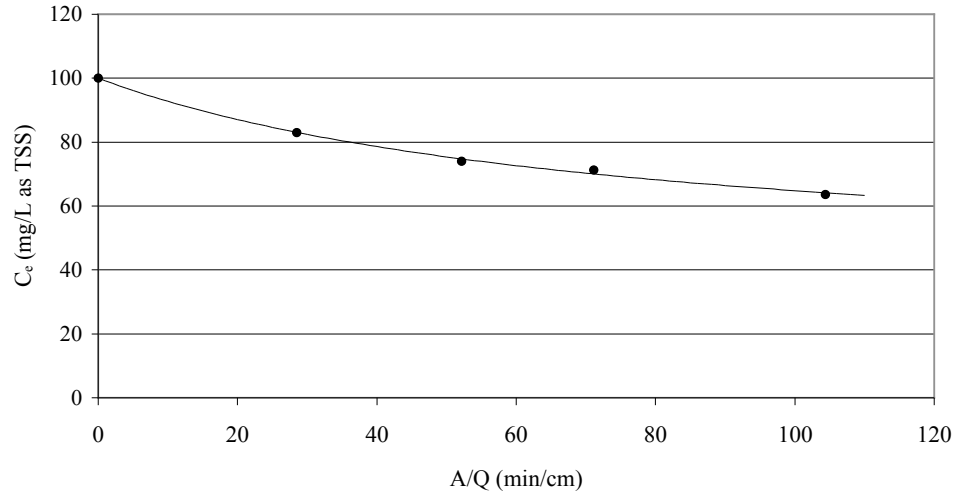

Appendix G-2. Effluent Min-U-Sil 10 Concentration vs. A/Q when C_i = 100 mg TSS/L

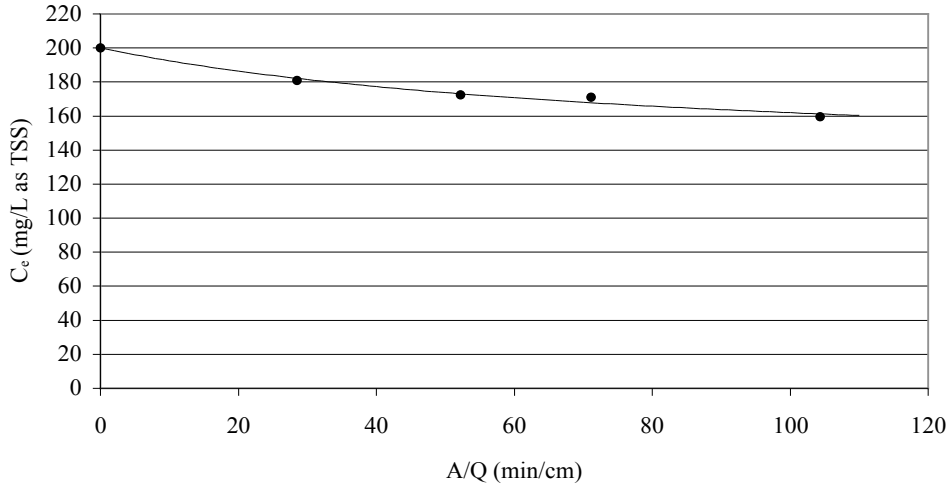

Appendix G-3. Effluent Min-U-Sil 10 Concentration vs. A/Q when C_i = 200 mg TSS/L

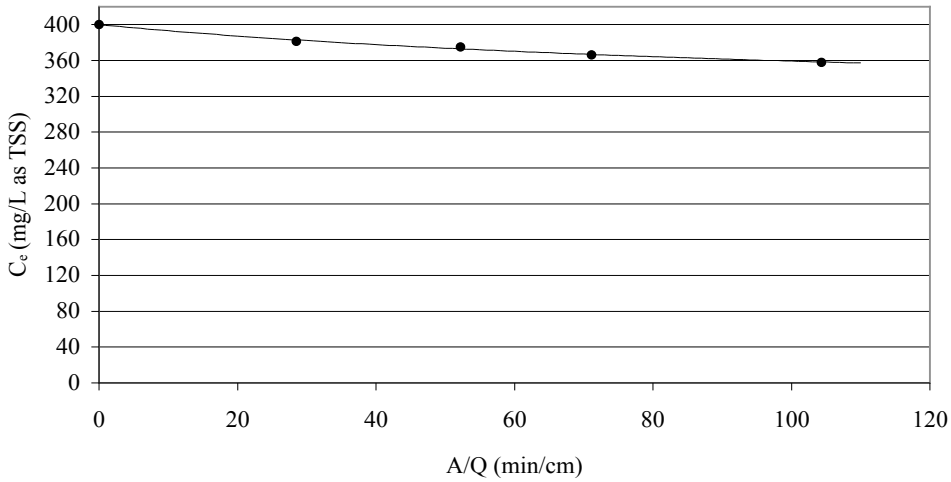

Appendix G-4. Effluent Min-U-Sil 10 Concentration vs. A/Q when C_i = 400 mg TSS/L

APPENDIX H

Appendix H-1. Methanol EPS Worksheet

EPS (ppm as TOC)	**Sample Mass** (g)	**Normalized EPS** (ppm as TOC)	**Extraction Area** (cm^2)	**EPS/Unit Area** (ppm as TOC/cm^2)	**Biofilm Thickness** (μm)
48.11	0.98	47.15	8.68	5.43	206
47.98	0.94	45.10	8.68	5.20	206
48.62	0.97	47.16	86.80	0.54	21
49.08	1.06	52.02	86.80	0.60	21
50.51	1.02	51.52	34.72	1.48	50
49.86	0.96	47.87	34.72	1.38	50
49.71	0.9825	48.84	17.36	2.81	103
49.84	0.9971	49.70	17.36	2.86	103
48.76	1.01	49.25	13.02	3.78	156
49.00	0.99	48.51	13.02	3.73	156

Appendix H-2. Organic Particle EPS Worksheet

EPS (ppm as TOC)	**Sample Mass** (g)	**Normalized EPS** (ppm as TEPC)	**Extraction Area** (cm^2)	**EPS/Unit Area** (ppm as TOC/cm^2)	**Biofilm Thickness** (μm)
59.14	0.96	56.77	13.02	4.36	156
58.93	1.01	59.52	13.02	4.57	156
52.14	0.97	50.58	86.80	0.58	32
57.61	0.99	57.03	86.80	0.66	32
60.31	1.03	62.12	34.72	1.79	68
59.22	0.94	55.67	34.72	1.60	62
55.21	1.06	58.52	17.36	3.37	108
56.74	0.97	55.04	17.36	3.17	111

APPENDIX I

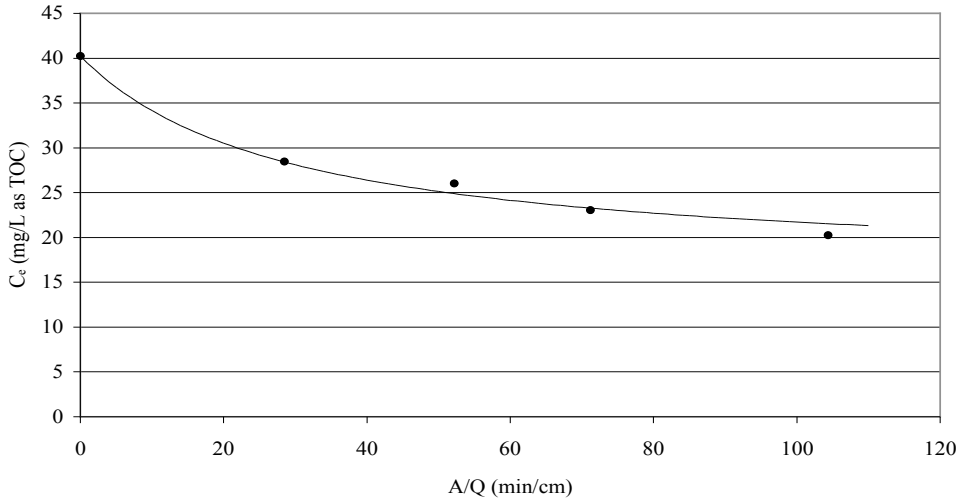

Appendix I-1. Effluent TOC vs. A/Q with 79% POC-21% DOC

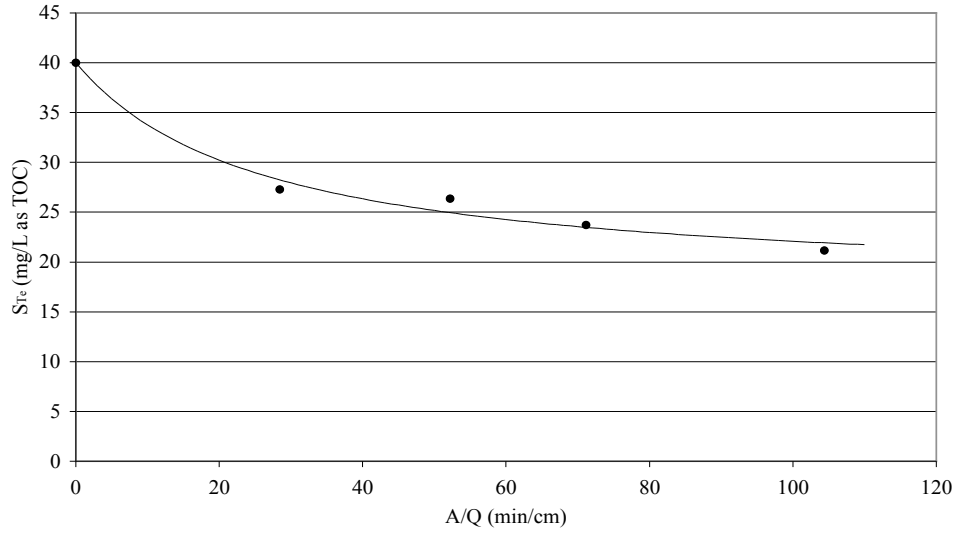

Appendix I-2. Effluent TOC vs. A/Q with 70% POC-30% DOC

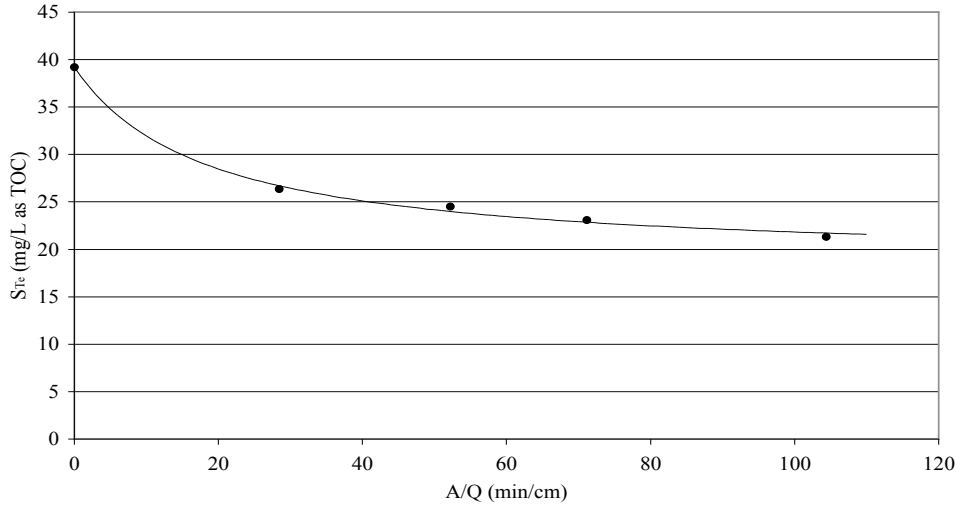

Appendix I-3. Effluent TOC vs. A/Q with 61% POC-49% DOC

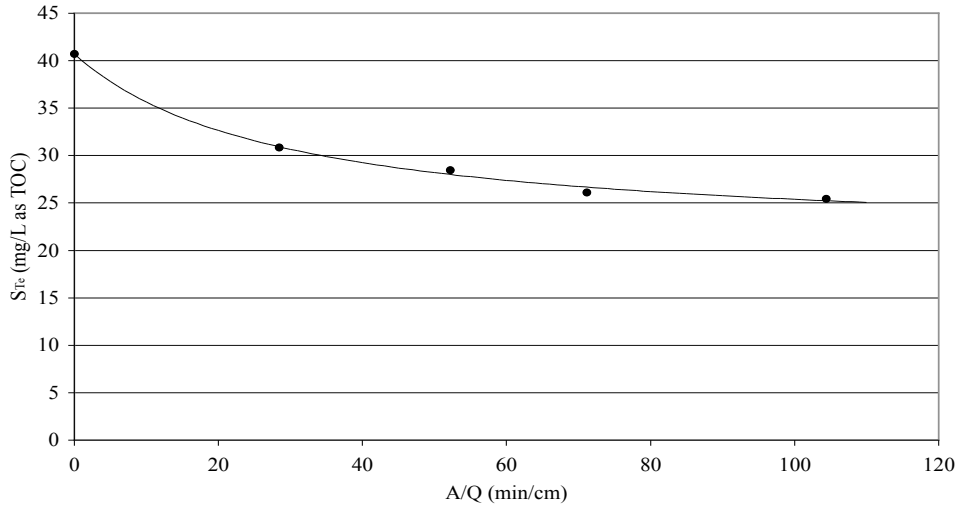

Appendix I-4. Effluent TOC vs. A/Q with 51% POC-49% DOC

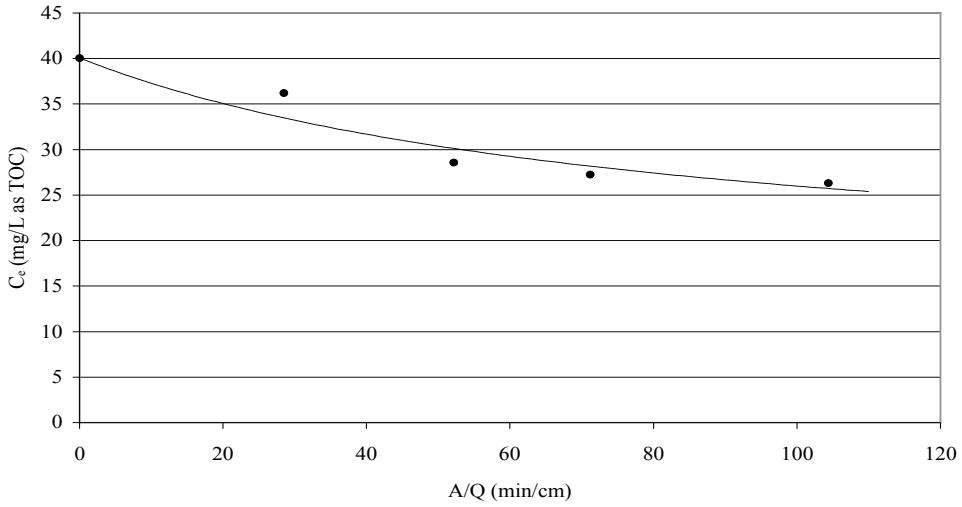

Appendix I-5. Effluent TOC vs. A/Q with 40% POC-60% DOC

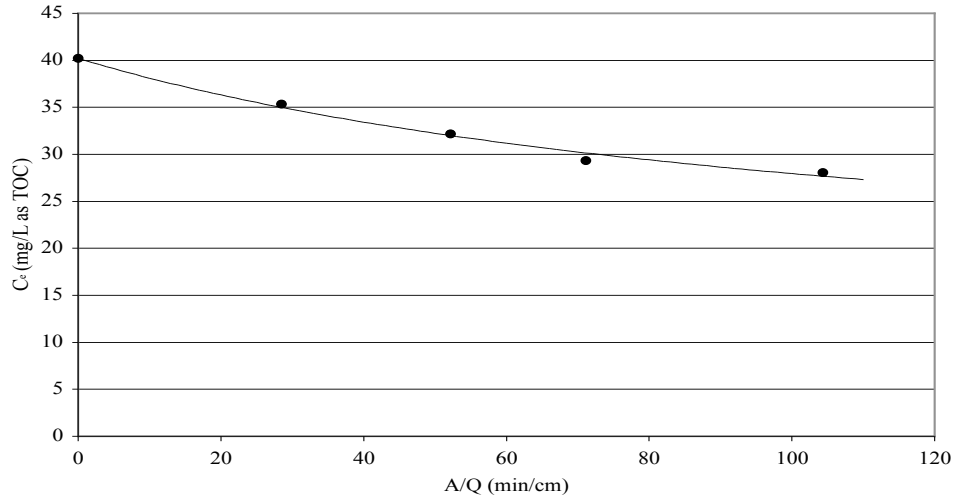

Appendix I-6. Effluent TOC vs. A/Q with 30% POC-70% DOC

APPENDIX J

Appendix J. Mixed-Order Model Confirmation Worksheet

Date	Q (cm^3/min)	A (cm^2)	TOC S_i (ppm as TOC)	TOC S_e (ppm as TOC)	Conversion (X)	δ (μm)	r (rpm)
1/4/05	30.00	3130.70	39.61	20.38	0.4855	45	120.0
1/4/05	44.00	3130.70	39.61	21.41	0.4595	45	120.0
1/4/05	60.00	3130.70	39.61	24.72	0.3759	45	120.0
1/4/05	110.00	3130.70	39.61	26.54	0.3300	45	120.0
1/5/05	30.00	3130.70	40.26	20.24	0.4973	45	120.0
1/5/05	44.00	3130.70	40.26	23.07	0.4270	45	120.0
1/5/05	60.00	3130.70	40.26	26.03	0.3535	45	120.0
1/5/05	110.00	3130.70	40.26	28.47	0.2928	45	120.0
1/6/05	30.00	3130.70	40.02	21.15	0.4715	46	120.0
1/6/05	44.00	3130.70	40.02	27.29	0.3181	46	120.0
1/6/05	60.00	3130.70	40.02	26.35	0.3416	46	120.0
1/6/05	110.00	3130.70	40.02	27.29	0.3181	46	120.0
1/7/05	30.00	3130.70	39.21	21.31	0.4565	47	120.0
1/7/05	44.00	3130.70	39.21	23.07	0.4116	47	120.0
1/7/05	60.00	3130.70	39.21	24.53	0.3744	47	120.0
1/7/05	110.00	3130.70	39.21	26.34	0.3282	47	120.0
1/8/05	30.00	3130.70	40.71	25.43	0.3753	49	120.0
1/8/05	44.00	3130.70	40.71	26.11	0.3586	49	120.0
1/8/05	60.00	3130.70	40.71	28.48	0.3004	49	120.0
1/8/05	110.00	3130.70	40.71	30.83	0.2427	49	120.0
3/1/05	30.00	3130.70	40.04	26.31	0.3429	45	120.0
3/1/05	44.00	3130.70	40.04	27.27	0.3189	45	120.0
3/1/05	60.00	3130.70	40.04	28.59	0.2860	45	120.0
3/1/05	110.00	3130.70	40.04	36.21	0.0957	45	120.0
3/2/05	30.00	3130.70	40.20	26.31	0.3455	47	120.0
3/2/05	44.00	3130.70	40.20	27.27	0.3216	47	120.0
3/2/05	60.00	3130.70	40.20	28.59	0.2888	47	120.0
3/2/05	110.00	3130.70	40.20	32.21	0.1988	47	120.0

VITA

Joshua Philip Boltz was born in Mobile, Alabama on March 18,1977. He graduated from S.S. Murphy High School in 1995, and went on to receive a Bachelor of Science in Civil Engineering from the University of South Alabama (USA), Mobile, Alabama in 2001. While attending USA, he earned membership to Alpha Theta Chi national honor society and Tau Beta Pi engineering honor society. He received his Master of Science in Environmental Engineering from the University of New Orleans, New Orleans, Louisiana in August 2003. His research emphasized on the kinetics of wastewater treatment processes, and he is a registered engineering intern in the state of Alabama.